DISSERTATION

DEVELOPING PRECLINICAL MODELS FOR INTERVERTEBRAL DISC DEGENERATION: ANALYZING MECHANICAL, MOLECULAR, AND IMMUNOLOGICAL INTERVENTIONS

Submitted by

Andres Bonilla

Department of Clinical Sciences

In partial fulfillment of the requirements

For the Degree of Doctor of Philosophy

Colorado State University

Fort Collins, Colorado

Fall 2024

Doctoral Committee:

Advisor: Jeremiah Easley

Steve Dow
Christian Puttlitz
Brian Johnstone

ABSTRACT

DEVELOPING PRECLINICAL MODELS FOR INTERVERTEBRAL DISC DEGENERATION: ANALYZING MECHANICAL, MOLECULAR, AND IMMUNOLOGICAL INTERVENTIONS

Low back pain is a prevalent global health issue, significantly affecting quality of life and contributing to economic burdens through reduced productivity and healthcare costs. Intervertebral disc degeneration (IVDD) is recognized as a major underlying cause of chronic low back pain. Despite advances in therapeutic strategies for IVDD, the translation of these treatments from preclinical research to clinical application remains challenging due to the lack of appropriate animal models that accurately mimic the complex pathophysiology of human IVDD. This document aims to address these limitations by developing and validating novel ovine and immune-induced animal models of IVDD, and to provide insights into the molecular, biomechanical, and immunological aspects of the disease.

Chapter 1 introduces the clinical significance of low back pain and the central role of IVDD in its development. The chapter highlights the unmet need for robust preclinical models to facilitate the evaluation of potential therapeutic interventions. Chapter 2 reviews the existing literature on ovine models of IVDD, emphasizing their relevance to human spinal disorders due to the anatomical, physiological, and histological similarities between sheep and humans. Ovine models are particularly valuable for studying both spontaneous and induced IVDD, providing a critical platform for translational research.

Chapter 3 presents a groundbreaking study that conducts the first comparative analysis of surgical, imaging, histological, and proteomic characteristics between cervical and lumbar intervertebral discs (IVDs) in an ovine model of IVDD. The results demonstrate a comparable progression of IVDD in both regions, challenging the longstanding emphasis on lumbar IVDs in research and underscoring the importance of cervical models in advancing our understanding of the disease.

These findings have substantial clinical and research implications, indicating that treatments traditionally developed and evaluated for lumbar IVDD may also be relevant for cervical pathology. Furthermore, the identification of specific biomarkers, could significantly enhance early diagnosis and inform the development of tailored therapeutic interventions.

Chapter 4 introduces a novel model utilizing extracorporeal shock wave therapy (ESWT) applied to ovine IVDs. While no significant evidence of IVDD was observed during the 12-week study period, localized bone formation at the treatment sites was identified. This finding provides important insight into the effects of ESWT, suggesting that while it is conventionally used as a therapeutic modality, it may also have unintended consequences, such as promoting bone formation, which could potentially lead to tissue damage. These results highlight the need for further refinement of shock parameters to reliably induce progressive IVDD, offering valuable data for future research into both the therapeutic and adverse effects of ESWT in spinal treatments.

In Chapter 5, a mechanical compression model utilizing MRI-compatible materials was developed to induce disc degeneration in ovine lumbar discs, marking the first report of its kind to our knowledge. This innovation allows for the longitudinal tracking of degeneration with a measurable rate of compression, leveraging MRI as the most critical tool for diagnosing IVDD.

While the model successfully induced biomechanical changes, including reduced disc height and altered neutral zone dynamics, no significant histological or biochemical degeneration was observed. However, these findings provide valuable insights for future researchers using mechanically induced models, offering a foundation to refine and optimize the model for tracking the progression of degeneration more accurately.

Chapter 6 explores the role of immune system in IVDD by developing an immune-induced model using a nucleus pulposus (NP) antigen vaccine. Rabbits were vaccinated against NP following IVD injury, leading to accelerated degeneration in comparison to non-vaccinated animals. This study highlights the potential of immune responses in accelerating disc degeneration, offering a novel avenue for understanding the interplay between immunity and IVDD progression.

This document contributes to the advancement of IVDD research by establishing and validating novel animal models, including ovine, mechanical compression, and immune-induced models. The proteomic findings and biomechanical evaluations presented in this document offer critical insights into the molecular pathways involved in IVDD and lay the foundation for the development of customized therapeutic strategies. Future research should focus on refining these models to better replicate the complexities of human IVDD and explore long-term therapeutic interventions that can mitigate degeneration and restore disc function.

ACKNOWLEDGMENTS

This work was made possible thanks to the invaluable guidance and support of many people. First, I am deeply grateful for the mentorship of Dr. Jeremiah Easley, who has been an incredible advisor and friend. Thank you for inspiring my ambition and coaching me through this challenging journey. I would also like to express my sincere gratitude to the members of my doctoral committee: Steve Dow, Brian Johnstone, and Christian Puttlitz. Your challenging but insightful mentorship has pushed me to pursue being better every day in my career as a researcher.

I would also like to extend my appreciation to the entire PSRL team, both past and present, for their continuous support. A special thanks to Kim Lebsock, who has helped me countless times throughout this journey. I am equally grateful to Katie Sikes, Lindsey Burton, Katie Bisazza, and Emily Van Zeeland for their unwavering support and friendship. To the OBRL crew—Ben Gandomski, Lucas Nakamura, Cecily Broomfield, and Devin von Stade—thank you for your all your collaboration. I am deeply thankful to Lynda Chow and Jade Kurihara from Dr. Dow's laboratory for their exceptional guidance. I would also like to express my gratitude to all the TMI staff and scientific members who collaborated with me and provided support whenever needed.

Especial thanks to the Fulbright ICETEX program and the Pasaporte a la Ciencia 2019 scholarship, which enabled me to pursue my doctoral studies. I am also grateful to Dr. Jorge Carmona for his invaluable support during my time in Manizales, as well as to Dr. Iang Rondón, who has been an incredible friend and mentor.

Finally, I am deeply grateful to all my family and friends who have supported me throughout this journey. Above all, I am profoundly thankful to my parents and my brother for their unwavering love and encouragement. Your constant support, belief in me, and your example as good people have been the foundation of my success. Thank you for instilling in me the ambition, resilience, and perseverance that made this achievement possible, and for supporting me despite the distance.

Los amo mucho, gracias por todo!

TABLE OF CONTENTS

CHAPTER 1 LOW BACK PAIN, INTERVERTEBRAL DISC DEGENERATION AND ANIMAL MODELS

1.1 Introduction

The prevalence of musculoskeletal conditions is growing worldwide, and low back pain (LBP) is significant among these as the leading cause of disability (1). It is estimated that approximately 80% of adults are affected by LBP at some point in their lifetime (2). LBP impacts individuals in both developed and developing countries alike, affects all age groups from children to the elderly (2,3), and thus represents a significant burden for patients, health care systems, and the economies of many countries. Approximately 40% of LBP cases are attributable to degeneration of the intervertebral discs (IVDs), making this the most common cause of chronic LBP (4). Intervertebral disc degeneration (IVDD) is a progressive, cell-mediated cascade involving each of the IVD's three main anatomical regions: the central, proteoglycan rich nucleus pulposus (NP); the peripheral, fibrocartilaginous annulus fibrosus (AF), and the two cartilage endplates (CEPs) that interface with the adjacent vertebrae. The earliest manifestations of IVDD commonly occur in the NP, where proteoglycan loss compromises the distribution of loads leading to structural and mechanical derangement of the entire spinal motion segment. While IVDD commonly occurs with increasing age, risk factors for accelerating its progression include genetics, smoking, lifestyle, obesity, trauma, and mechanical stress (5–7). IVDD may lead to LBP through direct compression of adjacent neural elements or by innervation of the IVD structures themselves, which combined with increased nerve sensitizing agents leads to increased pain (8–14).

This chapter includes content of published manuscript: Tang, S. N., Bonilla, A. F., Chahine, N. *et al.,* (2022). Controversies in spine research: Organ culture versus in vivo models for studies of the intervertebral disc. JOR Spine, 5(4) e1235

The complexity of IVDD pathophysiology poses great challenges for effective long-term treatment of associated LBP (15). Current clinical treatments are predominantly focused on managing symptoms (e.g. alleviation of pain) rather than addressing underlying causes. These treatments may involve medications such as non-steroidal anti-inflammatory drugs (NSAIDs), which can address acute symptoms but carry the risk of increased internal bleeding during long-term use (16). For more severe symptoms, opioid-based medications may be prescribed (17), but they pose a serious risk of addiction, exacerbating the opioid epidemic and associated morbidities (18–21). Where conservative treatments do not appear to modify disease progression, surgical interventions such as spinal fusion or total disc arthroplasty may be employed, but these fail to preserve disc structure or mechanical function long-term and may result in progression of IVDD in adjacent levels (15). Therefore, there is a significant clinical need for improved treatment options for patients suffering from IVDD and LBP that directly target the underlying causes.

The successful development, evaluation, and translation of new treatments for IVDD requires the use of appropriate preclinical models that recapitulate the structural, functional, and biological characteristics of the clinical condition as closely as possible. Therefore, a deeper understanding of the benefits and limitations of various approaches to implementing currently available preclinical models is critical for advancing investigations of IVDD pathophysiology and treatment.

1.2 Epidemiology and Clinical Significance of Low Back Pain

LBP is highly prevalent, and the main cause of years lived with disability (YLDs) (22,23). It is a widespread condition that most people experience at some point in their lives, making it a significant contributor to the global disease burden (24). It affects individuals of all ages, from

children to the elderly, and occurs in both sexes across all socioeconomic backgrounds (22). This widespread condition does not discriminate by age, gender, or socioeconomic status, making it a global health issue that spans diverse populations (Figure 1). Between 1990 and 2015, the YLDs due to LBP increased by 54%, largely driven by population growth and aging, with the most pronounced rise seen in low- and middle-income countries (25). In 2020, LBP affected around 619 million people globally, with a projection of 843 million prevalent cases by 2050 (22). Additionally, an increasing number of adolescents are also reporting LBP, although a specific diagnosis is often not identified in these cases (26).

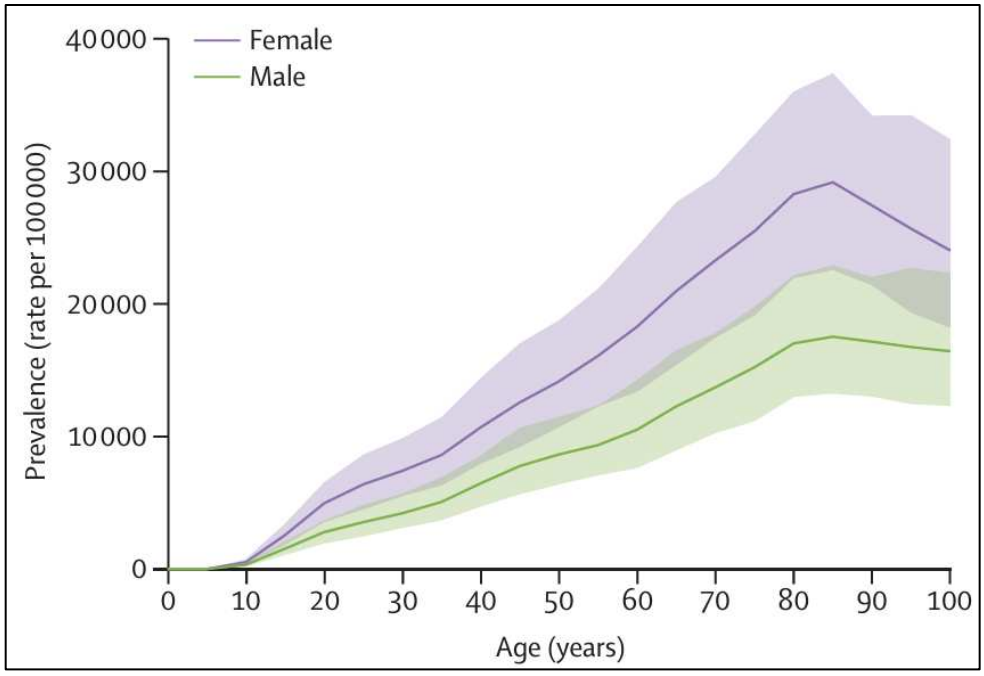

Figure 1. Global prevalence of low back pain by age and sex in 2020. Adapted from Ferreira et al, (2022) (22).

Individuals with physically demanding jobs, physical and mental health issues, smokers, and those who are obese face the highest risks of developing LBP (27). Additionally, the incidence of LBP peaks during the third decade of life and continues to increase until around age 60-65

(24,28). Other significant risk factors that influence the onset and progression of LBP include low educational attainment, psychological stress, anxiety, depression, job dissatisfaction, insufficient social support at work, and exposure to whole-body vibrations (29). These environmental and personal elements collectively contribute to the complex nature of LBP prevalence and its management challenges.

The costs, healthcare utilization, and disability associated with LBP vary widely across countries, largely influenced by cultural beliefs, social structures, and differing views on the causes and management of the condition (25,30). In the United States, annual healthcare expenditures related to LBP exceed $100 billion, driven by direct medical treatments, lost wages, and reduced productivity (31). Despite these variations, the global burden of LBP is projected to rise, particularly in low- and middle-income countries, where under-resourced healthcare systems are often ill-equipped to manage the increasing impact of this condition. Consequently, the associated disability and costs are expected to place even greater strain on these fragile systems in the coming decades (32).

Despite advancements in the assessment and treatment of LBP, managing this condition continues to be a significant challenge for both researchers and clinicians. One major obstacle to developing effective treatments is the considerable variation in how LBP manifests, its underlying causes, precipitating factors, and the course it takes over time (28). There is a pressing need for intensified research efforts and global initiatives to address LBP as a growing public health issue (32). In this endeavor, identification of the main causes of LBP has been a priority. Among these causes, IVD degeneration stands out as a critical contributor to LBP, linked with various structural abnormalities and disruptions in IVD physiology. IVD degeneration alters disc mechanics, contributes to nerve compression, and triggers inflammation—key factors driving LBP symptoms.

Understanding the relationship between IVD degeneration and LBP is crucial to addressing this growing public health concern effectively (33,34).

1.3 Structure of the Intervertebral Disc

The IVD is a critical component of the vertebral column to support the body and facilitate upper body motion. In the human spine, 23 IVDs form fibrocartilaginous joints between each of the articulating vertebrae. Overall, there are six IVDs in the cervical spine, twelve in the thoracic spine, and five in the lumbar spine. These IVDs consists of three main components: the cartilaginous endplates (CEP), nucleus pulposus (NP), and annulus fibrosus (AF) (Figure 2). Collectively, the CEP, NP, and AF function to transmit vertebral loads and facilitate spinal motion.

The CEP is a layer of hyaline cartilage found on the upper (cranial) and lower (caudal) surfaces of the intervertebral disc (IVD), where it connects to the vertebral bodies. It plays a crucial role in facilitating the transport of fluids and solutes into and out of the IVD. Similar to articular cartilage, the extracellular matrix (ECM) of the CEP is composed of type II collagen, embedded with chondrocytes (35,36).

The NP is a gelatinous tissue located centrally in the IVD which originates from the notochord, with notochordal cells remaining in the tissue after birth until around 10 years of age in humans. These cells are then replaced by smaller, chondrocyte-like cells that have lower metabolic activity (37). The ECM of the NP is composed of type II collagen fibers and elastin, which contain proteoglycans such as aggrecan and versican (38). The proteoglycans negatively charged side chains contribute to the high hydration and osmolarity of the NP, allowing the IVD to withstand compressive forces and deform reversibly.

The AF is made up of multiple concentric rings, or lamellae, with collagen fibers arranged parallel within each layer, providing tensile strength and the ability to withstand forces from any direction (39). The inner AF consists of several layers of fibrocartilage, while the outer AF is a fibrous tissue containing highly organized fibers composed mainly of type I collagen, allowing it to resist tensile loads (40).

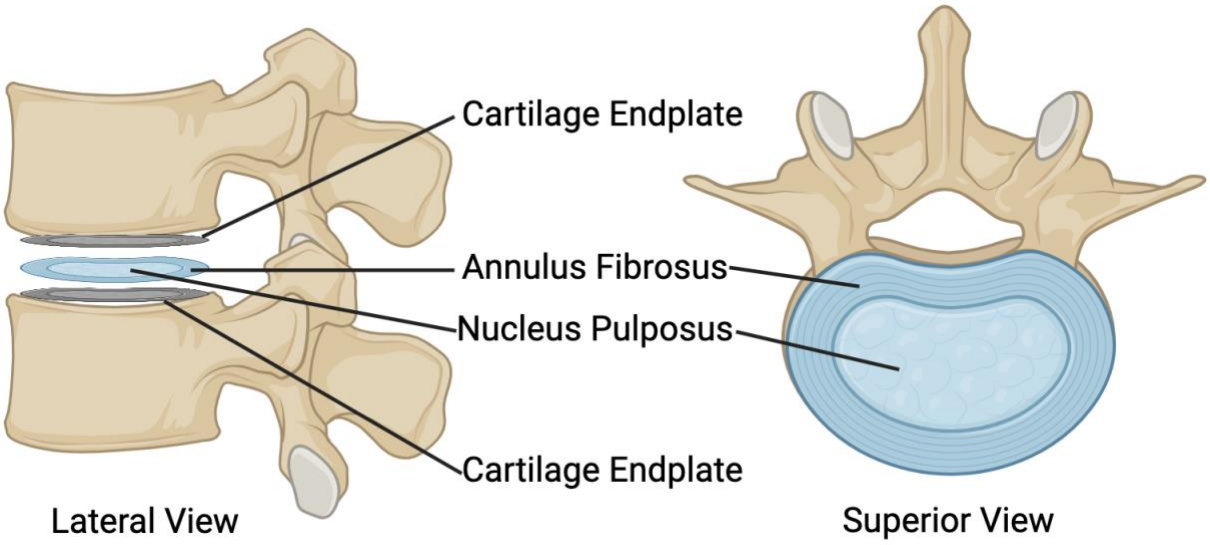

Figure 2. Illustration of the IVD and adjacent vertebrae in situ, highlighting key anatomical features and the structure of the disc. The main anatomical regions of the IVD are clearly demarcated. Figure created using BioRender.com by Andres Bonilla (2024).

1.4 Intervertebral Disc Disease

The most common IVD pathology is the degeneration of the disc, which brings about significant morphological, biochemical, and functional alterations in the intervertebral disc (41). IVDD develops during adolescence and progresses with age (38,42). Although the exact cause of IVD degeneration is not fully understood, it is generally seen as a multifactorial condition influenced by inadequate nutrient supply, excessive mechanical stress, injury, and genetic

predisposition (38,43). In comparison to other tissues, IVDs exhibit signs of age-related degeneration earlier in life. Organismal aging is driven by the gradual accumulation of molecular and cellular damage over time, leading to disrupted tissue homeostasis and, ultimately, to the physiological and functional decline (38).

As degeneration progresses, the distinct functional regions of the IVD become less well-defined, and the tissue structure loses its organization. The typically gelatinous NP undergoes a transformation into a more fibrotic tissue, while fissures form throughout the IVD (44). Degeneration is accompanied by increased vascularization and innervation throughout the intervertebral disc (Figure 3). Similarly, abnormal apoptosis, and senescence of IVD cells, along with ECM degradation and immune cell infiltration, are key molecular changes observed (45). From a biochemical standpoint, key features of intervertebral disc degeneration include a reduction in proteoglycan content within the NP and changes in the type and distribution of collagen fibers throughout the disc (46). These biochemical changes reduce the hydrostatic pressure generated by the NP and weaken the AF, leading to a decreased load-bearing capacity, reduced disc height, and bulging of the peripheral AF. These degenerative modifications in the intervertebral disc adversely affect spinal mechanics, often contributing to conditions such as spinal stenosis, facet joint arthritis, and alterations in the surrounding spinal ligaments (47).

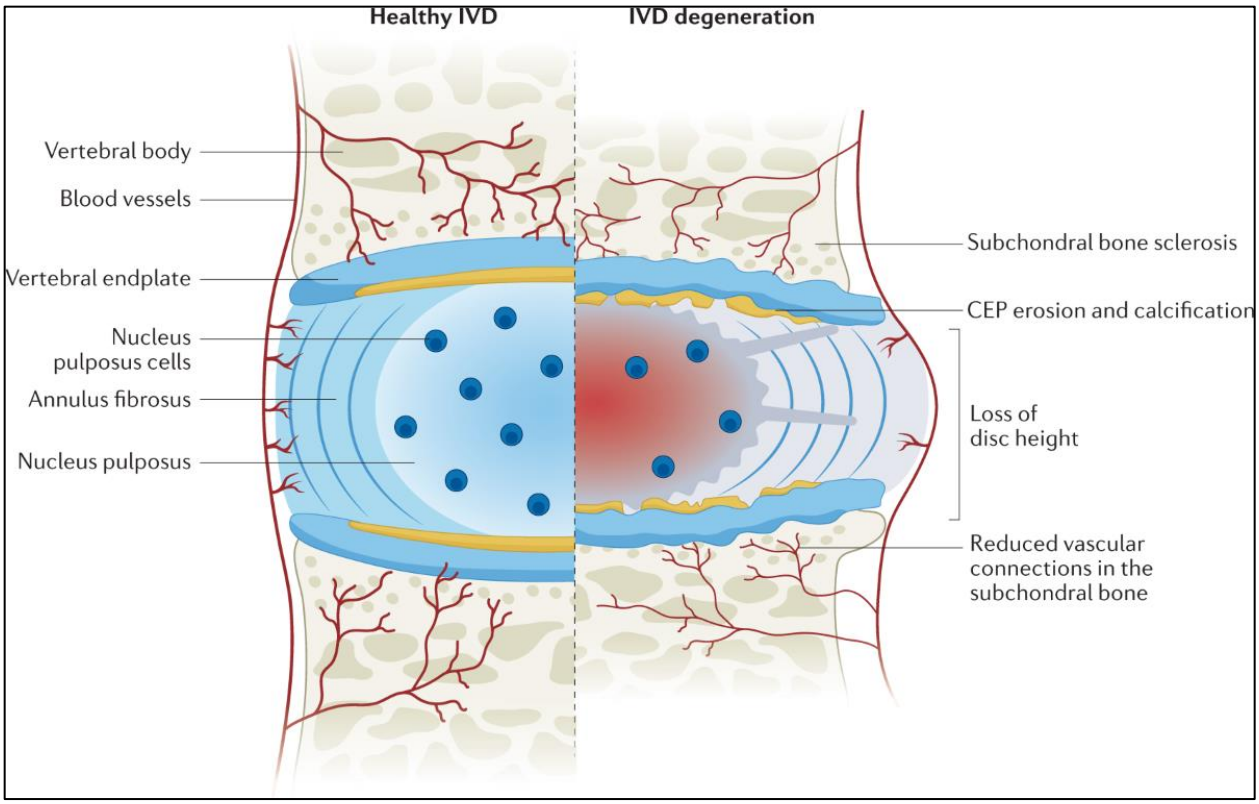

Figure 3. Illustrative comparison of Healthy (Left) and degenerated (Right) IVD. Changes in specific regions, function and structure of the IVD are demarcated. Adapted from Uruj Zehra et al, (2022) (48).

1.5 Animal Models

Animal models have played a critical role in advancing understanding of the temporal evolution of IVDD, including how constitutive, environmental, or biomechanical risk factors may initiate, promote, or otherwise regulate degenerative changes, and how therapeutic strategies may ameliorate, resolve, or prevent IVDD (49). Currently, *in vivo* studies of IVDD are conducted in small animals such as mice, rats, and rabbits; as well as larger animals such as dogs, pigs, goats, sheep, cows, and nonhuman primates (50). However, given the complexity of human IVDD, a perfect animal model does not exist (51). In general, *in vivo* models offer significant advantages

for the study of IVDD, including the ability to assess pain, evaluate nutrition and blood supply, account for systemic immune effects, and observe crosstalk with surrounding tissues (Figure 4). They also enable advanced imaging and meet regulatory requirements essential for the clinical translation of new IVDD treatments.

1.5.1 Pain Evaluation

Pain can be defined as cortical interactions that initiate changes in behavior (52). These pain behaviors are influenced by physiological and immunological factors, cognition, and conduct. In human patients, LBP as a result of IVDD results in significant morbidity, preventing patients from completing their daily routine, removing individuals from the workforce, and resulting in stress, anxiety, and depression (53). This pain is the main driver for patients seeking care, and a paramount factor in the diagnosis of IVDD (54). Importantly, studies have shown that IVDD does not always directly correlate with pain, and that IVDD may often be present in asymptomatic individuals (55).

While the direct connections between IVDD and pain remain complex, animal models have been and continue to be essential research tools for understanding physical and metabolic pathways of symptomatic IVDD ("discogenic pain"), and in the development of new therapeutics aimed at mitigating and preventing the onset of degeneration and pain. Put simply, only *in vivo* models can recreate the complex processes of pain resulting from disc degeneration, and permit assessments of behavioral and functional changes as outcome measures. This is not without its challenges, as each species has unique physical and behavioral manifestations of pain, and species-specific, repeatable, and standardized pain scores must be used (56). Amongst large animals, dogs provide an interesting model for discogenic pain as distinct and appreciable behavioral changes make these

animals particularly valuable when assessing analgesics (57–61). Nonetheless, the optimal way to measure pain in both pre-clinical models (and patients) is still the subject of extensive debate. Important aspects such as the nociceptive response generators, pain thresholds, and clinical and behavior manifestations need to be contemplated before selecting an animal model (56). Validated methods of pain measurement include physical performance (e.g., grimace scales, lameness examinations, gait measurements) (62), behavioral changes (e.g., decreased burrowing and rearing) (63,64), and response to mechanical stimuli (e.g., hind-paw mechanical hyperalgesia test). A recent study has shown that the Grimace scale (a subjective pain assessment method based on facial expressions) is highly reliable in mouse and rat models, and moderately reliable in rabbits, piglets, and sheep (65).

Large animal models have also led to the identification of molecular biomarkers of discogenic pain (66) Biomarkers not only represent potentially powerful, non-invasive diagnostic tools for evaluating IVDD progression and response to therapeutic intervention, but also provide mechanistic insights into how local pathophysiological changes lead to the manifestation of clinical symptoms, informing the development of new therapies. This simply cannot be accomplished using *ex vivo* models where clinical manifestations of IVDD (e.g. pain) cannot be measured.

1.5.2 Nutrition and Blood Supply

The IVDs are largely avascular structures. During human development, blood vessels penetrate deep into the lamellar structure of the AF from around 35 weeks gestation (67,68). Vessels then recede, and by the second decade of life remain only at the margins. At no point do blood vessels penetrate the central NP; instead, blood vessels terminate within the subchondral

bone adjacent to the CEP. These locations (AF margins and the vertebral endplates) are the sole sources of nutrition for cells within the IVD itself, with the latter considered the most important (69). Physiological nutrition via these routes is therefore critical for IVD cell survival, and alterations to the adjacent vasculature that disrupt nutrient supply are considered to play an important role in the onset and progression of IVDD. Importantly, the role of vasculature in IVDD can only be investigated using *in vivo* animal models with an intact circulatory system and cannot be achieved using *ex vivo* organ culture models.

At a fundamental level, *in vivo* models have been used to establish mechanisms of nutrient flow into the IVD. For example, historically, *in vivo* large animal models were used to establish that vertebral endplate vasculature is the primary nutrient diffusion pathway into the IVD (70,71). More recently, a rabbit model was used to demonstrate how alterations in microvasculature that occur with degeneration affect nutrient supply to the IVD (72). *In vivo* models have also been essential for studies investigating how certain drugs impact the vasculature supplying nutrients to the IVD. For example, *in vivo* models have been used to show how vasoactive agents such as acetylcholine and nicotine, as well as cigarette smoking itself, may alter vasculature and nutrient supply to the IVD, implicating smoking in the etiology of IVDD (73–76). *In vivo* models are also essential for evaluating the efficacy of therapeutic agents administered systemically to treat IVD pathologies, such as intravenous stem cells and antibiotics (77,78).

1.5.3 Long Term Evaluation

Irrespective of the factors initiating or driving IVDD, it is most often a long-lasting process with changes in the cellular environment and the different structures of the IVD occurring over months or years, before leading to the gross structural and functional alterations that are associated

with the manifestation of clinical symptoms (79). As such, *in vivo* models have been important tools for elucidating the natural history of IVDD (80). Furthermore, *in vivo* models are crucial for evaluating the long-term efficacy of novel treatments for IVDD (81). The primary goal of IVDD treatments is to both restore IVD function and structure and alleviate painful symptoms. Acute toxicity and initial structural (e.g., an increase in cellularity and ECM or IVD height) and functional changes can be assessed *ex vivo* and *in vivo*; however, potential therapeutic agents may have either a short half-life or may diffuse out of the IVD, so their long-term effects must be determined. Furthermore, initial treatment success may be diminished by the unfavorable degenerative environment of IVDD. *In vivo* models allow an observation period of several weeks (small animal models) to months or even years (large animal models), facilitating confirmation of sustained or permanent therapeutic effects. Furthermore, the same animal may be assessed over time using non-invasive, gold standard imaging techniques such as magnetic resonance imaging (MRI), radiographs or computed tomography, increasing the clinical relevance of findings and reducing the number of experimental animals required. In addition, it is crucial to ensure both acute (i.e., toxicity) and long-term safety (e.g. tumorgenicity) of novel biological treatments, which is only possible using *in vivo* models.

1.5.4 Systemic Factors

A major advantage of using *in vivo* animal models for IVDD and LBP research is the ability to assess the contributions of systemic biological processes such as the immune system, or co-morbidities such as diabetes or obesity on IVDD progression and treatment. Immune cell infiltration of mast cells, macrophages, neutrophils, and T lymphocytes has been identified in the painful human degenerate IVD following rupture of the AF or CEP (82–85); however, the

mechanisms underlying the roles of these cells in IVDD are underexplored. The healthy IVD is largely avascular and immune-privileged, yet with degeneration, there is evidence that these immune cells can infiltrate the disc from the bone marrow via lesions in the vertebral endplate and/or via aberrant blood vessel ingrowth into the endplate and AF (86). *In vivo* animal models of IVDD and LBP are valuable tools with which to investigate the recruitment, invasion, and function of immune cells in pathological environments, which cannot be readily investigated *ex vivo*. For example, transgenic mice over-expressing the pro-inflammatory cytokine TNFα demonstrate increased infiltration of Tryptase-expressing (Mast) cells or CD68+ (Macrophage) cells in IVD tissue regions associated with higher risks of herniation (87). The increased presence of immune cells, specifically macrophages in herniated IVD tissue, has been corroborated using a novel *in vivo* mouse model of IVD herniation induced radiculopathy (88). Green Fluorescent Protein (GFP) transgenic bone marrow chimeric mouse models of IVD injury have been used to determine the origin of M1 macrophages and demonstrated that following IVD injury, M1 macrophages are recruited specifically from outside the IVD (89). A subsequent study verified these findings by demonstrating increased recruitment of macrophages to the dorsal region of the IVD together with neo-innervation in an IVD injury model up to 12 months (90). These studies highlight the importance of *in vivo* models for investigating the role of the immune system in IVDD.

Systemic inflammatory diseases such as obesity and diabetes demonstrate a strong association with IVDD and back pain (91,92), and animal models (rodents in particular), demonstrating these disease phenotypes are useful tools to conduct the mechanistic and therapeutic studies in which changes in whole IVD joint structure/function and pain behaviors can be investigated. Obesity and diabetes co-exist and can be readily investigated simultaneously using *in vivo* animal models. Male and female leptin receptor-deficient mice fed with a control (low fat)

or high-fat diet to mimic the effects of obesity and diabetes on disc health have been used to examine obesity and type-2 diabetes on healthy intervertebral IVDs (93,94). Sex-dependent effects have been described, with only females developing diabetes and the most pronounced changes in IVD and bone structure, pointing toward a sex-dependent role for leptin in the spine (93).

In a type-2 diabetic rat model several changes have been identified in the IVD joint compared to healthy control and obese rats. Specifically decreases in the glycosaminoglycan (GAG) and water contents of the IVD, increases in mechanical stiffness, advanced glycation end-products (AGEs) and catabolic markers, as well as increases in vertebral endplate thickness and decreased porosity were found, suggesting a reduction in nutrition to the IVD (95). Similarly, AGE-fed mice demonstrated age-accelerated IVDD together with ectopic calcification of the spinal tissues and insulin resistance, highlighting a role for AGEs in promoting diabetes-induced IVDD (96). To further validate the role of AGEs in diabetes-induced IVDD, diabetic mice were treated with oral anti-inflammatory and anti-AGE drugs. These drugs mitigated pathological effects observed on disc height, GAG content and catabolic markers in the diabetic mice models, demonstrating broad clinical applications of anti-AGE drugs on spinal health (97). Together, these studies highlight the critical role of *in vivo* animal models in evaluating the effects of systemic co-morbidities on IVDD progression and response to treatment.

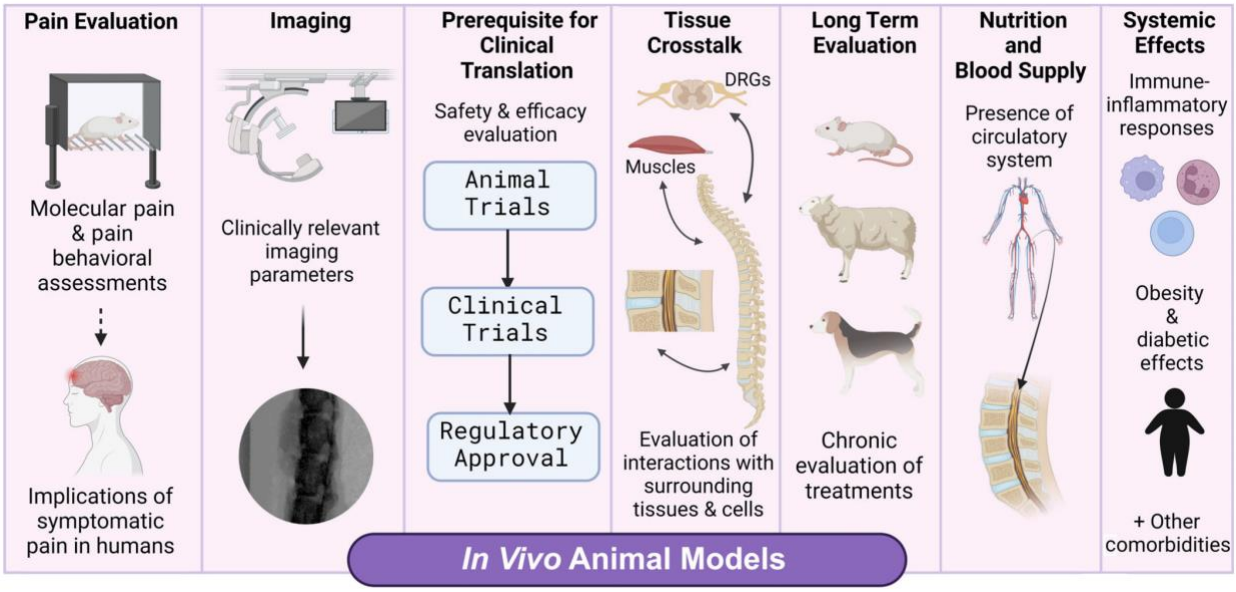

Figure 4. Summary of the advantages of *in vivo* models for the intervertebral disc. Figure modified from Tang, Bonilla, *et al.,*2022 (98).

1.5.5 Crosstalk with Surrounding Tissues

Investigating crosstalk with surrounding tissues is essential for a comprehensive understanding of IVDD progression and the development of LBP, and this is best achieved with the biological complexity inherent to *in vivo* models. For example, tissue crosstalk is important to consider when studying nociception. The dorsal root ganglion (DRG) has been suggested to interact with the NP in IVD herniation to elicit pathological consequences. This involves induction of pro-inflammatory signaling pathways (99,100), activation of microglia (101), and modulation of the AMPK-mTOR axis (102) in the DRG. *Ex vivo* co-culture models may be able to model some tissue interactions. For example, a gene-editing study using *ex vivo* co-culture systems suggested that inflammatory signals from degenerative IVDs can sensitize nociceptive neurons (103), and such sensitization can be manifested under mechanical stress (104), suggesting that IVDD may play a role in pain sensitization (105). However, even in *ex vivo* work, different results can be obtained depending on the study design. For example, differential effects of hypoxic stress

on neurite outgrowth in DRGs were reported between the single cell and tissue levels (106). Therefore, the study of neural activity in context of IVDD *in vivo* may yield contrasting results from those obtained *ex vivo*.

There are numerous examples of the importance of tissue crosstalk in IVDD pathophysiology. In a rabbit cornea implantation model, cartilaginous endplate explants may inhibit neovascularization while AF explants may promote it (107). This implies compartmental crosstalk can craft the nutritional pathway of the discs. On the other hand, loss of vertebral bone integrity, for example due to vertebroplasty (108), or bone loss in ovariectomized mice (109) may affect IVD health. Schmorl's nodes, an endplate defect, have been associated with IVDD (110), and is consistent with findings that experimental injury to the endplate can initiate disc degeneration in large animal models (111). IVD herniation may initiate at the endplate-annulus interface in aged rats (112) and involves systemic TNF-α upregulation (87). These studies support that endplate and vertebral bone have major influences on IVD tissue homeostasis. At the cellular level, IVDD is associated with remodeling of the NP, which transitions into a fibrocartilaginous tissue composed of chondrocyte-like and fibroblastic cells. NP ECM remodeling may in part be mediated by cell types originating in adjacent tissues (113–116). Thorough interrogation of such dynamic cellular exchange among tissue compartments/systems requires *in vivo* models.

1.5.6 Physiologically Relevant Imaging

To ensure the physiological relevance of IVD imaging findings, it is important to consider tissue interaction. Imaging of whole IVD motion segments in live animals can better reflect the physiological status of the IVDs. For example, when performed *in vivo*, radiographic assessments of disc height (an important surrogate of IVDD progression and response to treatment) can be

normalized to adjacent vertebral dimensions to account for variation across spine levels and individual animals. Moreover, *in vivo* imaging accounts for the mechanical constraints of para-spinal tissues such as muscles and ligaments when evaluating IVD geometry. Under deep sedation or anesthesia, animals can be ensured for proper position to avoid influence of muscle relaxation to accurately evaluate anatomical structures (56). Animals with altered muscle activity such as GDF-8 mouse mutants and botulinum toxin-treated monkeys exhibit reduced IVD height (117). Lastly, *in vivo* imaging permits long-term, longitudinal imaging evaluations that cannot be achieved *ex vivo*.

1.5.7 Regulatory Requirements and Prerequisites for Clinical Translation

In vivo animal models provide superior preclinical platforms to address regulatory requirements and accelerate clinical translation by answering critical questions regarding both the safety and efficacy of novel IVDD treatments. Regulatory agencies such as the U.S Food and Drug Administration (FDA) oversee the approval process of any drug or medical device aimed at IVDD treatment, with the exception of human-derived, minimally manipulated tissues. Preclinical studies must demonstrate that the benefits of the treatment outweigh its risks before approval for clinical use. Although animal testing is not required by the FDA, it is the most effective way to demonstrate the biological response in a living system and, therefore, is rarely excluded from the investigational new drug application process. The FDA has recognized this and has issued draft guidance to ensure such studies are rigorously conducted (118). Also recognized is the need to refine, reduce and replace animal models in device and therapeutic testing where possible (119). In most cases, preclinical animal study results are used to support an investigational new drug application and are followed by human clinical trials prior to FDA approval; however, in some specific instances,

animal study results alone may be used for approval. This type of approval is covered by the FDA Animal Rule in situations where human efficacy trials may not be ethical or feasible (120).

Several preclinical *in vivo* animal models may be utilized in combination to satisfy regulatory requirements. For example, initial discovery of pathological mechanisms and screening of therapeutic targets may be carried out in rodent models that permit genetic manipulation, while subsequently, large animal models provide platforms for long-term evaluation of safety and efficacy where IVD size and geometry are closer to that of humans. While organ culture models may also play a role in this process, *ex vivo* models are largely supportive to *in vivo* studies.

Intermixed with the FDA approval process is the concept of and strategy surrounding commercialization and translation to the clinic. Commercialization of a drug or device for the prevention or treatment of IVDD relies heavily on acceptance by medical physicians such as spine surgeons. A therapy could be groundbreaking with a high impact on affected patients but never realize its potential as a gold standard treatment if it is not considered sufficiently clinically relevant or if efficacy data is unconvincing. Preclinical *in vivo* animal models, and large animal models in particular, are vital to the commercialization process of any groundbreaking therapy by more closely recapitulating the human condition, anatomy, IVD size and geometry, and life span. With respect to novel device development, large animal models mimic the surgical application requirements of such devices, providing practical feedback in the development of instrumentation and delivery systems, which may be as impactful to the overall success of the therapy as the therapy itself. If a surgeon cannot safely or consistently instrument an implant or deliver a therapy, then said therapy is irrelevant. Organ culture models do not provide this realistic, clinically relevant scenario. Additionally, advanced diagnostic imaging, specifically MRI, has grown to be the gold standard modality for assessing IVDD severity. As such, clinicians rely on MRI as an essential

diagnostic tool for IVDD patients. Unlike organ culture models, MRI can be utilized in *in vivo* animal models to follow IVDD progression as well as to assess treatment efficacy, which is highly impactful with respect to the goal of achieving acceptance of therapies by clinicians and eventual commercialization. Ultimately, for a device or therapy to be useful, it must integrate seamlessly into the clinical environment, and leveraging clinically relevant *in vivo* animal models throughout the product development and translational process is the best way to achieve this.

Unfortunately, no model of IVDD mimics the human condition in all aspects. Despite their important role within the assessment for a new device or therapy, ethical considerations also impact the choice and use of *in vivo* models. For example, dog and primate models with spontaneous occurring IVDD closely translating to clinical findings in humans undergo increased public scrutiny making these models less accessible and more expensive. On the other hand, preclinical models utilizing livestock animals such as sheep, goats, and pigs are more widely accepted by the general public, although some are more limited for investigating human IVDD due to retention of notochordal cells (pigs). Animal models that keep notochordal cell-rich NPs, such as pigs and non- chondrodystrophic dogs presents different biomechanical properties to animal and humans such as sheep with absence of notochordal cells (121). While organ culture models carry little ethical stigma, it is currently unusual for a therapy to move from benchtop to the affected patient via solely the use of organ culture models. Even ©f organ culture models were acceptable by regulatory agencies to provide safety and efficacy, it would be challenging to translate those results into the clinical situation without additional analysis in living systems.

1.6 Appropriate Model Selection

It is clear that the selection of a model system for any project must be driven by the research

question. Just as an inappropriate sample size can invalidate the results of a project, so too can the use of an inappropriate model system. Therefore, an understanding of the strengths and weaknesses of the various *ex vivo* organ culture and *in vivo* models available is a critical step in study design. The relative strengths and weaknesses of these different models are not necessarily universal; again, they are driven by the question that is being asked and the outcome measures that best answer that question. A particularly obvious example would be that it would not be possible to test a new spinal implant intended for human use in a rat or rabbit, but it would be achievable in a sheep, pig, or calf model. When selecting amongst the available options, in this case, outcome measures are particularly important – what do you need to sample, how often, and over what period of time?

Both organ culture models and animal models have their limitations, but both also play a vital role in the overall successful understanding of the disease process and the development of potentially life-changing therapies for human patients. The types of available *in vivo* animal models used for spine research have ranged from non-mammalian vertebrates (such as zebrafish) to small mammals (such as rodents) to large mammals (such as dogs and livestock). With the increasing complexity of the model, there is more likely to be translation to human disease; however, the increased complexity may complicate the mechanistic understanding across multiple tissues. Furthermore, the cost of larger models is higher, both in dollars and potentially in negative public perception. In general, single-cell organisms, invertebrates, and non-mammalian vertebrates have the most utility in investigating the cellular or molecular basis of disease. Non-mammalian vertebrates and some rodents are amenable to genetic manipulation, allowing for the creation of genetic models that display a particular phenotype (which may include susceptibility or resistance to disease). This type of manipulation is not currently possible in most large

mammalian models, but these species are highly useful for the study of naturally occurring and induced models of disease. It should be noted that modern gene-editing technology is making genetic manipulation of larger animals more feasible (122). No animal model can perfectly recapitulate human disease, and the ability to use cadaveric human tissue in organ culture must be considered a potential advantage of that approach. Organ culture models may offer the benefit of systematic control of the biomechanics of the experimental system that more closely mimic the human condition.

There are many advantages to naturally occurring models of disease. Because they are closest to the "real mechanism", they can give the best insight into disease biology and the best evaluation of diagnostics and therapeutics. Furthermore, if companion animals can be used – for example, when studying IVDD in dogs – then researchers may be able to recruit client-owned cases, which may reduce costs and reduce unnecessary animal usage. Such investigations are also of dual benefit, with advances made for the treatment of the species being studied as well as potential translational benefits to humans. However, there are also possible disadvantages to studying naturally occurring diseases, including the fact that variables beyond the control of researchers (such as genetic diversity within highly outbred species) may affect results, and appropriate cases may be difficult to find.

In contrast, experimentally induced models have the advantage of enhanced reproducibility of the intervention/injury such as traumatic and mechanical injuries, in as many animals as needed and when they are needed. The downside is that induced disease may not exactly recapitulate natural disease and therefore response to therapeutics might not translate perfectly. Furthermore, there are significant costs and ethical concerns to navigate. When considering induced models of disease for spine research, surgical models are most common; however, other methods of inducing

disease may be considered, including genetic manipulation, dietary manipulation, and chemically induced disease (50).

There is no single "gold standard" model for IVD research precisely because different research questions lend themselves to different approaches. Thus, the path to selecting the right model starts with the research question. This will lead to the outcomes of interest, and the selection of the methods that will be used to measure them. These, in turn, will drive the selection of a specific model. In some cases, the elimination of clearly unsuitable models may be the easiest first step. From there, the strengths and weaknesses of potentially suitable options can be weighed. It may turn out that two models could answer your question equally well, and in this case, other factors such as cost, and convenience will certainly play a role. It is possible (even likely) that a broad research question cannot be answered effectively by a single model, and that multiple models must be used in sequence or simultaneously to address different aspects of the question. Indeed, complementary use of several IVD model types and leveraging the unique advantages of each is likely to result in the highest impact research in most instances. For example, taking the development of a novel biologic for IVDD treatment as a general case study, a study may commence by establishing and characterizing an IVDD phenotype in a naturally occurring or transgenic animal model, and identifying a putative therapeutic target. Subsequently, potential therapeutic agents could be screened in organ culture models under controlled experimental conditions and utilizing cadaveric human discs to confirm relevance to the human condition. Short-term safety and efficacy studies could then be undertaken in small animal models, followed by longer-term studies in large animal models using gold standard clinically relevant outcome measures. As access to such a wide array of model systems may be beyond the capabilities of a single laboratory, financially and/or logistically, such studies could be undertaken through

collaborations across laboratories and institutions.

1.7 References

1. De David CN, Deligne LDMC, Da Silva RS, Malta DC, Duncan BB, Passos VMDA, et al. The burden of low back pain in Brazil: Estimates from the Global Burden of Disease 2017 Study. Popul Health Metr. 2020 Sep 30;18(1):1–10.
2. Freburger JK, Holmes GM, Agans RP, Jackman AM, Darter JD, Wallace AS, et al. The Rising Prevalence of Chronic Low Back Pain. Arch Intern Med. 2009 Feb 9;169(3):251–8.
3. Hartvigsen J, Hancock MJ, Kongsted A, Louw Q, Ferreira ML, Genevay S, et al. What low back pain is and why we need to pay attention. 2018 Jun 1;391(10137):2356–67.
4. Zhang YG, Guo TM, Guo X, Wu SX. Clinical diagnosis for discogenic low back pain. Int J Biol Sci. 2009;5(7):647.
5. Chou L, Brady SRE, Urquhart DM, Teichtahl AJ, Cicuttini FM, Pasco JA, et al. The Association Between Obesity and Low Back Pain and Disability Is Affected by Mood Disorders: A Population-Based, Cross-Sectional Study of Men. Medicine. 2016 Apr 1;95(15).
6. Oichi T, Taniguchi Y, Oshima Y, Tanaka S, Saito T. Pathomechanism of intervertebral disc degeneration. JOR Spine. 2020 Mar 1;3(1).
7. Shiri R, Falah-Hassani K, Heliövaara M, Solovieva S, Amiri S, Lallukka T, et al. Risk Factors for Low Back Pain: A Population-Based Longitudinal Study. Arthritis Care Res (Hoboken). 2019 Feb 1;71(2):290–9.
8. Freemont AJA, Peacock TE, Goupille P, Hoyland JAJ, O'Brien J, Jayson MIV. Nerve ingrowth into diseased intervertebral disc in chronic back pain. The Lancet. 1997 Jul 19;350(9072):178–81.

9. Purmessur D, Freemont AJ, Hoyland JA. Expression and regulation of neurotrophins in the nondegenerate and degenerate human intervertebral disc. Arthritis Res Ther. 2008 Aug 27;10(4):R99.

10. Binch ALA, Cole AA, Breakwell LM, Michael ALR, Chiverton N, Creemers LB, et al. Nerves are more abundant than blood vessels in the degenerate human intervertebral disc. Arthritis Res Ther. 2015 Dec 21;17(1):370.

11. LA Binch A, Cole AA, Breakwell LM, Michael ALLR, Chiverton N, Cross AK, et al. Expression and regulation of neurotrophic and angiogenic factors during human intervertebral disc degeneration. Arthritis Res Ther. 2014 Oct 20;16(4):416.

12. Freemont AJ, Watkins A, Le Maitre C, Baird P, Jeziorska M, Knight MTNN, et al. Nerve growth factor expression and innervation of the painful intervertebral disc. J Pathol. 2002 Jul;197(3):286–92.

13. Richardson SM, Doyle P, Minogue BM, Gnanalingham K, Hoyland JA. Increased expression of matrix metalloproteinase-10, nerve growth factor and substance P in the painful degenerate intervertebral disc. Arthritis Res Ther. 2009 Aug 20;11(4):R126.

14. Olmarker K. Radicular pain – recent pathophysiologic concepts and therapeutic implications. Der Schmerz. 2001 Dec;15(6):425–9.

15. Alizadeh R, Sharifzadeh SR. Pathogenesis, etiology and treatment of failed back surgery syndrome. Neurochirurgie. 2021;

16. Mokhtare M, Mohammad Valizadeh S, Emadian O, Valizadeh SM. Lower Gastrointestinal Bleeding due to Non-Steroid Anti-Inflammatory Drug-Induced Colopathy Case Report and Literature Review. Middle East J Dig Dis. 2013;5(2):107.

17. Ravalli S, Musumeci G. New Horizons of Knowledge in Intervertebral Disc Disease. J

Invest Surg. 2021;34(8):912–3.

18. Lyden J, Binswanger IA. The United States opioid epidemic. Semin Perinatol. 2019 Apr 1;43(3):123–31.

19. Silverman LI, Heaton W, Farhang N, Saxon LH, Dulatova G, Rodriguez-Granrose D, et al. Perspectives on the Treatment of Lumbar Disc Degeneration: The Value Proposition for a Cell-Based Therapy, Immunomodulatory Properties of Discogenic Cells and the Associated Clinical Evaluation Strategy. Front Surg. 2020 Dec 16;7:554382.

20. Foster NEN, Anema JR, Cherkin D, Chou R, Cohen SP, Gross DP, et al. Prevention and treatment of low back pain: evidence, challenges, and promising directions. 2018 Jun 9;391(10137):2368–83.

21. Deyo RA, Von Korff M, Duhrkoop D. Opioids for low back pain. BMJ. 2015 Jan 5;350(jan05 10):g6380–g6380.

22. Ferreira ML, de Luca K, Haile LM, Steinmetz JD, Culbreth GT, Cross M, et al. Global, regional, and national burden of low back pain, 1990–2020, its attributable risk factors, and projections to 2050: a systematic analysis of the Global Burden of Disease Study 2021. Lancet Rheumatol. 2023 Jun;5(6):e316–29.

23. James SL, Abate D, Abate KH, Abay SM, Abbafati C, Abbasi N, et al. Global, regional, and national incidence, prevalence, and years lived with disability for 354 diseases and injuries for 195 countries and territories, 1990-2017: a systematic analysis for the Global Burden of Disease Study 2017. Lancet [Internet]. 2018 Nov 10 [cited 2023 Jan 29];392(10159):1789–858. Available from: https://pubmed.ncbi.nlm.nih.gov/30496104/

24. Hoy D, Brooks P, Blyth F, Buchbinder R. The Epidemiology of low back pain. Best Pract Res Clin Rheumatol. 2010 Dec;24(6):769–81.

25. De David CN, Deligne LDMC, Da Silva RS, Malta DC, Duncan BB, Passos VMDA, et al. The burden of low back pain in Brazil: Estimates from the Global Burden of Disease 2017 Study. Popul Health Metr. 2020 Sep 30;18.

26. Borenstein DG, Balagué F. Low Back Pain in Adolescent and Geriatric Populations. Rheumatic Disease Clinics of North America. 2021 May;47(2):149–63.

27. Knezevic NN, Candido KD, Vlaeyen JWS, Van Zundert J, Cohen SP. Low back pain. The Lancet. 2021 Jul;398(10294):78–92.

28. Vlaeyen JWS, Maher CG, Wiech K, Van Zundert J, Meloto CB, Diatchenko L, et al. Low back pain. Nat Rev Dis Primers. 2018 Dec 13;4(1):52.

29. Andersson GB. Epidemiological features of chronic low-back pain. The Lancet. 1999 Aug;354(9178):581–5.

30. Lo J, Chan L, Flynn S. A Systematic Review of the Incidence, Prevalence, Costs, and Activity and Work Limitations of Amputation, Osteoarthritis, Rheumatoid Arthritis, Back Pain, Multiple Sclerosis, Spinal Cord Injury, Stroke, and Traumatic Brain Injury in the United States: A 2. Vol. 102, Archives of Physical Medicine and Rehabilitation. 2021. p. 115–31.

31. Dagenais S, Caro J, Haldeman S. A systematic review of low back pain cost of illness studies in the United States and internationally. Vol. 8, Spine Journal. 2008. p. 8–20.

32. Hartvigsen J, Hancock MJ, Kongsted A, Louw Q, Ferreira ML, Genevay S, et al. What low back pain is and why we need to pay attention. The Lancet. 2018 Jun 1;391(10137):2356–67.

33. Mohd Isa IL, Teoh SL, Mohd Nor NH, Mokhtar SA. Discogenic Low Back Pain: Anatomy, Pathophysiology and Treatments of Intervertebral Disc Degeneration. Int J Mol Med.

2023;24(208):1–16.

34. Zhang Y gang, Guo T mao, Guo X, Wu S xun, Zhang gang. Clinical diagnosis for discogenic low back pain [Internet]. Vol. 5, Int. J. Biol. Sci. 2009. Available from: http://www.biolsci.org647

35. Lakstins K, Arnold L, Gunsch G, Flanigan D, Khan S, Gadde N, et al. Characterization of the human intervertebral disc cartilage endplate at the molecular, cell, and tissue levels. Journal of Orthopaedic Research. 2021 Sep 1;39(9):1898–907.

36. Yin S, Du H, Zhao W, Ma S, Zhang M, Guan M, et al. Inhibition of both endplate nutritional pathways results in intervertebral disc degeneration in a goat model. J Orthop Surg Res. 2019 May 16;14(1).

37. Peck SH, McKee KK, Tobias JW, Malhotra NR, Harfe BD, Smith LJ. Whole Transcriptome Analysis of Notochord-Derived Cells during Embryonic Formation of the Nucleus Pulposus. Sci Rep. 2017 Dec 1;7(1).

38. Oichi T, Taniguchi Y, Oshima Y, Tanaka S, Saito T. Pathomechanism of intervertebral disc degeneration. Vol. 3, JOR Spine. John Wiley and Sons Inc; 2020.

39. Humzah MD, Soames RW. Human intervertebral disc: Structure and function. Anat Rec. 1988 Apr 8;220(4):337–56.

40. Jin L, Liu Q, Scott P, Zhang D, Shen F, Balian G, et al. Annulus Fibrosus Cell Characteristics Are a Potential Source of Intervertebral Disc Pathogenesis. PLoS One [Internet]. 2014 May 5 [cited 2023 Feb 16];9(5):e96519. Available from: https://journals.plos.org/plosone/article?id=10.1371/journal.pone.0096519

41. Urban JP, Roberts S. Degeneration of the intervertebral disc. Arthritis Res Ther. 2003;5(3):120.

42. Wen P, Zheng B, Zhang B, Ma T, Hao L, Zhang Y. The role of ageing and oxidative stress in intervertebral disc degeneration. Front Mol Biosci. 2022;9(November):1–12.

43. Adams MA, Roughley PJ. What is Intervertebral Disc Degeneration, and What Causes It? Spine (Phila Pa 1976). 2006 Aug;31(18):2151–61.

44. Buckwalter JA. Aging and Degeneration of the Human Intervertebral Disc. Spine (Phila Pa 1976). 1995 Jun;20(11):1307–14.

45. Sun K, Jiang J, Wang Y, Sun X, Zhu J, Xu X, et al. The role of nerve fibers and their neurotransmitters in regulating intervertebral disc degeneration. Ageing Res Rev. 2022 Nov;81:101733.

46. Lyons G, Eisenstein SM, Sweet MBE. Biochemical changes in intervertebral disc degeneration. Biochimica et Biophysica Acta (BBA) - General Subjects. 1981 Jan;673:443–53.

47. Simpson ST. Intervertebral Disc Disease. Veterinary Clinics of North America: Small Animal Practice. 1992 Jul;22(4):889–97.

48. Zehra U, Tryfonidou M, Iatridis JC, Illien-Jünger S, Mwale F, Samartzis D. Mechanisms and clinical implications of intervertebral disc calcification. Nat Rev Rheumatol. 2022 Jun 9;18(6):352–62.

49. Jin L, Balian G, Li XJ. Animal models for disc degeneration-an update. Vol. 33, Histology and Histopathology. NIH Public Access; 2018. p. 543–54.

50. Fusellier M, Clouet J, Gauthier O, Tryfonidou M, Le Visage C, Guicheux J. Degenerative lumbar disc disease: in vivo data support the rationale for the selection of appropriate animal models. Eur Cell Mater. 2020 Jan 6;39:18–47.

51. Reitmaier S, Graichen F, Shirazi-Adl A, Schmidt H. Separate the Sheep from the Goats:

Use and Limitations of Large Animal Models in Intervertebral Disc Research. Vol. 99, Journal of Bone and Joint Surgery - American Volume. Lippincott Williams and Wilkins; 2017. p. e102.

52. Shi C, Qiu S, Riester SM, Das V, Zhu B, Wallace AA, et al. Animal models for studying the etiology and treatment of low back pain. 2018 May 1;36(5):1305–12.

53. Andersson GBJ. Epidemiological features of chronic low-back pain. The Lancet. 1999 Aug 14;354(9178):581–5.

54. Fujii K, Yamazaki M, Kang JD, Risbud M V., Cho SK, Qureshi SA, et al. Discogenic Back Pain: Literature Review of Definition, Diagnosis, and Treatment. Vol. 3, JBMR Plus. 2019.

55. Lotz JC. Animal Models of Intervertebral Disc Degeneration. Spine (Phila Pa 1976). 2004 Dec 1;29(23):2742–50.

56. Lee NN, Salzer E, Bach FC, Bonilla AF, Cook JL, Gazit Z, et al. A comprehensive tool box for large animal studies of intervertebral disc degeneration. JOR Spine. 2021 Jun 14;4(2):e1162.

57. Testa B, Reid J, Scott ME, Murison PJ, Bell AM. The Short Form of the Glasgow Composite Measure Pain Scale in Post-operative Analgesia Studies in Dogs: A Scoping Review. Front Vet Sci. 2021 Sep 30;8:1084.

58. Fujii K, Yamazaki M, Kang JD, Risbud M V, Cho SK, Qureshi SA, et al. Discogenic Back Pain: Literature Review of Definition, Diagnosis, and Treatment. JBMR Plus. 2019 May;3(5):e10180.

59. Pelled G, Salas MM, Han P, Gill HE, Lautenschlager KA, Lai TT, et al. Intradiscal quantitative chemical exchange saturation transfer MRI signal correlates with discogenic pain in human patients. Sci Rep. 2021 Dec 1;11(1).

60. Chen, Y. T., Cotter, A., & Isaac Z. Back Pain: Discogenic. In Clinical Guide to Musculoskeletal Medicine. Springer, Cham.; 2022. 25–32 p.

61. Thompson K, Moore S, Tang S, Wiet M, Purmessur D. The chondrodystrophic dog: A clinically relevant intermediate-sized animal model for the study of intervertebral disc-associated spinal pain. JOR Spine. 2018 Mar 28;1(1):1–13.

62. Millecamps M, Czerminski JT, Mathieu AP, Stone LS. Behavioral signs of axial low back pain and motor impairment correlate with the severity of intervertebral disc degeneration in a mouse model. The Spine Journal. 2015 Dec;15(12):2524–37.

63. Lai A, Moon A, Purmessur D, Skovrlj B, Winkelstein BA, Cho SK, et al. Assessment of functional and behavioral changes sensitive to painful disc degeneration. Journal of Orthopaedic Research. 2015 May 1;33(5):755–64.

64. Leimer EM, Gayoso MG, Jing L, Tang SY, Gupta MC, Setton LA. Behavioral Compensations and Neuronal Remodeling in a Rodent Model of Chronic Intervertebral Disc Degeneration. Scientific Reports 2019 9:1. 2019 Mar 6;9(1):1–10.

65. Evangelista MC, Monteiro BP, Steagall P V. Measurement properties of grimace scales for pain assessment in non-human mammals. Pain. 2021 Sep 9;Publish Ah.

66. Willems N, Tellegen AR, Bergknut N, Creemers LB, Wolfswinkel J, Freudigmann C, et al. Inflammatory profiles in canine intervertebral disc degeneration. BMC Vet Res. 2016 Dec 13;12(1):10.

67. Nerlich AG, Schaaf R, Wälchli B, Boos N. Temporo-spatial distribution of blood vessels in human lumbar intervertebral discs. European Spine Journal. 2007 Apr 1;16(4):547–55.

68. Rudert M, Tillmann B. Detection of lymph and blood vessels in the human intervertebral disc by histochemical and immunohistochemical methods. Ann Anat. 1993;175(3):237–42.

69. Grunhagen T, Shirazi-Adl A, Fairbank JCT, Urban JPG. Intervertebral Disk Nutrition: A Review of Factors Influencing Concentrations of Nutrients and Metabolites. Orthopedic Clinics of North America. 2011 Oct;42(4):465–77.

70. 1980 Volvo award winner in basic science. Nutritional pathways of the intervertebral disc. An experimental study using hydrogen washout technique - PubMed [Internet]. [cited 2022 Apr 19]. Available from: https://pubmed.ncbi.nlm.nih.gov/7268543/

71. Van Der Werf M, Lezuo P, Maissen O, Van Donkelaar CC, Ito K. Inhibition of vertebral endplate perfusion results in decreased intervertebral disc intranuclear diffusive transport. J Anat. 2007 Dec;211(6):769.

72. Ashinsky BG, Bonnevie ED, Mandalapu SA, Pickup S, Wang C, Han L, et al. Intervertebral Disc Degeneration Is Associated With Aberrant Endplate Remodeling and Reduced Small Molecule Transport. J Bone Miner Res. 2020 Aug 1;35(8):1572–81.

73. Holm S, Nachemson A. Nutrition of the Intervertebral Disc: Acute Effects of Cigarette Smoking: An Experimental Animal Study. Ups J Med Sci. 1988 Jan 23;93(1):91–9.

74. Iwahashi M, Matsuzaki H, Tokuhashi Y, Wakabayashi K, Uematsu Y. Mechanism of intervertebral disc degeneration caused by nicotine in rabbits to explicate intervertebral disc disorders caused by smoking. Spine (Phila Pa 1976). 2002 Jul 1;27(13):1396–401.

75. Wallace AL, Wyatt BC, McCarthy D, Hughes SP. Humoral regulation of blood flow in the vertebral endplate. Spine (Phila Pa 1976). 1994;19(12):1324–8.

76. Gullbrand SE, Peterson J, Mastropolo R, Lawrence JP, Lopes L, Lotz J, et al. Drug-induced changes to the vertebral endplate vasculature affect transport into the intervertebral disc in vivo. J Orthop Res. 2014 Dec 1;32(12):1694–700.

77. Cunha C, Almeida CR, Almeida MI, Silva AM, Molinos M, Lamas S, et al. Systemic

Delivery of Bone Marrow Mesenchymal Stem Cells for In Situ Intervertebral Disc Regeneration. Stem Cells Transl Med. 2017 Mar 1;6(3):1029–39.

78. Walters R, Rahmat R, Fraser R, Moore R. Preventing and treating discitis: cephazolin penetration in ovine lumbar intervertebral disc. European Spine Journal. 2006 Sep;15(9):1397.

79. Urban JPGG, Roberts S. Degeneration of the intervertebral disc. Arthritis Res Ther. 2003;5(3):120–30.

80. Alini M, Eisenstein SM, Ito K, Little C, Kettler AA, Masuda K, et al. Are animal models useful for studying human disc disorders/degeneration? European Spine Journal. 2008 Jan 14;17(1):2–19.

81. Daly C, Ghosh P, Jenkin G, Oehme D, Goldschlager T. A Review of Animal Models of Intervertebral Disc Degeneration: Pathophysiology, Regeneration, and Translation to the Clinic. Biomed Res Int. 2016;2016:1–14.

82. Zhang W, Nie L, Wang Y, Wang X ping, Zhao H, Dongol S, et al. CCL20 Secretion from the Nucleus Pulposus Improves the Recruitment of CCR6-Expressing Th17 Cells to Degenerated IVD Tissues. PLoS One. 2013 Jun 18;8(6):e66286.

83. Nakazawa KR, Walter BA, Laudier DM, Krishnamoorthy D, Mosley GE, Spiller KL, et al. Accumulation and localization of macrophage phenotypes with human intervertebral disc degeneration. The Spine Journal. 2018 Feb 1;18(2):343–56.

84. Wiet MG, Piscioneri A, Khan SN, Ballinger MN, Hoyland JA, Purmessur D. Mast Cell-Intervertebral disc cell interactions regulate inflammation, catabolism and angiogenesis in Discogenic Back Pain. Sci Rep. 2017 Dec 2;7(1):12492.

85. Peng B, Hao J, Hou S, Wu W, Jiang D, Fu X, et al. Possible pathogenesis of painful

intervertebral disc degeneration. Spine (Phila Pa 1976). 2006 Mar;31(5):560–6.

86. Ye F, Lyu F, Wang H, Zheng Z. The involvement of immune system in intervertebral disc herniation and degeneration. JOR Spine. 2022 Mar 15;5(1).

87. Gorth DJ, Shapiro IM, Risbud M V. Transgenic mice overexpressing human TNF-α experience early onset spontaneous intervertebral disc herniation in the absence of overt degeneration. Cell Death Dis. 2019 Jan 18;10(1):7.

88. Jin L, Xiao L, Ding M, Pan A, Balian G, Sung SSJ, et al. Heterogeneous macrophages contribute to the pathology of disc herniation induced radiculopathy. Spine Journal. 2022;22(4):677–89.

89. Kawakubo A, Uchida K, Miyagi M, Nakawaki M, Satoh M, Sekiguchi H, et al. Investigation of resident and recruited macrophages following disc injury in mice. Journal of Orthopaedic Research®. 2020 Aug 1;38(8):1703–9.

90. Lee S, Millecamps M, Foster DZ, Stone LS. Long-term histological analysis of innervation and macrophage infiltration in a mouse model of intervertebral disc injury–induced low back pain. Journal of Orthopaedic Research. 2020 Jun 25;38(6):1238–47.

91. Mahmoud M, Kokozidou M, Auffarth A, Schulze-Tanzil G. The Relationship between Diabetes Mellitus Type II and Intervertebral Disc Degeneration in Diabetic Rodent Models: A Systematic and Comprehensive Review. Cells. 2020 Sep 29;9(10).

92. Ruiz-Fernández C, Francisco V, Pino J, Mera A, González-Gay MA, Gómez R, et al. Molecular relationships among obesity, inflammation and intervertebral disc degeneration: Are adipokines the common link? Int J Mol Sci. 2019 Apr 2;20(8).

93. Natelson DM, Lai A, Krishnamoorthy D, Hoy RC, Iatridis JC, Illien-Jünger S. Leptin signaling and the intervertebral disc: Sex dependent effects of leptin receptor deficiency and

Western diet on the spine in a type 2 diabetes mouse model. PLoS One. 2020 May 1;15(5):e0227527.

94. Lintz M, Walk RE, Tang SY, Bonassar LJ. The degenerative impact of hyperglycemia on the structure and mechanics of developing murine intervertebral discs. JOR Spine. 2022 Mar 23;5(1).

95. Fields AJ, Berg-Johansen B, Metz LN, Miller S, La B, Liebenberg EC, et al. Alterations in intervertebral disc composition, matrix homeostasis and biomechanical behavior in the UCD-T2DM rat model of type 2 diabetes. J Orthop Res. 2015 May 1;33(5):738–46.

96. Svenja IJ, Young L, Sheeraz AQ, Andrew CH, Weijing C, Helen V, et al. Chronic ingestion of advanced glycation end products induces degenerative spinal changes and hypertrophy in aging pre-diabetic mice. PLoS One. 2015 Feb 10;10(2).

97. Illien-Junger S, Grosjean F, Laudier DM, Vlassara H, Striker GE, Iatridis JC. Combined Anti-Inflammatory and Anti-AGE Drug Treatments Have a Protective Effect on Intervertebral Discs in Mice with Diabetes. PLoS One. 2013 May 17;8(5):e64302.

98. Tang SN, Bonilla AF, Chahine NO, Colbath AC, Easley JT, Grad S, et al. Controversies in spine research: Organ culture versus in vivo models for studies of the intervertebral disc. Vol. 5, JOR Spine. John Wiley and Sons Inc; 2022.

99. Xie L, Zhao Z, Chen Z, Ma X, Xia X, Wang H, et al. Melatonin Alleviates Radiculopathy Against Apoptosis and NLRP3 Inflammasomes Via the Parkin-Mediated Mitophagy Pathway. Spine (Phila Pa 1976). 2021 Aug 1;46(16):E859–68.

100. Huang SJ, Yan JQ, Luo H, Zhou LY, Luo JG. IL-33/ST2 signaling contributes to radicular pain by modulating MAPK and NF-KB activation and inflammatory mediator expression in the spinal cord in rat models of noncompressive lumber disk herniation. J

Neuroinflammation. 2018 Jan 12;15(1):1–12.

101. Huang X, Wang W, Liu X, Xi Y, Yu J, Yang X, et al. Bone mesenchymal stem cells attenuate radicular pain by inhibiting microglial activation in a rat noncompressive disk herniation model. Cell Tissue Res. 2018 Oct 1;374(1):99–110.

102. Liu Y, Li J, Li H, Shang Y, Guo Y, Li Z, et al. AMP-Activated Protein Kinase Activation in Dorsal Root Ganglion Suppresses mTOR/p70S6K Signaling and Alleviates Painful Radiculopathies in Lumbar Disc Herniation Rat Model. Spine (Phila Pa 1976). 2019 Aug 1;44(15):E865–72.

103. Stover JD, Farhang N, Lawrence B, Bowles RD. Multiplex Epigenome Editing of Dorsal Root Ganglion Neuron Receptors Abolishes Redundant Interleukin 6, Tumor Necrosis Factor Alpha, and Interleukin 1β Signaling by the Degenerative Intervertebral Disc. Hum Gene Ther. 2019 Sep 1;30(9):1147–60.

104. Stover JD, Lawrence B, Bowles RD. Degenerative IVD conditioned media and acidic pH sensitize sensory neurons to cyclic tensile strain. J Orthop Res. 2021 Jun 1;39(6):1192–203.

105. Ma J, Stefanoska D, Grad S, Alini M, Peroglio M. Direct and Intervertebral DiscMediated Sensitization of Dorsal Root Ganglion Neurons by Hypoxia and Low pH. Neurospine. 2020 Mar 31;17(1):42–59.

106. Ma J, Stefanoska D, Stone LS, Hildebrand M, van Donkelaar CC, Zou X, et al. Hypoxic stress enhances extension and branching of dorsal root ganglion neuronal outgrowth. JOR Spine. 2020 Jun 1;3(2).

107. Carreon LY, Ito T, Yamada M, Uchiyama S, Takahashi HE. Neovascularization induced by anulus and its inhibition by cartilage endplate. Its role in disc absorption. Spine (Phila Pa 1976). 1997 Jul 1;22(13):1429–34.

108. Feng Z, Chen L, Hu X, Yang G, Chen Z, Wang Y. Vertebral Augmentation can Induce Early Signs of Degeneration in the Adjacent Intervertebral Disc: Evidence from a Rabbit Model. Spine (Phila Pa 1976). 2018;43(20):E1195–203.

109. Xiao ZF, He JB, Su GY, Chen MH, Hou Y, Chen SD, et al. Osteoporosis of the vertebra and osteochondral remodeling of the endplate causes intervertebral disc degeneration in ovariectomized mice. Arthritis Res Ther. 2018 Sep 10;20(1):207.

110. Samartzis D, Mok FPS, Karppinen J, Fong DYT, Luk KDK, Cheung KMC. Classification of Schmorl's nodes of the lumbar spine and association with disc degeneration: a large-scale population-based MRI study. Osteoarthritis Cartilage. 2016 Oct 1;24(10):1753–60.

111. Cinotti G, Rocca C Della, Romeo S, Vittur F, Toffanin R, Trasimeni G. Degenerative changes of porcine intervertebral disc induced by vertebral endplate injuries. Spine (Phila Pa 1976). 2005 Jan 15;30(2):174–80.

112. Kuga N, Kawabuchi M. Histology of intervertebral disc protrusion: an experimental study using an aged rat model. Spine (Phila Pa 1976). 2001;26(17).

113. Kim KW, Lim TH, Kim JG, Jeong ST, Masuda K, An HS. The origin of chondrocytes in the nucleus pulposus and histologic findings associated with the transition of a notochordal nucleus pulposus to a fibrocartilaginous nucleus pulposus in intact rabbit intervertebral discs. Spine (Phila Pa 1976). 2003 May 15;28(10):982–90.

114. Kim KW, Ha KY, Park JB, Woo YK, Chung HN, An HS. Expressions of membrane-type I matrix metalloproteinase, Ki-67 protein, and type II collagen by chondrocytes migrating from cartilage endplate into nucleus pulposus in rat intervertebral discs: a cartilage endplate-fracture model using an intervertebral disc organ culture. Spine (Phila Pa 1976). 2005;30(12):1373–8.

115. Au TYK, Lam TK, Peng Y, Wynn SL, Cheung KMC, Cheah KSE, et al. Transformation of resident notochord-descendent nucleus pulposus cells in mouse injury-induced fibrotic intervertebral discs. Aging Cell. 2020 Nov 1;19(11):e13254.

116. Xiong C jie, Huang B, Zhou Y, Cun Y ping, Liu L tao, Wang J, et al. Macrophage migration inhibitory factor inhibits the migration of cartilage end plate-derived stem cells by reacting with CD74. PLoS One. 2012 Aug 27;7(8).

117. Han SK, Lee Y, Hong JJ, Yeo HG, Seo J, Jeon CY, et al. In vivo study of paraspinal muscle weakness using botulinum toxin in one primate model. Clin Biomech (Bristol, Avon). 2018 Mar 1;53:1–6.

118. Administration USF and D. General Considerations for Animal Studies for Medical Devices [Internet]. 2015. Available from: https://www.fda.gov/regulatory-information/search-fda-guidance-documents/general-considerations-animal-studies-medical-devices

119. Hampshire VA, Gilbert SH. Refinement, Reduction, and Replacement (3R) Strategies in Preclinical Testing of Medical Devices. Toxicol Pathol. 2019 Apr 1;47(3):329–38.

120. Administration USF and D. Animal Rule Approvals [Internet]. 2002. Available from: https://www.fda.gov/drugs/nda-and-bla-approvals/animal-rule-approvals

121. Smolders LA, Kingma I, Bergknut N, Van Der Veen AJ, Dhert WJA, Hazewinkel HAW, et al. Biomechanical assessment of the effects of decompressive surgery in non-chondrodystrophic and chondrodystrophic canine multisegmented lumbar spines. European Spine Journal. 2012 Sep;21(9):1692.

122. Hay AN, Farrell K, Leeth CM, Lee K. Use of Genome Editing Techniques to Produce Transgenic Farm Animals. Adv Exp Med Biol. 2022;1354:279–97.

CHAPTER 2. OVINE MODELS OF INTERVERTEBRAL DISC DEGENERATION

2.1 Summary

The development of effective therapeutic strategies for intervertebral disc degeneration is a major focus of research worldwide. However, the translation of these therapies into clinical practice remains challenging due to the lack of an appropriate preclinical animal model that reliably tests their efficacy and safety. The study of the biological processes and potential treatments for IVDD necessitates such reliable animal models to bridge this critical gap between research and clinical application. Historically, both induced and spontaneous IVDD in small and large animal models have been utilized to study human spine disorders. While these models provide valuable insights, they also have inherent limitations. Recently, growing evidence has highlighted spontaneously occurring spine disorders in sheep as a highly translatable model, addressing many limitations of other animal or *in vitro* models. Sheep share critical cellular, anatomical, physiological, histological, and molecular similarities with humans concerning spinal disorders, making them particularly valuable for translational research and for meeting regulatory requirements for clinical translation. In this review, we outline the key features of IVDD that are shared between sheep and humans and examine the current ovine models, both spontaneous and induced, used to study IVDD. We also emphasize the critical role of these models in advancing our understanding of the disease mechanisms, diagnosis, prevention, and treatment. Ongoing efforts to refine these models and address their limitations will further enhance their value in developing effective strategies for managing IVDD in humans. This review covers the advantages, similarities, ethical considerations, spontaneous and induced methods, limitations, and future directions of ovine models in the study of intervertebral disc degeneration.

2.2 Introduction

Animal models have played an important role in the attempt to clarify how IVDD evolves over time to determine how structural, environmental, or biomechanical risk factors may initiate, promote, or otherwise regulate these degenerative changes (123). To investigate these degenerative changes, a plethora of animal models have been developed. Commonly these animal models are divided between small and large animal models. While mice, rats, and rabbits represent common choices among small animals, large animals like dogs, pigs, goats, and sheep are frequently employed (124). Nevertheless, given the complexity of human intervertebral disc degeneration, a perfect animal model does not exist (125). Additionally, the selection of an appropriate animal model depends on the research questions, but also need to considerate the size, similarities with the human intervertebral disc, absence of notochordal cells, biomechanical forces similar to the clinical condition, and ethical considerations (126).

The ovine spine emerges as a prominent model for studying IVDD due to its cellular, biomechanical, and anatomical similarities to the human spine (126–130). Like human, the ovine discs undergo chondroid metaplasia with skeletal maturation, with the consequently loss of their notochordal cell remnants (131). Despite its quadrupedal conformation, the ovine spine has been shown to exhibit significant biomechanical similarities to the human spine with intradiscal loads up to 3.5 Mpa (132,133). When testing the biomechanical range of motion of spines with implanted devices, the qualitative effects of the devices on range of motion have been shown to be very similar between human and sheep spines (134). The ovine species also aligns with humans in body weight, bone mineral composition, metabolic rate, and bone healing rates (135,136). Beyond these physiological similarities, ethical considerations further endorse the use of ovine models over non-human primate alternatives or companion animals. In this literature review, we seek to delineate

the key features of IVDD shared between sheep and humans, elucidate current ovine models of IVDD, and underscore the relevance of these models in advancing our understanding of disease mechanisms, diagnosis, prognosis, prevention, and treatment of intervertebral disc degeneration.

2.3 Advantages of the Ovine Model

2.3.1Anatomical and Physiological Similarities

The ovine intervertebral disc closely resembles the size and cellular phenotype of the human disc, making it a superior model compared to other animal models. Macroscopically, the ovine intervertebral disc exhibits a structure like the human disc, featuring an organized and well-defined AF, a discernible transition zone between the AF and a clearer, gelatinous NP (**Figure 1**). The most pronounced parallels in the principal dimensions of the sheep and human spine are predominantly evident in the thoracic and lumbar regions (137). However, the sheep cervical spine has been deemed a suitable model for cervical spine research, particularly supported by quantitative data, with the motion segment C3–C4 demonstrating the most reliability as a model for its human counterpart (138). These anatomical similarities observed between the spines of sheep and humans underscore the potential utility of sheep as a valuable comparative model for studying various aspects of spinal anatomy and function.

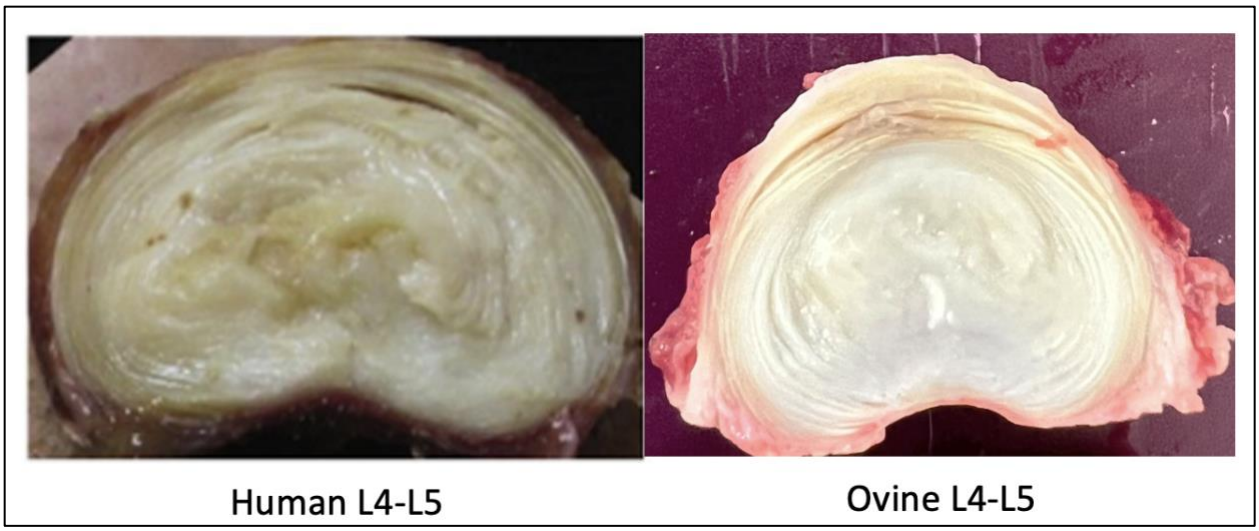

Figure 1. Representative images illustrate comparative axial gross views of lumbar intervertebral discs from human (Left Image) and ovine (Right Image) specimens, showcasing remarkable anatomical similarities. These visual comparisons accentuate shared structural features, enhancing our comprehension of the inter-species parallels in disc anatomy.

The lumbar IVD in adult humans is marked by relatively large size, susceptibility to biomechanical stresses influenced by bipedalism, and most notably the absence of notochordal cells (124). Notochordal cells are specialized cells that form the notochord, a temporary, rod-like structure present in the embryos of vertebrate animals (139). The notochord serves as a structural support during early development and plays a crucial role in the patterning of the embryonic body (140). In the context of intervertebral discs, notochordal cells are initially present in the NP, the inner core of the disc (141). In many species, including humans, notochordal cells in the intervertebral discs undergo a process of differentiation of these type of cell as part of the natural aging and development process (142,143). The persistent existence of notochordal cells is crucial, as they significantly influence processes into the intervertebral disc, including proteoglycan metabolism, hyaluronan production, and potential contributions to progenitor cell function (124). In adulthood, the intervertebral discs lose these notochordal cells, and this loss is associated with changes in the disc structure and function. Therefore, whether notochordal cells are present in IVDs

could indicate some limitations with animal models used to research IVD studies which unlike humans contain abundant notochordal cell populations and gelatinous NPs late into IVD maturation (144,145).

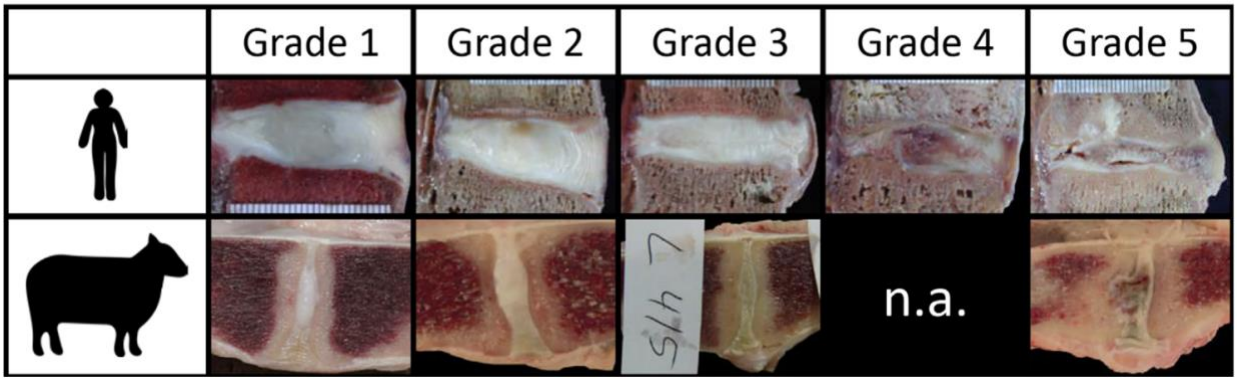

Figure 2. Representative images present comparative sagittal views of lumbar intervertebral discs from human (first row) and ovine (second row) specimens, showcasing notable anatomical similarities. These visual comparisons emphasize shared structural features, enhancing our understanding of interspecies parallels in gross disc anatomy. Image modified from Lee et al (146).

The lumbar IVD in adult humans is marked by relatively large size, susceptibility to biomechanical stresses influenced by bipedalism, and most notably the early differentiation of notochordal cells (124). Notochordal cells are specialized cells that form the notochord, a temporary, rod-like structure present in the embryos of vertebrate animals (139). These notochordal cells are present in the NP, the inner core of the IVDs since embryonic development (140,141). Within the IVD, these cells proliferate and produce a gelatinous, glycosaminoglycan-rich extracellular matrix, which divides the original cell mass into a network of small cell clusters, acting therefore as the embryonic precursors to all cells found within the NP of the mature IVD (147). Beyond their developmental features, notochord cells are crucial for promoting ECM synthesis and regulating cellular activity in the NP, playing a key part in maintaining normal IVDs homeostasis (148,149).

In many species, including humans, these notochordal cells in the IVDs undergo a process of cellular differentiation as part of the natural aging and development process, with the eventual

replacement of the notochord cells by a chondrocyte phenotype cells in the NP (140,142,143,150). Although the exact mechanisms driving the differentiation of notochordal cells are still under investigation, both molecular and physical factors have been proposed as contributors to the transition of these cells from a notochordal to a chondrocyte-like phenotype in the NP (140,151,152).

Studies have demonstrated that the reduction or loss of notochordal cells is a critical trigger in the onset of IDD, underscoring their essential role in maintaining disc health. (131,152,153). Specifically, evidence suggest that the loss of this type of cells mainly because their differentiation of the chondrocyte phenotype cells in the NP leads to an imbalance in homeostasis into the IVDs and the subsequent degradation of the ECM (154,155), both of which are critical factors contributing to IDD, suggesting that these cells are required for the maintenance of the NP (154,156).

Whether notochordal cells are present in IVDs could indicate some limitations with animal models used to research IVD studies which unlike humans contain abundant notochordal cell populations and gelatinous NPs late into IVD maturation (144,145). Sheep are among the few animals to also lose the notochordal cells rapidly following birth (141,144,157,158). Similar to humans during adolescence, sheep undergo through a differentiation process of their notochord cells linked to skeletal maturation (131,159). Therefore, ovine models may have greater relevance following this differentiation of notochordal cells than those animal models that conserve these types of cells (145). The similarities in the process of differentiation of notochordal cells in ovine models presents a clear advantage, closely mirroring clinical conditions observed in human patients with IVDD (131). This similarity enhances the relevance of these models, particularly in evaluating potential cellular therapeutic interventions for disc-related conditions.

Sheep also have similarities with humans in body weight and bone mineral composition (135). For instance, adult sheep present the advantage of possessing body weights (60-100 kg)

more akin to humans and possessing long bones with dimensions suitable for the implantation of human implants and prostheses, a feature not feasible in smaller species (135). In addition, research examining bone ingrowth into porous implants implanted into the distal femur of sheep, a weight-bearing model, indicates that sheep and humans exhibit a similar pattern of bone ingrowth into porous implants over time (160–162).

2.3.2 Biomechanical Similarities

Despite its quadrupedal position, sheep experience mechanical stresses very similar to those of the human spine. Biomechanical assessments and intradiscal pressure evaluation have demonstrated favorable comparability between ovine and human lumbar spines in terms of overall disc shape and most biomechanical parameters, including range of motion, neutral zone, and load distribution between the intervertebral disc (163). Similarly, hydration patterns between human and ovine discs over time were observed, shedding light on the importance of disc hydration and its impact on stiffness under various loading conditions, findings reinforcing the utility of the ovine model for disc research (164). Additionally, when testing the biomechanical range of motion of spines with implanted devices, the qualitative effects of the devices have been shown to be very similar between human and sheep spines (134). These biomechanical changes are also age-related comparable. For instance, research indicates that the intra-lamellar matrix within individual AF lamellae of sheep is weaker and more compliant in middle-aged and elderly ovine IVDs compared to young IVDs, mirroring observations in humans (163). Considering the relevance of the ovine model to understand spine conditions even cutting-edge technological advancements such as computational finite element models have been developed to validate both sheep cervical and lumbar spine models. These studies indicate that despite geometric variations, the human and ovine

discs are functionally adapted to generate similar internal stresses (163,165).

2.3.3 Ethical Considerations

Preclinical animal models have historically played a pivotal role in investigating the disc as they represent a critical surrogate in clinical translation with the purpose of furthering our understanding about the pathophysiology, treatment and prevention of IVDD. Successful translation of these preclinical studies necessitates the identification of suitable animal models that replicate the human condition to be studied. The sheep model, in particular, is being increasingly applied to the field of biomedical research and is arguably one of the most influential models of human organ systems (125,163). Its utility extends across cardiovascular, orthopedic, reproductive, gene therapy, and neurodegenerative research domains (166). Ovine models are also more widely accepted, from an ethical perspective, than non-human primate models such as baboon and macaque models due to major ethical and practical considerations (e.g., expense and housing) (167). The growing utilization of sheep as animal models for orthopedic research is partly due to ethical Concerns and public apprehension regarding the use of companion animals for medical research. Furthermore, their availability as animals for consumption makes sheep less ethically objectionable compared to companion animals or non-human primates, contributing to their growing popularity in orthopedic research. Unlike companion animals or non-human primates, sheep have less emotional attachment from owners or caregivers, further facilitating their use as research subjects (135,163).

2.4 Methods for Inducing IVDD in Ovine Models

Numerous methods have been devised to assess and induce IVDD in sheep, positioned as a

one of the most common large animal models to gauge clinical conditions, potential targets, and therapeutic approaches. It is crucial to emphasize that while these methods aim to mimic human IVDD by instigating a degenerative sequence through acute injuries, none of these approaches can perfectly replicate a condition identical to human disorders. These *in vivo* approaches can be broadly categorized into three groups: Spontaneous, Damage-induced, and Mechanical models. Additionally*, in vitro* methods have proven valuable in advancing our understanding of the pathophysiology of IVDD. Each model contributes uniquely to our understanding of IVDD in sheep and other large animal models, offering valuable insights for translational research and therapeutic advancements in the context of human degenerative disc diseases.

2.4.1 Spontaneous Models

Aging is considered the most relevant factor associated to the occurrence of IVDD, and this is not different in the ovine specie. Spontaneous age-related changes indicative of IVDD has been observed in sheep as early as 2 years of age through various imaging modalities such as x-ray, computed tomography (CT), and magnetic resonance imaging (MRI), revealing signs of IVDD (168). The alignment of these imaging findings with histologic evaluations further confirmed that skeletally mature sheep, aged four years and above, exhibit signs of IVDD compared to their younger counterparts (169). Studies performed by our group have similarly revealed that measurements of bone volume, osteoid volume, and mineral apposition rate old ewes are comparable to those observed in men and post-menopausal women in their 6-7th decade of life (170). Therefore, considering that most animal models require an experimentally induced or injury to the IVD to induce IVDD; the spontaneous age-related degeneration observed in sheep mirrors the natural progression of IVDD in humans, without the need for additional intervention or trauma,

making it an ideal model for studying this degenerative condition.

Figure 3. Photograph of an ovine lumbar intervertebral disc from an elderly sheep (~10 years old), exhibiting characteristic features of disc degeneration, including evident dehydration and discoloration of the nucleus pulposus.

2.4.2 Damage-induced Models

Needle Puncture

The needle puncture model involves puncturing the AF, the outer structure of the IVDs, using various types and sizes of needles. While this model is predominantly used in small animals, it has also been established in larger animal models, including sheep (171). Induction of IVDD by needle puncture model is relatively straightforward, entailing the insertion of a needle into the AF, with or without disrupting the NP, leading to depressurization and/or AF damage, depending primarily on the needle size (172). Studies have shown that when sheep discs are punctured with a 27-gauge needle, which accounts for approximately 10% of the disc height in the ovine lumbar disc, were no significant differences in axial properties compared to intact discs, except for a

roughly 15% change in the torque range (173). Researchers have observed that NP migration can occur through an 18-gauge needle puncture, suggesting that the likelihood of acute herniation increases with the needle diameter (174). However, other studies have reported that needle puncture, regardless of needle size, has minimal or no significant impact on inducing disc degeneration (175). This discrepancy highlights the need for further investigation into the role of needle size in disc degeneration models.

The insertion depth can be precisely determined through radiographic imaging or by observing the length of the emerged needle. This method is typically approached surgically, is commonly attempted through a lateral or transpedicular approach under fluoroscopic guidance to ensure accurate needle placement within the disc space (176,177). CT-guided puncture has been demonstrated in sheep cadavers as a straightforward procedure, allowing for precise positioning of the needle into the lumbo-sacral disc (178,179). This method could prove valuable in training less experienced surgeons or radiologists for disc injections but could result in increased radiation exposure. One of the main limitations of this method is that needle punctured will disrupt the AF, but it will not necessarily cause herniation of the NP material due to the different and more viscous consistency of the NP, and the fast-healing response of the AF. Nonetheless, development of even more minimally invasive approaches is anticipated to reduce healing time and minimize inflammatory factors inherent to the surgical process, in addition to the induced damage to the disc.

Induced Chemical

Chemonucleolysis, involving the chemical digestion of the NP, originally served as a non-surgical treatment to digest the herniated NP tissue (180). Nowadays, this method is used to induce

IVDD in several animal models (181). Several chemical agents have been investigated as potential initiators of the pathophysiological progression of disc degeneration, with some of the most commonly studied agents including chymopapain, chondroitinase ABC (C-ABC), and 5-bromodeoxyuridine (182–184).

The use of chymopapain, was first reported clinically as a treatment for disc protrusion (182). This proteolytic enzyme derived from the papaya latex, digests disc glycosaminoglycan chains within the disc and therefore induced IVDD through the loss of disc height and alteration of its biomechanical properties (158). This enzyme degrades intervertebral disc proteoglycans in a manner that is dependent on the dosage, with higher doses even inducing destruction of the AF in small animal models (185,186). In sheep, the first report of its use was in 1986 evidencing at the moment that chymopapain had a bactericidal effect (187). Subsequent studies provided further evidence regarding the ease of removing the NP following the administration of chymopapain to ovine discs (188).

Chondroitinase ABC is an enzyme that digests chondroitin sulfate isomers. Injecting the enzyme C-ABC induces degradation of the polysaccharide chains within the proteoglycan, with the consequent disc height loss and alteration of biomechanical stability (181). Similar to chymopapain, studies using C-ABC have demonstrated a dose-related reduction in intradiscal pressure when C-ABC is administered (189,190).

Another agent to in induce chemonucleolysis is 5-bromodeoxyuridine (BrdU). BrdU is known for consistently triggering genome instability, leading to a senescence-like phenomenon in mammalian cells, irrespective of cell types or species (191). It is believed that employing an animal model that integrates age-related alterations in disc cells presents advantages compared to more invasive degenerative models that directly damage the matrix of disc tissue. In the specific case

for sheep, injection of BrdU resulted loss of T2- weighted signal intensity on MRI, decrease in disc height, and loss of the normal architecture and cell density after 14-weeks (192).

As mentioned earlier, the injection of these enzymes results mostly in the loss of proteoglycan, a crucial element in the clinically observed pathophysiological process of IVDD (193). Nonetheless, there is controversy about the models using chemical components to induce IVDD, because just the placement of the needle to inject the chemical agent would be causing degeneration basically through a needle puncture method. It has been demonstrated that techniques employing small-gauge needles to puncture the IVD led to an expedited progression of IVDD, herniation, diminished disc height and signal, along with the emergence of reactive endplate changes (194). Therefore, prudent evaluation of the risks and benefits is essential when considering procedures involving any type of disc injection.

Induced Physical

The deliberate surgical injury to the intervertebral disc is a well-established approach for inducing IVDD. This injury can be directed towards the endplate, the AF, or both the AF and NP.

Endplate Damage

Studies have shown that the vertebral endplate serves as the primary pathway for intravascular solute transport into the NP of intervertebral discs (195). Therefore, impeding endplate perfusion can result in restricted solute transport into the intranuclear tissue of the disc and lead to IVDD. After nucleotomy through the transpedicular approach across the endplates it is observed that mechanical nucleotomy facilitates the formation of a cavity within IVD, preserving the integrity of the AF (196). This preservation has allowed the injection of different

volumes of hydrogels, scaffolds, and different tissue engineering constructs, facilitating preclinical testing (171,196). However, in addition to inducing damage to the endplates, this transpedicular approach can lead to neurological impairment and leakage of injected materials into the systemic circulation (197). Complete consideration of these adverse effects is imperative before proceeding with this surgical approach.

Annular defect /annulotomy

Annular lesions have been demonstrated to cause immediate changes to the mechanics of the ovine IVD (198). Among the most common type of lesions are the needle puncture, stabs or Slid incisions, (also known as cruciate and box/window defects). These type of lesions to AF have been compared in mature sheep showing the *in vivo* and ex vivo advantages and limitations for each method (198,199). For instance, cruciate-style AF defects with removal of NP material has been recently used to evaluated whether experimental, injectable, and bioactive biomaterials could slow IVD degeneration (200). Induced damage to the AF in ovine discs has been also performed by concentric tears using injection of saline solution into the AF. These concentric tears of the AF induce mechanical changes by decreasing the stiffness of the disc (201). Interestingly, studies inducing annulotomy have shown that while the outer annulus displayed some healing capacity, the initial defect caused deformation and bulging of collagen bundles, ultimately resulting in tear extension towards the inner annulus and complete failure (191). In our experience, AF defects trend towards natural healing and then a longer inflammatory process causes a fibrotic scare that could lead to bone formation causing fusion of the disc level (data nonpublished).

Overall, these defects induced to the exterior lateral layers of the disc aim to recreate a model of disc herniation. However, one important consideration is that even aggressive removal

of AF does not result in disc herniation (199). According to the definition of disc herniation, a displacement of at least 25% of the disc circumference is required to classify it as a herniation (202). Unfortunately, this level of NP displacement has not been demonstrated in sheep. Therefore, careful consideration needs to be addressed in the selection of the sheep as a disc herniation model.

Nucleotomy

In ovine models, a combination of methods, such as the transpedicular approach and chemonucleolysis, is often utilized to achieve complete nucleotomy (203,204). Nucleotomy, whether partial or total depending on the research question or therapeutic intervention being tested, involves the surgical removal or partial excision of the NP (205). By creating a focal defect within the intervertebral disc, nucleotomy disrupts the structural integrity of the disc, resulting in altered biomechanics, tissue remodeling, and degenerative changes reminiscent of human disc degeneration. Studies employing nucleotomy in ovine models have yielded valuable insights into the pathophysiology of disc degeneration, shedding light on the role of mechanical loading, biochemical changes, and inflammatory responses in disease progression. Notably, the establishment of a model with an intact AF has revealed that mechanical nucleotomy results in a more reproducible and less destructive cavity within the NP (196). This facilitates the creation of a cavity in the IVD, allowing for the injection of consistent volumes of hydrogel and tissue engineering constructs (204).

Mechanical Models

Alteration of spine kinematics in sheep has been utilized to induce IVDD, with the most common method being the stabilization of spinal motion segments. However, compression has also been reported, leading to a decrease in disc height and range of motion (206). Inducing

mechanical destabilization through annular incision has been shown to result in reduced disc height, an increase in the neutral zone in biomechanical testing, and depletion of proteoglycan and collagen. This method also leads to upregulation of collagen types I and II, aggrecan, versican, perlecan, matrix metalloproteinase 1 & 13, and ADAMTS-5 expression (129).

Mechanical immobilization of the ovine lumbar spine has been achieved via pedicle screw and rod implantation, keeping the annulus and endplates intact. Results indicate a reduction in disc height after 6 and 26-week of immobilization, with significant disc degeneration observed compared to the control group. Interestingly, no statistical difference was detected between the 6 and 26-week terms, suggesting that only 6 weeks are required to develop this model, with progressive degenerative changes in facet joints (207).

In vitro models

The organ culture system for ovine intervertebral discs, including the vertebral endplates, has been well established and provides a valuable model for investigating the effects of nutrition and mechanical loading on intact disc explants. This culture system maintains disc cells in their native three-dimensional environment under uniaxial diurnal loading for seven days. Studies have demonstrated that during this period, cell viability and glycosaminoglycan synthesis rates remain unchanged. However, the expression of catabolic genes is significantly upregulated, while the expression of anabolic genes tends to be downregulated (208). Another study showed *in vitro* the regulation of matrix metalloproteinase-2 (MMP-2) in ovine NP cells. These results also indicated that Transforming Growth Factor-beta 1 (TGF-beta 1) and Insulin-like Growth Factor-1 (IGF-I) decreased active MMP-2 levels. These findings shed light on the poor healing potential of dense, avascular tissues like the intervertebral disc (209).

IVD degeneration under various loading conditions have been extensively used *in vitro*

with the ovine discs to explore the mechanisms of structural failure. For instance, an *in vitro* evaluation of healthy mature ovine lumbar motion segments subjected to flexion and vibration loading (1300 ± 500 N) was conducted to simulate moderately severe physiological exposure. Microstructural analysis of the damaged discs revealed delamination and disruption of the inner and mid-AF layers, along with limited diffuse tracking of NP material (210).

Further *in vitro* studies using ovine lumbar spinal segments in a disc loading simulator investigated the impact of five different loading combinations. These studies demonstrated that such loading could lead to endplate junction failures and AF failures. The combination of flexion, lateral bending, axial rotation, and axial compression posed the highest risk for caudal endplate junction failures. Notably, herniation was not observed in any of the segments subjected to these loading combinations (211). In addition to mechanical loading studies, MR imaging has been used to evaluate relaxation times and to obtain detailed anatomic and dynamic information about the ovine lumbar intervertebral disc during uniaxial compression. This advanced imaging technique provides a thorough evaluation of disc structure and function under load, offering valuable insights into the behavior of intervertebral discs *in vitro* and advancing our understanding of their biomechanical properties (212). Similarly, MR T2 relaxation time analysis was used to evaluate the effects of advanced glycation end-products (AGEs) on *in vitro* disc hydration in ovine IVD. AGEs, are known to accumulate in intervertebral disc tissue with aging and degeneration (213). Results showed that increased AGEs reduced water content in a dose-dependent manner without affecting proteoglycan and collagen composition (214). Another *in vitro* study showed that ovine IVDs can be sustained in culture for up to 21 days under simulated physiological loading, both with sufficient and limited nutrition. When nutrition was restricted, cell viability dropped to 50%-60% within days and remained at this level throughout the 3-week period (215).

2.5 Pathological Changes Associated with IVDD in Sheep

Following induced degeneration in sheep IVDs, several histological, biochemical, and biomechanical changes are observed. These changes closely mimic human disc degeneration, confirming the similarities between species and highlighting the sheep a valuable model for studying IVD pathophysiology and evaluating potential treatments. Among the histological changes, the most relevant is the decreased cell density of NP, with an increased cell clustering, and presence of cell death (146). The NP also loses its gelatinous consistency and becomes more fibrous. For the **AF**, the clearest change is the disorganization of collagen fibers, presence of clefts, and fissures (216). Additionally, an increased vascular infiltration and inflammatory cell presence in the AF is observed. In the case of the e**ndplates**, an increased calcification and irregularities, with reduced cell viability has been shown (217).

Among the most common biochemical changes observed in IVDD in sheep are the alterations in proteoglycan, collagen, matrix metalloproteinases (MMPs), and inflammatory mediators. Changes in the proteoglycan content are mainly related to a significant reduction in proteoglycan levels, particularly aggrecan, leading to decreased water content (218,219). For collagen content, there is an increased level of collagen I and a decreased level of collagen II in the NP, reflecting fibrosis, and altered ratios of collagen types in the AF (220). Another change is the elevated levels of MMPs and other degradative enzymes, contributing to extracellular matrix breakdown (221). Similarly, increased production of pro-inflammatory cytokines such as IL-1β, TNF-α, and other inflammatory markers is noted (222,223).

In relation to humans with IDD, biomechanical changes observed in sheep are related to reduced disc height due to loss of proteoglycans and water, leading to a loss of disc turgor. These changes also lead to an increase *in stiffness* and decrease in elasticity, reducing the disc's ability to absorb and distribute loads (224). As a result, there is an alteration in the load distribution across the disc and adjacent vertebrae, potentially leading to increased stress on other spinal structures.

Table 1. Overview of Intervertebral Disc Degeneration changes in human and sheep.

	Description	
Histological Changes	**Nucleus Pulposus**	Reduction in cell density, increased fibrosis, and loss of gelatinous consistency.
	Annulus Fibrosus	Disorganized collagen fibers, annular tears, vascular ingrowth, and increased inflammation.
	Endplates	Endplate sclerosis, calcification, and reduced nutritional support due to impaired endplate function
Biochemical Changes	**Proteoglycan Content**	Reduction in proteoglycans, contributing to disc dehydration and reduced disc height.
	Collagen Content	Increase in collagen I and decrease in collagen II, reflecting fibrotic changes.
	Matrix Metalloproteinases	Elevated MMP activity contributing to extracellular matrix degradation.
	Inflammatory Mediators	Increase in inflammatory cytokines, contributing to pain and degeneration.
Biomechanical Changes	**Disc Height**	Reduction in disc height, leading to reduced intervertebral space and potential nerve compression.
	Stiffness and Elasticity	Increased stiffness, reduced flexibility, contributing to altered spinal mechanics.

	Load Distribution	Changes in load distribution, leading to increased stress on adjacent vertebrae and facet joints.

2.6 Evaluation of Potential Therapeutic Strategies for IVDD in the ovine model

Cell-Based Therapies

Research on cell-based therapies for IVDD is emerging, along with the interest in biological therapy to treat disc disease without reducing the mobility of the spinal motion segment (225). Efficacy of stem cell therapy, especially Mesenchymal stem cells (MSCs) are highly favored for their capacity to transform into disc cells and foster the production of crucial extracellular matrix elements. Bone marrow mesenchymal stromal/stem cells, adipose tissue derived stem cells, synovial stem cells, muscle-derived stem cells, olfactory neural stem cells, induced pluripotent stem cells, hematopoietic stem cells, disc stem cells, and embryonic stem cells have been studied as a treatment for IVDD (226). Research has highlighted the multifaceted benefits of MSCs, including inflammation reduction, facilitation of regeneration, and enhancement of disc height and moisture content. Over the last decade, regenerative medicine approaches for IVDD, employing injections of IVD cells, chondrocytes, or stem cells, have undergone extensive investigation across various animal models of induced IVD degeneration (227). These endeavors have advanced to clinical trials aimed at treating a spectrum of spinal conditions.

One important cell-based therapy has been the injection of notochordal cells or efforts to maintain them in a healthy IVD (228). In particular, *in vitro* studies have shown the potential benefits of cell-derived matrix and cell-conditioned medium in supporting notochordal cell differentiation and prolonging their survival in the NP(229,230) . This is crucial, as the loss of

these cells is associated with the onset of degenerative processes in the IVD (139). Research has demonstrated that notochordal cell-conditioned medium can stimulate matrix production by NP cells in the NP environment (231,232). Similarly, notochordal cell-derived matrix from animals has been shown to promote glycosaminoglycan and matrix production in NP cells (233). However, as mentioned earlier, these therapies have mainly been validated *in vitro*, and further *in vivo* validation is required. Additionally, as previously noted, the injection of any substance into the disc necessitates puncturing the IVD structure, which could disrupt tissue homeostasis and contribute to IVDD.

Despite promising initial outcomes demonstrating the positive impacts of cell injection methods on IVD regeneration, comprehensive foundational studies on IVD cells and their microenvironment have revealed a challenge: transplanted cells struggle to survive and acclimate within the avascular setting of the IVD. Key obstacles include ensuring the viability of transplanted cells, their seamless integration into the existing disc architecture, and the creation of a conducive regenerative milieu amidst the harsh characteristic conditions of degenerated discs (234). Moreover, addressing concerns regarding immunogenicity and ensuring sustained functionality over the long term pose significant hurdles in the pursuit of effective stem cell therapy for IVD degeneration.

Gene Therapy

Gene therapy aims to modify the expression of specific genes involved in disc degeneration, such as those coding for anti-inflammatory cytokines or anabolic growth factors (e.g., TGF-β, BMPs). Preclinical studies have shown that gene therapy can enhance the production of extracellular matrix components and inhibit inflammatory pathways, indicating potential for

reversing or halting degeneration. However, key challenges include developing safe and efficient delivery methods, managing potential off-target effects, and ensuring long-term regulation of gene expression.

Tissue Engineering Approaches

Biomaterial scaffolds provide a supportive structure for cell attachment and growth. These can be combined with cells and growth factors to promote disc regeneration. Research has demonstrated that hydrogels, natural polymers, and synthetic scaffolds can support cell viability, encourage matrix production, and restore disc height in animal models (235). However, challenges in evaluating scaffold-based regeneration include ensuring mechanical strength, biocompatibility, and the ability to integrate with surrounding tissue, which are ongoing areas of research. Additionally, the complex structure of the IVDs makes it difficult to fully replicate its biomechanical properties.

A detailed examination of annulus-endplate integration in ovine lumbar discs conducted across various maturity stages, has unveiled a persistent branching mechanism within AF bundles (236). These findings have prompted the consideration of using the ovine endplate disc, characterized by its physiological curvature, as a valuable model for evaluating biomechanical prostheses designed for human cervical disc replacement (237). Despite notable changes in endplate morphology over time, the intricate fibril-level integration of sub-bundles into the cartilaginous endplate tissue indicates a dynamic maturation process that influences the microstructural characteristics of annulus-endplate integration in the intervertebral disc (238,239).

Cell-based therapies are promising for regeneration but require improvements in cell survival and integration. Gene therapy is effective in modulating disease processes at the molecular

level but needs refinement in delivery and safety. Tissue engineering offers structural support and regeneration potential but faces challenges in replicating the intervertebral disc's complex mechanics. Combining these strategies might offer the most comprehensive solution to address the multifaceted nature of IVD degeneration.

2.7 Limitations of the Ovine Model

There is a scientific consensus which concluded that all models appeared to lack translatability and justification for the selection of one model over another (125). The sheer fact that a plethora of models exists accentuates the fact that no single model is better than another at this time. Therefore, the selection of a model needs to be addressed considering the research question that wants to be solved (98). In that sense, sheep models could be not the most appropriate model for the evaluations of behavioral or pain reaction during IVDD. Although some studies could study the neurological changes specially in dorsal root ganglion of animals with IVDD, ovine are very rustic animals who can hide any signs of pain (240). This makes difficult to make any type of clinical or even mechanical evaluation to determinate pain sensations.

Where a larger animal may be desired, husbandry may be prohibitive, particularly if a high number of animals are required for a well powered sample study. Availability is also important, making small animals such as rodents an attractive option due to ease of breeding and thus their improved attain- ability, study reproducibility, relatively quick maturation and aging, and lower maintenance costs. Therefore, funding considerations can influence the choice of model to be utilized and becomes an important aspect when planning a study that features a preclinical animal model (241).

Sheep offer several advantages as a model for IDD research. They are more acceptable to animal ethics committees compared to companion animals and are readily available, reasonably outbred, and less expensive to purchase than other large species. Additionally, sheep are easy to manage and handle during surgical procedures. Their long bones are suitable for implant systems, making them excellent for studying osteoporosis. Moreover, sheep do not require environmental enrichment as they thrive in their natural pastures, providing increased clinical translation and more accurate indication of dosage, drug distribution, and safety of potential therapies. Clinically relevant technologies like MRI, CT, and PET scans, as well as clinical equipment such as anesthesia, physiological monitoring, and surgical tools, can be used with sheep. However, there are also disadvantages, including higher ethical considerations compared to small animals, higher maintenance costs, and the need for larger facilities. Additionally, unlike rodents, there is no standardized behavioral testing protocol for sheep (242).

2.8 Future Directions of ovine models of IVDD

Recent advancements in sheep models of disc degeneration hold promise for furthering our understanding of this complex condition and facilitating the development of novel therapeutic strategies. One avenue of exploration involves the utilization of genetically modified sheep, offering researchers the opportunity to study specific genetic factors implicated in disc degeneration. By introducing targeted genetic modifications, such as gene knockouts or overexpression, researchers can elucidate the role of individual genes or pathways in the pathogenesis of disc degeneration, paving the way for targeted interventions. For example, employing genetic modifications using CRISPR/Cas9 technology could enable the spontaneous

simulation of disc degeneration by activating senescence pathways. Looking ahead, the introduction of inducible Cas9 in the intervertebral discs of sheep may establish programmable translational models for testing therapeutic interventions.

One of the most significant limitations of the ovine model of IDD is the measurement of pain. Due to their stoic nature, clinical signs of pain are difficult to recognize. However, recent efforts have been made to subjectively measure pain behavior in sheep. The Grimace scale is a system used to identify pain through facial expressions in several animal species (243). A specific ovine Grimace scale has been established and applied to interpret sheep facial expressions as a response to pain and distress following unilateral tibial osteotomy (244). Further validation of this system is required for its use in ovine models of IDD. Another possible technique to assess pain related to IDD in sheep could be the analysis of pain mechanisms or anatomical structures involved in pain transmission, such as the dorsal root ganglion These neuronal ganglia house the cell bodies of sensory nerves, which transmit pain signals to the spinal cord. Recently, the functional characterization of DRG in sheep was performed to evaluate peripheral sensitization following osteochondral defects (240). Further investigation into these ganglia is needed to determine specific changes associated with IDD in the ovine model.

Additionally, the refinement of surgical techniques in sheep models has contributed to more accurate and reproducible induction of disc degeneration. Innovations such as minimally invasive approaches, advanced imaging guidance, and tissue engineering technologies enable precise manipulation of the intervertebral disc, mimicking clinical scenarios more closely. These advancements not only enhance the reliability and validity of sheep models but also facilitate the translation of findings to clinical practice. By leveraging genetic manipulation and refined surgical

techniques, sheep models of disc degeneration hold immense potential for advancing our understanding of disease mechanisms and accelerating the development of effective therapies.

2.9 Conclusion

The ovine model for IVDD exhibits several favorable traits as an ideal intervertebral disc model, including the absence of notochordal cells, comparable body mass to humans, and exposure to similar biomechanical forces affecting the intervertebral disc. A significant potential critique of this model relates to the quadrupedal nature of sheep, as previous biomechanical studies have indicated substantial comparability in many biomechanical properties between ovine and human lumbar spines, despite the quadrupedal/bipedal distinction (245).

When choosing a preclinical model for spine research, it is critical to consider that biologic and biomechanical components of the healthy intervertebral disc and DDD are inextricably linked. Furthermore, it is important to acknowledge and address limitations of ovine models including subtle differences in biomechanics, genetics, physiology, and lifestyles. As such, comprehensive outcome assessments with correlations among metrics are important for validity and translatability. Taken together, preclinical studies using the spontaneous aging, induced in vivo, and in vitro ovine models of ovine models can guide targeted research toward developing valid and effective tools for early diagnosis, prevention, and treatments both for veterinary and human patients.

2.10 References

1. Lotz JC. Animal Models of Intervertebral Disc Degeneration. Spine (Phila Pa 1976). 2004 Dec 1;29(23):2742–50.

2. Daly C, Ghosh P, Jenkin G, Oehme D, Goldschlager T. A Review of Animal Models of Intervertebral Disc Degeneration: Pathophysiology, Regeneration, and Translation to the Clinic. Biomed Res Int. 2016;2016:1–14.

3. Reitmaier S, Graichen F, Shirazi-Adl A, Schmidt H. Separate the Sheep from the Goats: Use and Limitations of Large Animal Models in Intervertebral Disc Research. Journal of Bone and Joint Surgery - American Volume. 2017;99(19):e102.

4. Lim KZ, Daly CD, Ghosh P, Jenkin G, Oehme D, Cooper-White J, et al. Ovine Lumbar Intervertebral Disc Degeneration Model Utilizing a Lateral Retroperitoneal Drill Bit Injury. J Vis Exp. 2017;(123):55753.

5. Melrose J, Burkhardt D, Taylor TKF, Dillon CT, Read R, Cake M, et al. Calcification in the ovine intervertebral disc: A model of hydroxyapatite deposition disease. European Spine Journal. 2009 Apr;18(4):479–89.

6. Shu C, Hughes C, Smith SM, Smith MM, Hayes A, Caterson B, et al. The ovine newborn and human foetal intervertebral disc contain perlecan and aggrecan variably substituted with native 7D4 CS sulphation motif: Spatiotemporal immunolocalisation and co-distribution with Notch-1 in the human foetal disc. Glycoconj J. 2013 Oct;30(7):717–25.

7. Melrose J, Shu C, Young C, Ho R, Smith MM, Young AA, et al. Mechanical destabilization induced by controlled annular incision of the intervertebral disc dysregulates metalloproteinase expression and induces disc degeneration. Spine (Phila Pa 1976). 2012 Jan 1;37(1):18–25.

8. Schollum ML, Appleyard RC, Little CB, Melrose J. A detailed microscopic examination of alterations in normal anular structure induced by mechanical destabilization in an ovine model of disc degeneration. Spine (Phila Pa 1976). 2010 Oct 15;35(22):1965–73.

9. Hunter CJ, Matyas JR, Duncan NA. Cytomorphology of notochordal and chondrocytic cells from the nucleus pulposus: a species comparison. J. Anat. 2004.

10. Wilke HJ, Kettler A, Claes LE. Are Sheep Spines a Valid Biomechanical Model for Human Spines? Spine (Phila Pa 1976). 1997 Oct 15;22(20):2365–74.

11. Reitmaier S, Schmidt H, Ihler R, Kocak T, Graf N, Ignatius A, et al. Preliminary Investigations on Intradiscal Pressures during Daily Activities: An In Vivo Study Using the Merino Sheep. PLoS One. 2013 Jul 24;8(7).

12. Kettler A, Liakos L, Haegele B, Wilke HJ. Are the spines of calf, pig and sheep suitable models for pre-clinical implant tests? European Spine Journal. 2007;16(12):2186–92.

13. Pearce AI, Richards RG, Milz S, Schneider E, Pearce SG. Animal models for implant biomaterial research in bone: A review. Vol. 13, European Cells and Materials. AO Research Institute Davos; 2007. p. 1–10.

14. den Boer FC, Patka P, Bakker FC, Wippermann BW, van Lingen A, Vink GQ, et al. New segmental long bone defect model in sheep: quantitative analysis of healing with dual energy x-ray absorptiometry. J Orthop Res. 1999 Sep;17(5):654–60.

15. Wilke HJ, Kettler A, Wenger KH, Claes LE. Anatomy of the sheep spine and its comparison to the human spine. Anat Rec. 1997 Apr 1;247(4):542–55.

16. Kandziora F, Pflugmacher R, Scholz M, Schnake K, Lucke M, Schröder R, et al. Comparison between sheep and human cervical spines: An anatomic, radiographic, bone mineral density, and biomechanical study. Spine (Phila Pa 1976). 2001;26(9):1028–37.

17. Risbud M V., Shapiro IM. Notochordal Cells in the Adult Intervertebral Disc: New Perspective on an Old Question. Crit Rev Eukaryot Gene Expr. 2011;21(1):29–41.

18. Lawson L, Harfe BD. Notochord to Nucleus Pulposus Transition. Curr Osteoporos Rep.

2015 Oct 1;13(5):336–41.

19. Hunter CJ, Matyas JR, Duncan NA. Cytomorphology of notochordal and chondrocytic cells from the nucleus pulposus: A species comparison. J Anat. 2004;205(5):357–62.

20. Yurube T, Hirata H, Kakutani K, Maeno K, Takada T, Zhang Z, et al. Notochordal cell disappearance and modes of apoptotic cell death in a rat tail static compression-induced disc degeneration model. Arthritis Res Ther. 2014 Jan 29;16(1):R31.

21. Richardson SM, Ludwinski FE, Gnanalingham KK, Atkinson RA, Freemont AJ, Hoyland JA. Notochordal and nucleus pulposus marker expression is maintained by sub-populations of adult human nucleus pulposus cells through aging and degeneration. Sci Rep. 2017 May 4;7(1):1501.

22. Williams RJ, Laagland LT, Bach FC, Ward L, Chan W, Tam V, et al. Recommendations for intervertebral disc notochordal cell investigation: From isolation to characterization. JOR Spine. 2023;6(3):1–22.

23. Alini M, Diwan AD, Erwin WM, Little CB, Melrose J. An update on animal models of intervertebral disc degeneration and low back pain: Exploring the potential of artificial intelligence to improve research analysis and development of prospective therapeutics. Vol. 6, JOR Spine. John Wiley and Sons Inc; 2023.

24. Lee NN, Salzer E, Bach FC, Bonilla AF, Cook JL, Gazit Z, et al. A comprehensive tool box for large animal studies of intervertebral disc degeneration. JOR Spine. 2021;(July 2020):1–36.

25. McCann MR, Tamplin OJ, Rossant J, Séguin CA. Tracing notochord-derived cells using a Noto-cre mouse: implications for intervertebral disc development. Dis Model Mech. 2012 Jan 1;5(1):73–82.

26. Hunter CJ, Matyas JR, Duncan NA. The three-dimensional architecture of the notochordal nucleus pulposus: novel observations on cell structures in the canine intervertebral disc. J Anat. 2003 Mar 10;202(3):279–91.

27. Li Y, Zhang H, Zhu D, Yang F, Wang Z, Wei Z, et al. Notochordal cells: A potential therapeutic option for intervertebral disc degeneration. Cell Prolif. 2023 Sep 11;

28. McCann M, Séguin C. Notochord Cells in Intervertebral Disc Development and Degeneration. J Dev Biol. 2016 Jan 21;4(1):3.

29. Kerr GJ, Veras MA, Kim MKM, Séguin CA. Decoding the intervertebral disc: Unravelling the complexities of cell phenotypes and pathways associated with degeneration and mechanotransduction. Semin Cell Dev Biol. 2017 Feb;62:94–103.

30. McCann MR, Bacher CA, Séguin CA. Exploiting notochord cells for stem cell-based regeneration of the intervertebral disc. J Cell Commun Signal. 2011 Mar 16;5(1):39–43.

31. Erwin WM, Islam D, Inman RD, Fehlings MG, Tsui FW. Notochordal cells protect nucleus pulposus cells from degradation and apoptosis: implications for the mechanisms of intervertebral disc degeneration. Arthritis Res Ther. 2011 Dec 29;13(6):R215.

32. Williams RJ, Laagland LT, Bach FC, Ward L, Chan W, Tam V, et al. Recommendations for intervertebral disc notochordal cell investigation: From isolation to characterization. JOR Spine. 2023;6(3):1–22.

33. Bedore J, Leask A, Séguin CA. Targeting the extracellular matrix: Matricellular proteins regulate cell–extracellular matrix communication within distinct niches of the intervertebral disc. Matrix Biology. 2014 Jul;37:124–30.

34. Aguiar DJ, Johnson SL, Oegema TR. Notochordal Cells Interact with Nucleus Pulposus Cells: Regulation of Proteoglycan Synthesis. Exp Cell Res. 1999 Jan;246(1):129–37.

35. Li Y, Zhang H, Zhu D, Yang F, Wang Z, Wei Z, et al. Notochordal cells: A potential therapeutic option for intervertebral disc degeneration. Cell Prolif. 2023;(August):1–17.

36. Alini M, Diwan AD, Erwin WM, Little CB, Melrose J. An update on animal models of intervertebral disc degeneration and low back pain: Exploring the potential of artificial intelligence to improve research analysis and development of prospective therapeutics. JOR Spine. 2023 Mar 1;6(August 2022):1–29.

37. He T, Guo W, Yang G, Su H, Dou A, Chen L, et al. A Single-Cell Atlas of an Early Mongolian Sheep Embryo. Vet Sci. 2023 Aug 28;10(9):543.

38. Willie BM, Bloebaum RD, Bireley WR, Bachus KN, Hofmann AA. Determining relevance of a weight-bearing ovine model for bone ingrowth assessment. J Biomed Mater Res A. 2004 Jun 14;69A(3):567–76.

39. Schouman T, Schmitt M, Adam C, Dubois G, Rouch P. Influence of the overall stiffness of a load-bearing porous titanium implant on bone ingrowth in critical-size mandibular bone defects in sheep. J Mech Behav Biomed Mater. 2016 Jun;59:484–96.

40. Malhotra A, Pelletier MH, Yu Y, Christou C, Walsh WR. A Sheep Model for Cancellous Bone Healing. Front Surg. 2014 Sep 8;1.

41. Martini L, Fini M, Giavaresi G, Giardino R. Sheep model in orthopedic research: a literature review. Comp Med. 2001 Aug;51(4):292–9.

42. Costi JJ, Hearn TC, Fazzalari NL. The effect of hydration on the stiffness of intervertebral discs in an ovine model. Clinical Biomechanics. 2002 Jul;17(6):446–55.

43. Casaroli G, Galbusera F, Jonas R, Schlager B, Wilke HJ, Villa T. A novel finite element model of the ovine lumbar intervertebral disc with anisotropic hyperelastic material properties. Smith LJ, editor. PLoS One. 2017 May 4;12(5):e0177088.

44. Banstola A, Reynolds JNJ. The Sheep as a Large Animal Model for the Investigation and Treatment of Human Disorders. Biology (Basel). 2022;11(9):1–26.

45. Liang T, Gao B, Zhou J, Qiu X, Qiu J, Chen T, et al. Constructing intervertebral disc degeneration animal model: A review of current models. Front Surg. 2023 Mar 10;9.

46. Nisolle JF, Bihin B, Kirschvink N, Neveu F, Clegg P, Dugdale A, et al. Prevalence of age-related changes in ovine lumbar intervertebral discs during computed tomography and magnetic resonance imaging. Comp Med. 2016 Aug 1;66(4):300–7.

47. Bouhsina N, Decante C, Hardel JB, Madec S, Abadie J, Hamel A, et al. Correlation between magnetic resonance, X-ray imaging alterations, and histological changes in an ovine model of age-related disc degeneration. Eur Cell Mater. 2021;Soumis:166–78.

48. Turner AS. The Sheep as a Model for Osteoporosis in Humans. The Veterinary Journal. 2002 May;163(3):232–9.

49. Vadalà G, Russo F, Pattappa G, Schiuma D, Peroglio M, Benneker LM, et al. The Transpedicular Approach As an Alternative Route for Intervertebral Disc Regeneration. Spine (Phila Pa 1976). 2013 Mar;38(6):E319–24.

50. K K, M N, R K, S N. The effect of needle puncture injury on the biomechanical response of intervertebral discs. Orthop Procs. 2017;99-B No.SU:122.

51. Elliott DM, Yerramalli CS, Beckstein JC, Boxberger JI, Johannessen W, Vresilovic EJ. The Effect of Relative Needle Diameter in Puncture and Sham Injection Animal Models of Degeneration. Spine (Phila Pa 1976). 2008 Mar;33(6):588–96.

52. van Heeswijk VM, Thambyah A, Robertson PA, Broom ND. Does an Annular Puncture Influence the Herniation Path? Spine (Phila Pa 1976). 2018 Apr 1;43(7):467–76.

53. Schwan S, Ludtka C, Friedmann A, Heilmann A, Baerthel A, Brehm W, et al. Long-Term

Pathology of Ovine Lumbar Spine Degeneration Following Injury Via Percutaneous Minimally Invasive Partial Nucleotomy. Journal of Orthopaedic Research. 2019 Nov 1;37(11):2376–88.

54. Wang Y, Wu Y, Deng M, Kong Q. Establishment of a Rabbit Intervertebral Disc Degeneration Model by Percutaneous Posterolateral Puncturing of Lumbar Discs Under Local Anesthesia. World Neurosurg. 2021 Oct 1;154:e830–7.

55. Bonilla AF, Sikes KJ, Burton LH, Chow L, Kurihara J, Santangelo K, et al. Immunization against nucleus pulposus antigens to accelerate degenerative disc disease in a rabbit model. Front Vet Sci. 2024 May 13;11.

56. Neveu F, Vandeweerd JM, Kirschvink N, Nozry K, Gustin P, Dugdale A, et al. Assessment of a computed tomography guided injection technique of the lumbo-sacral disc in sheep. Veterinary and Comparative Orthopaedics and Traumatology. 2016 Mar 19;29(02):136–41.

57. Nisolle JF, Neveu F, Hontoir F, Clegg P, Kirschvink N, Vandeweerd JM. CT-guided injection technique into intervertebral discs in the ovine lumbar spine. European Spine Journal. 2013 Dec 11;22(12):2760–5.

58. Masaryk TJ, Boumphrey F, Modic MT, Tamborrello C, Ross JS, Brown MD. Effects of Chemonucleolysis Demonstrated by MR Imaging. J Comput Assist Tomogr. 1986 Nov;10(6):917–23.

59. Hoogendoorn RJ, Wuisman PI, Smit TH, Everts VE, Helder MN. Experimental intervertebral disc degeneration induced by chondroitinase ABC in the goat. Spine (Phila Pa 1976). 2007;32(17):1816–25.

60. Smith L. Enzyme Dissolution of the Nucleus Pulposus in Humans. JAMA. 1964 Jan 11;187(2).

61. Sasaki M, Takahashi T, Miyahara K, Hirose T. Effects of Chondroitinase ABC on Intradiscal Pressure in Sheep An In Vivo Study. Vol. 26, SPINE.

62. Eriko M, Nakabayashi K, Suzuki T, Kaul SC, Ogino H, Fujii M, et al. 5-Bromodeoxyuridine Induces Senescence-Like Phenomena in Mammalian Cells Regardless of Cell Type or Species. J Biochem [Internet]. 1999 Dec 1;126(6):1052–9. Available from: https://academic.oup.com/jb/article-lookup/doi/10.1093/oxfordjournals.jbchem.a022549

63. Melrose J, Taylor TKF, Ghosh P, Holbert C, Macpherson C, Bellenger CR. Intervertebral Disc Reconstitution After Chemonucleolysis With Chymopapain is Dependent on Dosage. Spine (Phila Pa 1976). 1996 Jan;21(1):9–17.

64. Kiester DP, Williams JM, Andersson GBJ, Thonar EJMA, McNeill TW. The Dose-Related Effect of Intradiscal Chymopapain on Rabbit Intervertebral Discs. Spine (Phila Pa 1976). 1994 Apr;19(7):747–51.

65. Fraser RD, Osti OL, Vernon-Roberts B. Discitis following chemonucleolysis. An experimental study. Spine (Phila Pa 1976). 1986 Sep;11(7):679–87.

66. Dang L, Wardlaw D, Hukins DW. Removal of nucleus pulposus from the intervertebral disc – the use of chymopapain enhances mechanical removal with rongeurs: a laboratory study. BMC Musculoskelet Disord. 2007 Dec 13;8(1):122.

67. Sasaki M, Takahashi T, Miyahara K, Hirose T. Effects of chondroitinase ABC on intradiscal pressure in sheep: An in vivo study. Spine (Phila Pa 1976). 2001;26(5):463–8.

68. Borem R, Walters J, Madeline A, Madeline L, Gill S, Easley J, et al. Characterization of chondroitinase-induced lumbar intervertebral disc degeneration in a sheep model intended for assessing biomaterials. J Biomed Mater Res A. 2021 Jul 22;109(7):1232–46.

69. Eriko M, Nakabayashi K, Suzuki T, Kaul SC, Ogino H, Fujii M, et al. 5-Bromodeoxyuridine

Induces Senescence-Like Phenomena in Mammalian Cells Regardless of Cell Type or Species. J Biochem. 1999 Dec 1;126(6):1052–9.

70. Zhou HW, Hou SX, Shang WL, Wu WW, Cheng Y, Mei F, et al. A new in vivo animal model to create intervertebral disc degeneration characterized by MRI, radiography, CT/discogram, biochemistry, and histology. Spine (Phila Pa 1976). 2007;32(8):864–72.

71. Johnstone B, Bayliss MT. The Large Proteoglycans of the Human Intervertebral Disc. Spine (Phila Pa 1976). 1995 Mar;20(6):674–84.

72. Carragee EJ, Don AS, Hurwitz EL, Cuellar JM, Carrino J, Herzog R. 2009 ISSLS Prize Winner: Does Discography Cause Accelerated Progression of Degeneration Changes in the Lumbar Disc. Spine (Phila Pa 1976). 2009 Oct;34(21):2338–45.

73. Van Der Werf M, Lezuo P, Maissen O, Van Donkelaar CC, Ito K. Inhibition of vertebral endplate perfusion results in decreased intervertebral disc intranuclear diffusive transport. J Anat. 2007 Dec 22;211(6):769–74.

74. Vadalà G, Russo F, Pattappa G, Peroglio M, Stadelmann VA, Roughley P, et al. A Nucleotomy Model with Intact Annulus Fibrosus to Test Intervertebral Disc Regeneration Strategies. Tissue Eng Part C Methods. 2015;21(11):1117–24.

75. Le Fournier L, Fusellier M, Halgand B, Lesoeur J, Gauthier O, Menei P, et al. The transpedicular surgical approach for the development of intervertebral disc targeting regenerative strategies in an ovine model. European Spine Journal. 2017 Aug 3;26(8):2072–83.

76. Latham JM, Pearcy MJ, Costi JJ, Moore R, Fraser RD, Vernon-Roberts B. Mechanical consequences of annular tears and subsequent intervertebral disc degeneration. Clinical Biomechanics. 1994 Jul;9(4):211–9.

77. Constant C, Hom WW, Nehrbass D, Carmel E, Albers CE, Deml MC, et al. Comparison and optimization of sheep in vivo intervertebral disc injury model. JOR Spine. 2022;(September 2021):1–18.

78. Panebianco CJ, Constant C, Vernengo AJ, Nehrbass D, Gehweiler D, DiStefano TJ, et al. Combining adhesive and nonadhesive injectable hydrogels for intervertebral disc repair in an ovine discectomy model. JOR Spine. 2023;(April):1–16.

79. Fazzalari NL, Costi JJ, Hearn TC, Fraser RD, Vernon-Roberts B, Hutchinson J, et al. Mechanical and Pathologic Consequences of Induced Concentric Anular Tears in an Ovine Model. Spine (Phila Pa 1976). 2001 Dec;26(23):2575–81.

80. Fardon DF, Milette PC. Nomenclature and Classification of Lumbar Disc Pathology. Spine (Phila Pa 1976). 2001 Mar;26(5):E93–113.

81. Vadalà G, Russo F, De Strobel F, Bernardini M, De Benedictis GM, Cattani C, et al. Novel stepwise model of intervertebral disc degeneration with intact annulus fibrosus to test regeneration strategies. Journal of Orthopaedic Research. 2018;36(9):2460–8.

82. Russo F, Hartman RA, Bell KM, Vo N, Sowa GA, Kang JD, et al. Biomechanical Evaluation of Transpedicular Nucleotomy With Intact Annulus Fibrosus. Spine (Phila Pa 1976). 2017 Feb 15;42(4):E193–201.

83. Daly CD, Ghosh P, Badal T, Shimmon R, Jenkin G, Oehme D, et al. A Comparison of Two Ovine Lumbar Intervertebral Disc Injury Models for the Evaluation and Development of Novel Regenerative Therapies. Global Spine J. 2018;8(8):847–59.

84. Bonilla A, Burton L, Page M, von Stade D, Regan D, Dow S, et al. 2020 Research Grant. Development of a clinically-relevant large animal model of intervertebral disc disease. The Spine Journal. 2023 Sep;23(9):S35.

85. Melrose J, Shu C, Young C, Ho R, Smith MM, Young AA, et al. Mechanical destabilization induced by controlled annular incision of the intervertebral disc dysregulates metalloproteinase expression and induces disc degeneration. Spine (Phila Pa 1976). 2012 Jan 1;37(1):18–25.

86. Gantenbein B, Grünhagen T, Lee CR, van Donkelaar CC, Alini M, Ito K. An In Vitro Organ Culturing System for Intervertebral Disc Explants With Vertebral Endplates. Spine (Phila Pa 1976). 2006 Nov;31(23):2665–73.

87. Pattison ST, Melrose J, Ghosh P, Taylor TKF. Regulation of Gelatinase -A (MMP-2) production by ovine Intervertebral disc nucleus pulposus cells grown in alginate bead culture by transforming growth factor-β and insulin like growth factor-I A. Cell Biol Int [Internet]. 2001 Jul 2;25(7):679–89. Available from: https://onlinelibrary.wiley.com/doi/10.1006/cbir.2000.0718

88. Wade KR, Schollum ML, Robertson PA, Thambyah A, Broom ND. ISSLS prize winner: Vibration really does disrupt the disc. Spine (Phila Pa 1976). 2016;41(15):1185–98.

89. Berger-Roscher N, Casaroli G, Rasche V, Villa T, Galbusera F, Wilke HJ. Influence of complex loading conditions on intervertebral disc failure. Spine (Phila Pa 1976). 2017;42(2):E78–85.

90. Drew SC, Silva P, Crozier S, Pearcy MJ. A diffusion and T2 relaxation MRI study of the ovine lumbar intervertebral disc under compression in vitro. Phys Med Biol. 2004 Aug 21;49(16):3585–92.

91. Yang F, Zhu D, Wang Z, Ma Y, Huang L, Kang X, et al. Role of Advanced Glycation End Products in Intervertebral Disc Degeneration: Mechanism and Therapeutic Potential. Oxid Med Cell Longev. 2022 Dec 17;2022:1–12.

92. Jazini E, Sharan AD, Morse LJ, Dyke JP, Aronowitz EB, Chen LKH, et al. Alterations in T 2 relaxation magnetic resonance imaging of the ovine intervertebral disc due to nonenzymatic glycation. Spine (Phila Pa 1976). 2012;37(4).

93. Jünger S, Gantenbein-Ritter B, Lezuo P, Alini M, Ferguson SJ, Ito K. Effect of Limited Nutrition on In Situ Intervertebral Disc Cells Under Simulated-Physiological Loading. Spine (Phila Pa 1976). 2009 May;34(12):1264–71.

94. Constant C, Hom WW, Nehrbass D, Carmel EN, Albers CE, Deml MC, et al. Comparison and optimization of sheep in vivo intervertebral disc injury model. JOR Spine. 2022 Jun 1;5(2).

95. Bouhsina N, Decante C, Hardel JB, Rouleau D, Abadie J, Hamel A, et al. Comparison of MRI T1, T2, and T2* mapping with histology for assessment of intervertebral disc degeneration in an ovine model. Sci Rep. 2022 Dec 1;12(1).

96. Hayes AJ, Melrose J. Aggrecan, the Primary Weight-Bearing Cartilage Proteoglycan, Has Context-Dependent, Cell-Directive Properties in Embryonic Development and Neurogenesis: Aggrecan Glycan Side Chain Modifications Convey Interactive Biodiversity. Biomolecules. 2020 Aug 27;10(9):1244.

97. Melrose J, Smith SM, Appleyard RC, Little CB. Aggrecan, versican and type VI collagen are components of annular translamellar crossbridges in the intervertebral disc. European Spine Journal. 2008 Feb 31;17(2):314–24.

98. Du J, Garcia JP, Bach FC, Tellegen AR, Grad S, Li Z, et al. Intradiscal injection of human recombinant BMP-4 does not reverse intervertebral disc degeneration induced by nuclectomy in sheep. J Orthop Translat. 2022 Nov;37:23–36.

99. Melrose J, Shu C, Young C, Ho R, Smith MM, Young AA, et al. Mechanical destabilization

induced by controlled annular incision of the intervertebral disc dysregulates metalloproteinase expression and induces disc degeneration. Spine (Phila Pa 1976). 2012 Jan 1;37(1):18–25.

100. Shen B, Melrose J, Ghosh P, Taylor T. Induction of matrix metalloproteinase-2 and -3 activity in ovine nucleus pulposus cells grown in three-dimensional agarose gel culture by interleukin-1β: a potential pathway of disc degeneration. European Spine Journal. 2003 Feb;12(1):66–75.

101. Le Maitre CL, Freemont AJ, Hoyland JA. The role of interleukin-1 in the pathogenesis of human intervertebral disc degeneration. Arthritis Res Ther. 2005;7(4):R732-45.

102. Wilke HJ, Kettler A, Claes LE. Are Sheep Spines a Valid Biomechanical Model for Human Spines? Spine (Phila Pa 1976) [Internet]. 1997 Oct 15 [cited 2020 Apr 7];22(20):2365–74. Available from: http://journals.lww.com/00007632-199710150-00009

103. Sakai D. Future perspectives of cell-based therapy for intervertebral disc disease. European Spine Journal. 2008 Dec 13;17(S4):452–8.

104. Vadalà G, Russo F, Ambrosio L, Loppini M, Denaro V. Stem cells sources for intervertebral disc regeneration. World J Stem Cells. 2016;8(5):185.

105. Sakai D, Andersson GBJ. Stem cell therapy for intervertebral disc regeneration: obstacles and solutions. Nat Rev Rheumatol. 2015 Apr 24;11(4):243–56.

106. McCann MR, Bacher CA, Séguin CA. Exploiting notochord cells for stem cell-based regeneration of the intervertebral disc. J Cell Commun Signal. 2011 Mar 16;5(1):39–43.

107. Zhang Y, Liang C, Xu H, Li Y, Xia K, Wang L, et al. Dedifferentiation-like reprogramming of degenerative nucleus pulposus cells into notochordal-like cells by defined factors. Molecular Therapy. 2024 Aug;32(8):2563–83.

108. Korecki CL, Taboas JM, Tuan RS, Iatridis JC. Notochordal cell conditioned medium stimulates mesenchymal stem cell differentiation toward a young nucleus pulposus phenotype. Stem Cell Res Ther. 2010 Jun 16;1(2):18.

109. Abbott RD, Purmessur D, Monsey RD, Iatridis JC. Regenerative potential of TGFβ3 + Dex and notochordal cell conditioned media on degenerated human intervertebral disc cells. Journal of Orthopaedic Research. 2012 Mar 22;30(3):482–8.

110. de Vries SAH, van Doeselaar M, Meij BP, Tryfonidou MA, Ito K. The Stimulatory Effect of Notochordal Cell-Conditioned Medium in a Nucleus Pulposus Explant Culture. Tissue Eng Part A. 2016 Jan;22(1–2):103–10.

111. Schmitz TC, van Doeselaar M, Tryfonidou MA, Ito K. Detergent-Free Decellularization of Notochordal Cell-Derived Matrix Yields a Regenerative, Injectable, and Swellable Biomaterial. ACS Biomater Sci Eng. 2022 Sep 12;8(9):3912–23.

112. Nerurkar NL, Sen S, Huang AH, Elliott DM, Mauck RL. Engineered Disc-Like Angle-Ply Structures for Intervertebral Disc Replacement. Spine (Phila Pa 1976). 2010 Apr;35(8):867–73.

113. Henry N, Clouet J, Le Bideau J, Le Visage C, Guicheux J. Innovative strategies for intervertebral disc regenerative medicine: From cell therapies to multiscale delivery systems. Biotechnol Adv. 2018 Jan;36(1):281–94.

114. Rodrigues SA, Wade KR, Thambyah A, Broom ND. Micromechanics of annulus–end plate integration in the intervertebral disc. The Spine Journal [Internet]. 2012 Feb;12(2):143–50. Available from: https://linkinghub.elsevier.com/retrieve/pii/S1529943012000046

115. Rodrigues SA, Wade KR, Thambyah A, Broom ND. Micromechanics of annulus–end plate integration in the intervertebral disc. The Spine Journal. 2012 Feb;12(2):143–50.

116. Rodrigues SA, Thambyah A, Broom ND. How maturity influences annulus-endplate integration in the ovine intervertebral disc: a micro- and ultra-structural study. J Anat. 2017 Jan 18;230(1):152–64.

117. Wade KR, Robertson PA, Broom ND. Influence of maturity on nucleus–endplate integration in the ovine lumbar spine. European Spine Journal. 2014 Apr 20;23(4):732–44.

118. Tang SN, Bonilla AF, Chahine NO, Colbath AC, Easley JT, Grad S, et al. Controversies in spine research: Organ culture versus in vivo models for studies of the intervertebral disc. Vol. 5, JOR Spine. John Wiley and Sons Inc; 2022.

119. Chakrabarti S, Ai M, Wong K, Newell K, Henson FMD, Smith EStJ. Functional Characterization of Ovine Dorsal Root Ganglion Neurons Reveal Peripheral Sensitization after Osteochondral Defect. eNeuro. 2021 Sep;8(5):ENEURO.0237-21.2021.

120. Poletto DL, Crowley JD, Tanglay O, Walsh WR, Pelletier MH. Preclinical in vivo animal models of intervertebral disc degeneration. Part 1: A systematic review. JOR Spine. 2022;(October 2022):1–20.

121. Banstola A, Reynolds JNJ. The Sheep as a Large Animal Model for the Investigation and Treatment of Human Disorders. Biology (Basel). 2022;11(9):1–26.

122. Evangelista MC, Monteiro BP, Steagall P V. Measurement properties of grimace scales for pain assessment in nonhuman mammals: a systematic review. Pain. 2022 Jun;163(6):e697–714.

123. Häger C, Biernot S, Buettner M, Glage S, Keubler LM, Held N, et al. The Sheep Grimace Scale as an indicator of post-operative distress and pain in laboratory sheep. PLoS One. 2017 Apr 19;12(4):e0175839.

124. Wilke HJ, Kettler A, Claes LE. Are Sheep Spines a Valid Biomechanical Model for Human

Spines? Spine (Phila Pa 1976). 1997 Oct;22(20):2365–74.

CHAPTER 3 DISC DEGENERATION IN AN OVINE MODEL: CHARACTERIZATION AND INSIGHTS

3.1 Summary

This study is the first to explore the differences in proteomic profiles and histological characteristics between cervical and lumbar IVDs in an ovine model of IVDD. The findings reveal a similar progression of IVDD in both regions, challenging the traditional emphasis on lumbar IVDs in research and highlighting the relevance of cervical models for understanding the disease. The study documents clear evidence of IVDD progression through gross morphological changes, imaging evaluation, and histological assessment, aligning with existing literature while filling critical gaps regarding cervical IVDs. Notably, this research identified distinct patterns in differentially expressed proteins (DEPs) and imaging changes, with significant implications for clinical practices. Clinicians may need to reconsider treatment approaches for IVDD, recognizing that both cervical and lumbar IVDs exhibit comparable degenerative characteristics. The identification of specific biomarkers, including proteins like C-reactive protein and Asporin, could enhance early diagnosis and guide the development of tailored therapeutic interventions. These findings suggest that treatments traditionally focused on lumbar degeneration may require adaptations for cervical pathology, addressing the unique kinematic features of each anatomical region. Additionally, the translational potential of the study is significant, providing a foundation for future experimental designs in IVDD research. By identifying key molecular pathways and targets associated with degeneration, researchers can design experiments aimed at exploring therapeutic strategies. Lastly, the findings emphasize the need for comparisons across species and animal models to understand potential differences in IVDD progression and treatment responses. The insights gained from this research can refine the selection of animal models for preclinical

studies and inform the development of targeted therapies for IVDD in clinical practice. By fostering a better understanding of the mechanisms underlying degeneration, future research can contribute to innovative treatment strategies and improved patient outcomes.

3.2 Introduction

Animal models have been essential in efforts to understand the progression of IVDD and to identify how structural, environmental, or biomechanical risk factors may trigger or influence these degenerative changes (123). A wide range of animal models has been developed to study these processes, typically categorized into small and large animal models (246–249). Common small animal models include mice, rats, and rabbits, while larger animals such as dogs, pigs, goats, and sheep are frequently used (124). However, due to the complexity of human intervertebral disc degeneration, no animal model perfectly replicates the condition (125). The selection of the most suitable animal model depends not only on the specific research questions but also on factors such as the size and anatomical similarities to the human disc, the absence of notochordal cells, biomechanical forces comparable to clinical conditions, and ethical considerations (126).

Among animal models developed to understand the pathophysiology IVDD and explore potential treatments for this condition, the ovine model stands out as one of the most relevant large animal models. Specific similarities, such as spinal size, cellularity, and biomechanics, make the ovine model particularly valuable for comparison to human IVDD (216,250,251). Additionally, recent studies have shown that sheep, like humans, experience spontaneous IVDD as they age. These age-related changes have been observed in long-living sheep, which closely mimic elderly

humans. Imaging, histological, and mechanical findings in sheep with IVDD demonstrate changes similar to those in humans, along with clinical signs of degeneration (252,253).

Despite the recognized advantages of the ovine model for studying IVDD, this animal model remains incompletely characterized. Many researchers utilize the ovine model to examine how different stages of IVDD affect intervertebral disc structure, as well as the associated biochemical and molecular changes. The lumbar discs are often preferred due to the ease of surgically inducing degeneration and their similarity to the human lumbar spine. The size of the ovine lumbar spine closely mimics the human lumbar spine, making it a valuable model for evaluating novel surgical instruments and scaffolds as potential treatments for IVDD (254,255). On another hand, the ovine cervical spine has been used to test various scaffolds and interbody fusion cages, offering promising insights for translation to human medicine (256,257).

The objectives of this study were to use a multidimensional approach, including gross morphometry, MR imaging, histological analysis, and proteomic profiling, to explore clinical, structural, histological, and molecular changes in cervical and lumbar intervertebral discs in the ovine model. By combining these methodologies, the study aimed to deepen the understanding of disc degeneration and support the development of targeted diagnostic and therapeutic strategies.

3. 3 Materials and methods

3.3.1 Animals

This study was conducted with the approval of the Institutional Animal Care and Use Committee at Colorado State University (protocol#: 3382). Six skeletally mature female Rambouillet sheep were enrolled and randomly assigned to one of two observation periods: 8

weeks and 32 weeks (n = 3 sheep per period). Each sheep underwent partial discectomy, involving a box-cut AF defect and standardized removal of 100 mg of NP at three cervical and three lumbar levels. The procedures were performed using a lateral retroperitoneal surgical approach. Additionally, three other animals from a separate study were used as intact control naïve IVDs for comparison of IVDs. All animals were musculoskeletal and neurologically normal prior to surgery.

Procaine penicillin G (22,000 units/kg, subcutaneous (SQ) and two fentanyl patches (100 and 50 mcg) were applied to all sheep 24 hr. prior to surgery and maintained for three days. The auricular vein and artery were catheterized, and anesthesia was induced using a combination of ketamine (3.3 mg/kg, intravenous (IV)) and diazepam (0.1 mg/kg, IV). Following anesthetic induction, the sheep were intubated with a cuffed endotracheal tube, placed in dorsal recumbency, and maintained on isoflurane (1.5%–3%) with 100% oxygen using positive pressure ventilation (20 cm H2O) for the duration of the procedure. Atracurium (15 mg/kg) was administered IV intraoperatively to facilitate muscle dissection and retraction.

Preoperatively, the sheep were required to be in good health based on a complete physical assessment performed by a veterinarian and a complete blood cell count and free of signs of degenerative lumbar disease based on pre-operative lumbar spine radiographs. Animal welfare assessment was performed by clinical physical exami- nation using a score sheet twice daily for the first 3 days postopera- tively followed by daily evaluation for 4 additional days, and then once weekly in conjunction with complete physical examinations per- formed regularly by an experienced veterinarian.

3.3.2 Surgical intervention

All surgical procedures were conducted under aseptic conditions. The auricular vein and

artery were accessed for catheter placement. A combination of ketamine (3.3 mg/kg, IV) and diazepam (0.1 mg/kg, IV) was used to initiate anesthesia. After achieving the anesthetic state, the sheep were intubated using a cuffed endotracheal tube.

Initially, animals were positioned in dorsal recumbency and maintained on isoflurane (1.5%-3%) combined with 100% oxygen. An open surgical approach to the ventral cervical space was completed and C2-3 to C4-5 discs were exposed. After blunt dissection a 11 blade was used to create a box-cut defect (full-thickness partial annulectomy) of each selected disc with the creation of 4 cuts of 8-mm depth of 84niport. 5-mm length and 3-mm wide rectangular window in the ventral aspect of AF (Figure 1). With a Kerrison rongeur instrument partial nucleotomy was performed at C2-3, C3-4, C4-5 discs levels removing ~100 mg of NP tissue. Routine closure was performed of the musculature and ventral fascia with absorbable suture, subcutaneous tissue with absorbable suture, and skin with non-absorbable suture.

Then, the sheep was repositioned to a right lateral recumbency. Through a left lateral retroperitoneal method, the intervertebral spaces from L2 to L5 were made visible by dissecting through the oblique abdominal muscles, leading to the muscle layer in front of the transverse processes. After blunt dissection a 11 blade was used to create a box-cut defect (full-thickness partial annulectomy) of each selected disc with the creation of 4 cuts of 8-mm depth of 84niport. 5-mm length and 3-mm wide rectangular window in the in the left lateral aspect of the AF. With a rongeur instrument partial nucleotomy was performed at L2-3, L3-4, L4-5 discs levels removing ~100 mg of NP tissue. Routine closure was performed of the epaxial musculature and dorsal fascia with absorbable suture, subcutaneous tissue with absorbable suture, and skin with non-absorbable suture.

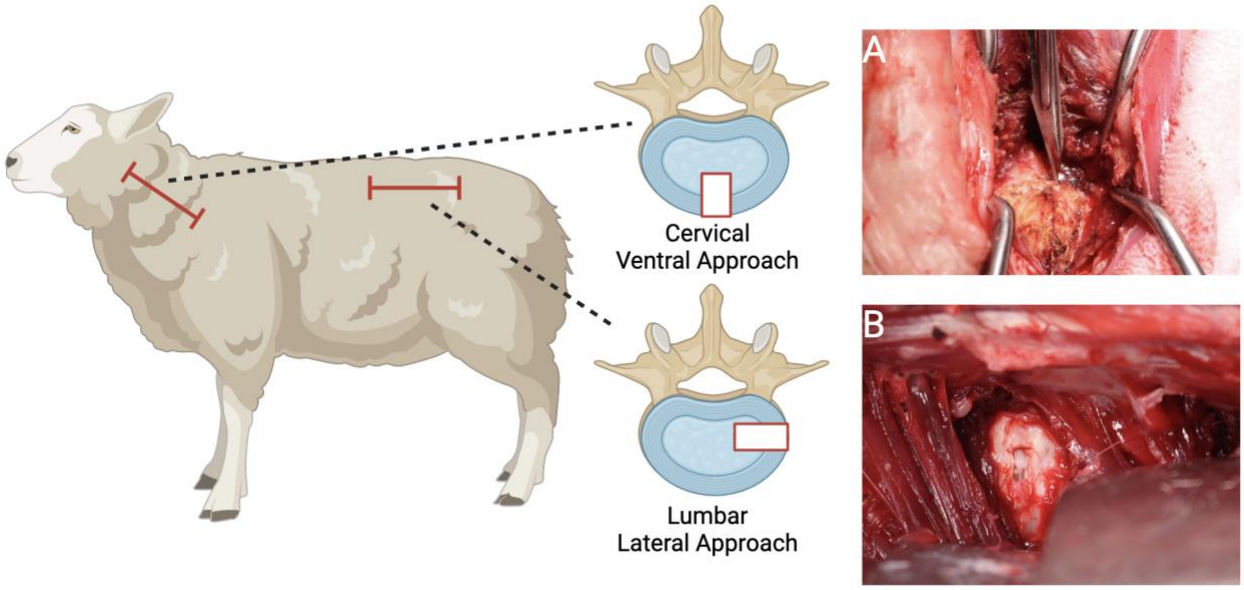

Figure 1: Illustration of the full-thickness partial discectomy performed ventral and lateral for the cervical (C2-3, C3-4, C4-5) and lumbar (L2-3, L3-4, L4-5) intervertebral discs respectively. The cervical spine was visualized through a ventral surgical approach and the intervertebral discs were exposed (A), similarly lumbar spine was visualized through a lateral surgical approach and the intervertebral discs were exposed (B).

3.3.3 In vivo Imaging

Radiographic imaging of the cervical and lumbar spine was performed for each animal both pre- and post-IVD injury creation surgery. For animals in the 8-week study period, additional imaging was conducted at 8 weeks pre sacrifice. Animals in the 32-week study period underwent imaging pre- and post-IVD injury creation surgery, as well as at 8, 16, and 32 weeks postoperatively, to assess disc height loss and degenerative changes over time. For these procedures, sheep were pre-medicated and anesthetized with an initial induction of 4% isoflurane, followed by maintenance at 1-3%. The animals were positioned prone for radiographic imaging, which was performed in both dorsoventral and later lateral views. A blinded observer analyzed the radiographic images to evaluate spinal and bone abnormalities

MR images were used to determine disc height index (DHI) (258,259), and Pfirrmann

grade (260). MR images were chosen to assess DHI due to its superior resolution, which enables precise evaluation of disc height changes within the same slice or plane, enhancing the accuracy of measurements and analysis. MR Imaging was similarly completed in the same times that radiographic imaging. Sheep were pre-medicated and anesthetized by initial induction of 4% isoflurane, and maintenance at 1 – 3%, and placed in the prone position. A 3T MR scanner (Siemens Magnetom Skyra MR Scanner) was used to obtain to obtain 2-dimensional T1 and T2-weighted sequences in sagittal orientation (1.5mm slices). The following basic protocol parameters were used for image acquisition: RT 4590 ms, ET 89 ms, 1.5 mm slices, acquisition matrix 384 x 288, Flip Angle of 260 degrees, and bandwidth of 480 Hz. The MRI scans were analyzed by a blinded observer for cervical and lumbar Pfirrmann grades, and any other noted spinal abnormalities.

3.3.4 Euthanasia and sample harvest

The sheep were humanely euthanized at 8 weeks (n = 3 sheep) or 32 weeks (n = 3 sheep) after surgery according to their respective observation period by intravenous overdose of pentobarbitone sodium (88mg/kg), in accordance with the American Veterinary Medical Association (AVMA) guidelines, and the cervical and lumbar spine harvested and removed to complete the *ex vivo* evaluation.

3.3.5 Gross Evaluation

The cervical and lumbar spines were meticulously dissected, ensuring precise removal of all peripheral musculature surrounding the cervical and lumbar region and the respective IVDs that had undergone partial discectomy. Using a 60 blade, axial cuts were made at the cranial edge

of the C3-4 and L3-4 intervertebral discs. Digital photographs were taken to evaluate and compare the gross morphology of each disc, providing visual documentation for further comparative analysis of structural changes.

3.3.6 Proteomic analysis

Posteriorly, using biopsy punches, tissue samples of approximately 100 mg were obtained from the NP with an 8 mm punch, and from AF with a 6 mm punch, precisely delineating each region (Figure 2). Tissue collections were carefully replicated to represent regions directly and indirectly impacted by the surgically induced injury. Samples stored at -80°C were transferred to 2 mL reinforced tissue bead grinding tubes, with 1 mL of tissue grinding buffer (Thermo Lysis buffer, 2% SDS, 1X HALT Protease Inhibitor Cocktail) added to each. After homogenization and centrifugation at 8,000xg for 10 minutes, the supernatant was collected. Protein pellets were washed three times and posteriorly centrifuged at 16,000xg for 10 minutes at 4°C, and solubilized in 150-300 µL of Thermo Fisher Lysis Buffer. Protein content was measured using the Pierce BCA Protein Assay Kit (ThermoFisher Scientific).

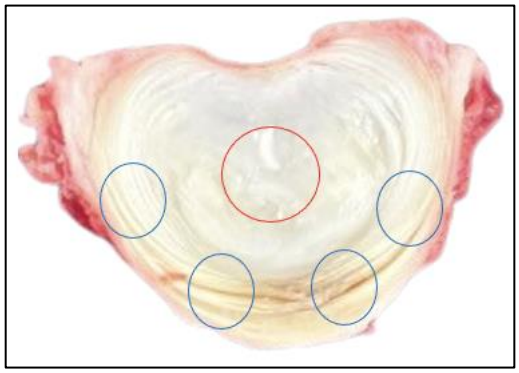

Figure 2. Diagram representing the anatomic locations were Nucleus Pulposus (red circle) and Annulus fibrosus (blue circles) sample tissue were collected.

After this, samples were digested using the EasyPep Mini MS Sample Prep Kit

(ThermoFisher Scientific). Peptide eluate was dried in a vacuum evaporator and resuspended in 3% acetonitrile/0.1% formic acid. Once resolubilized, absorbance at 205nm was measured on a NanoDrop (ThermoScientific). The samples were analyzed by Mass Spectrometry Analysis – LC-MS/MS. Briefly, reverse phase chromatography was performed. A total of 1µg of peptides was purified and concentrated using an on-line enrichment column (Thermo Scientific PepMap Neo). Subsequent chromatographic separation was performed on a Vanquish Neo (Thermo Scientific). Peptides were eluted directly into the mass spectrometer (Orbitrap Eclipse, Thermo Scientific).

Proteome Discoverer 3.0 was used for data processing (Thermo Scientific). Raw data was interrogated against the FASTA for the reference proteome for sheep taxon ID9940 "88niport_Sheep_ID9940_061523.fasta". Additionally, the cRAP proteome was included (The common Repository of Adventitious Proteins -cRAPcontains commonly found contaminant proteins in proteomics experiments). Thresholds were set such that a false discovery rate (FDR) of ≤1% and protein identification was defined with at least one peptide.

3.3.7 Histopathological analysis

The C4-5 and L4-5 IVDs, along with their respective cranial and caudal vertebral body segments, were harvested, bisected in the sagittal plane, and processed for decalcified histological analysis. Following fixation in 10% formalin, specimens were decalcified using 10% EDTA. Standard histological processing techniques (Tissue-Tek VIP, Sakura, Torrance, CA) were employed, and the specimens were embedded in paraffin. Slides were stained with Hematoxylin and Eosin and Alcian Blue. The histological sections were meticulously evaluated by a certified veterinary pathologist using a histological grading scheme for disc degeneration. A histological score system modified for the evaluation of IDD large animals was used (Table1) (146). This

scored included various parameters, including the NP (cell clusters, cell loss, matrix integrity, cellularity), AF (integrity, morphology, cellular and ECM metaplasia), the presence of tears and clefts in the AF/NP, CEP morphology, and bone modeling at the AF/bone interface.

Table 1. Consensus-based histological grading scheme for all large animal models. The scoring item related to notochordal cells is not included.

Nucleus pulposus cell clusters	
No clusters	0
Scattered small cell clusters (*i.e.* 2-7 nuclei per cluster)	1
Frequent large cell clusters (*i.e.* >8 nuclei per cluster)	2
Presence of huge cell clusters (*i.e.* >15 nuclei per cluster)	3
NP cell loss (karyolysis) and cell necrosis (pyknosis or karyorrhexis)	
None – lacunae all contain viable nuclei	0
Rarely present. Few (<25%) lacunae demonstrate karyolysis, pyknosis, or karyorrhexis	1
Frequently present. 25%-50% of lacunae demonstrate karyolysis, pyknosis, or karyorrhexis	2
Karyolysis, pyknosis, or karyorrhexis predominates (>50%)	3
NP Matrix staining (AB-PSR)	
Blue proteoglycan matrix stain dominates	0
Reduction in blue proteoglycan matrix staining (*i.e.* fading)	1
Reduction in blue proteoglycan matrix staining with presence of collagen staining (up to 50% of area)	2
Loss of blue proteoglycan matrix staining and/or dominance of collagen staining (>50% of area)	3
AF morphology (AB-PSR)	
Well-organized; uniform collagen lamellae form concentric half-ring arcs throughout entire AF	0
Mild disorganization of collagen fiber lamellae with some disruption or loss of concentric layers (<25%)	1
Moderately disorganization of collagen fiber lamellae with progressive disruption or loss	2

of concentric layer (25–75%)	
Complete disorganization/collapse of AF; almost all concentric collagen lamellae are severely disrupted or lost (>75%)	3
AF Cellular (H&E) and matrix metaplasia (AB-PSR) / distinction between AF and NP –	
Clear distinction between AF and NP tissue with intense blue proteoglycan matrix staining in NP: spindle-shaped fibroblasts populate AF with no or rare individual metaplastic cells resembling NPCs in the AF	0
Distinction less clear: loss of annular-nuclear demarcation. Proliferation of cells resembling NPCs limited to inner most AF layers with >75% lacunae containing single nuclei (*i.e.* rare to few small NPC-like clusters)	1
Distinction less clear: loss of annular-nuclear demarcation. Moderate proliferation of cells resembling NPCs extending to mid-layers of AF with 25-50% lacunae containing more than one cell nucleus (*i.e.* frequent NPC-like clusters)	2
No discernable annular-nuclear demarcation. Marked proliferation of cells resembling NPCs extending to outer layers of the AF with >50% lacunae containing more than one cell nucleus or presence of lacunae containing >4 nuclei (*i.e.* frequent extremely large NBC-like clusters)	3
Tears and cleft formation[&] in the AF/ NP (H&E, AB-PSR)	
Absent	0
Rarely present. Few small concentric-oriented clefts limited to inner AF without transverse clefts that bridge inner to outer layers of AF	1
Larger and more numerous clefts that extend from inner through mid-layers of AF	2
Abundantly present, large clefts that bridge more than one layer of the AF or presence of fibroblast infiltration/neovascularization	3
CEP morphology (Saf O/FG, AB-PSR)	
Uniformly thickness and contour without disruption	0
Focal to multifocal thickness and/or contour irregularities without disruption	1
Focal endplate disruptions (thin clefts, fissures or chondroid matrix extrusion up to 10%	2

total area with or without irregularities in thickness/contour	
Frequent or large areas of endplate disruption with chondroid matrix extrusion >10% total area with or without formation of Schmorl's nodes	3
Bone modeling – at the external AF/bone interface (H&E)	
Absent	0
Limited, bone remodeling that forms pointed EP contours or small nodular exostoses that to not impinge on AF	1
Larger vertebral exostoses that protrude cranio-caudally and impinge on outer layers of the AF	2
Abundant new bone formation with partial to complete bridging spondylosis	3

NP: nucleus pulposus; NPC: NP cells; AF: annulus fibrosus; CEP: cartilaginous endplate; H&E: hematoxylin & eosin stain; AB-PSR: alcian blue/picrosirius red stain; Saf O/FG: safranin O/fast green stain. Adapted from Leet et al 2021(21).

3.3.8 Statistical analysis

After processing the data, statistical analyses were conducted on all outcome parameters. Normality tests were performed, followed by a one-way ANOVA and Tukey's multiple comparison test to identify statistically significant differences ($p \leq 0.05$) (GraphPad Prism 8.3.0, San Diego, CA). Results for histological grading, DHI, and Pfirrmann grading are reported as mean ± SD. For graphical presentation, DHI values from the control group (week 0) were normalized to 100%, ensuring consistent comparison across time points.

For protein abundance comparison, sample were analyzed by type of tissue separately (AF and NP). Differences among groups (control, 8 and 32 weeks) were assessed by ANOVA and Benjamini-Hochberg corrected p value <0.05 were considered statistically significant. For those proteins showing a statistically significant ANOVA test, the Tukey post hoc test was applied to determine which pair (s) of groups were different. For graphics, proteomic data global comparisons were assessed for statistical significance in MetaboAnalyst version 6.0 (261). KEEG pathway and

GO molecular function analysis of differentially expressed proteins (DEPs) was conducted using ShinyGO v.0.80, with the Ensembl genome assembly for "sheep genes Oar_rambouillet_v1.0" as the reference (262). Venn diagrams of DEPs between comparisons were generated using the Bioinformatics & Evolutionary Genomics Venn diagram tool (https://bioinformatics.psb.ugent.be/webtools/Venn/).

3. 4. Results

3.4.1 Surgical procedure

All animals tolerated without complications the surgical procedure. Partial annulectomy was completed successfully ventrally and laterally in the cervical and lumbar levels respectively. Around 100 mg of NP tissue were extracted from each intervertebral disc through the window defect created in the AF. Animals recovered successfully and without particularities after the procedure.

3.4.2 Gross Evaluation

Control naïve IVDs in both cervical and lumbar regions exhibited well-defined structures of the NP and AF. The NP appeared intact as a uniformly pale white structure with a viscous, water-rich consistency, while the AF exhibited well-defined fibrous rings of consistent pale-yellow coloration, encircling the NP. At the 8-week mark, notable degenerative changes were observed in both cervical and lumbar IVDs (Figure 3). In the cervical discs, the NP changed from white to amber, accompanied by disorganization and disruption of the fibrous rings in the AF, particularly around the injury site. There was also a marked infiltration of blood vessels and the formation of scar tissue with a hard, bone-like consistency. Lumbar discs exhibited similar changes, with the

NP turning brown, particularly near the injury site, with mild signs of desiccation showed by a reduction in its gel-like, water-rich consistency. The AF also showed disruption or fissuring of its rings, along with notable blood vessel proliferation and significant but smaller-scale scar tissue formation compared to the cervical discs. Besides the evident desiccation of the IVDs, no clear visual differentiation of the NP to AF was possible at this time point.

Figure 3: Representative Images of the gross evaluation demonstrates a clear time-dependent progression of intervertebral disc degeneration in both the cervical and lumbar regions.

At 32 weeks, the cervical NP had completely turned brown with a dry appearance, losing its water-rich consistency. The AF rings had also changed color, with a brownish-pink hue likely due to increased vascular infiltration. Severe bone formation at the injury site led to near-complete fusion of the IVD. In the lumbar discs, the changes were less drastic compared to the 8-week time point, but the NP showed a darker brown color and further loss of water content. Disruption of the AF rings was still evident, and there was clear scar tissue formation with minor bone development, indicating early fusion processes.

3.4.3 Imaging Evaluation

Radiographic images taken before an at 8, 16 at 32 weeks were used to evaluate clinical aspects of the cervical and lumbar spine. No significant abnormalities were noted at radiographic images in both cervical or lumbar spine before or after the surgery (Figure 4). Similar and normal bone density were observed for spine structures in all the animals. MR images were selected to assess DHI due to their superior resolution, allowing for precise evaluation of disc height changes within the same slice or plane (Figure 5). This enhanced resolution improves the accuracy of both measurements and overall analysis.

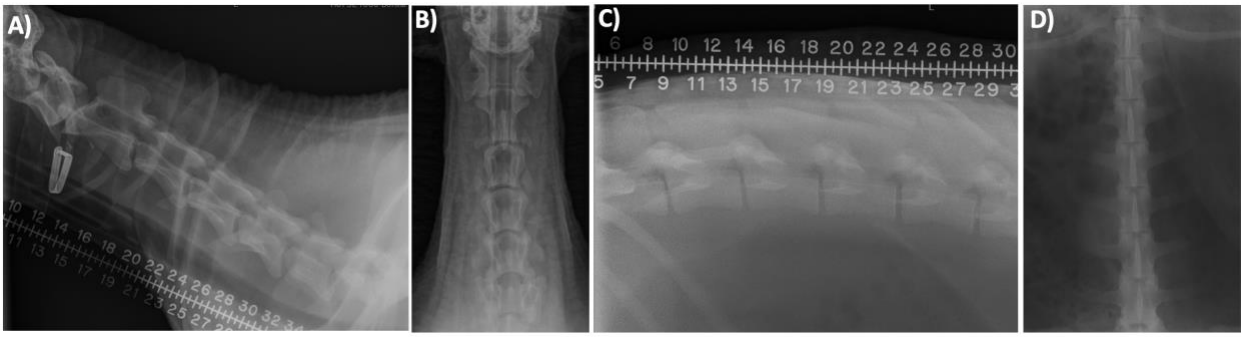

Figure 4: Representative images of radiographic evaluation of the cervical (A-B) and Lumbar (C-D) spine. Images were used to evaluated evaluate spine conformation and discard or note the presence of spine abnormalities.

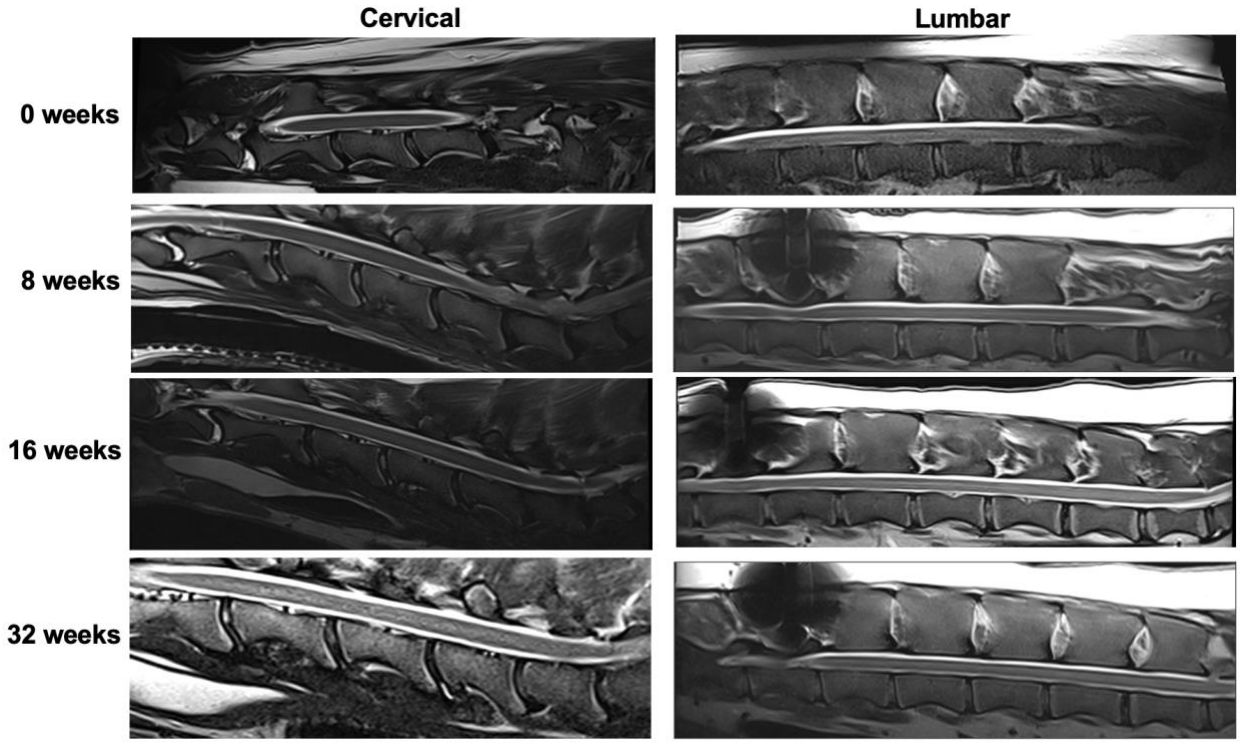

Figure 5: Representative MRI images of the cervical (Left column) and Lumbar (Right Column) spine at the different time points (Rows). MR images were selected to assess DHI and Pfirrmann grade.

Evaluation of the DHI showed a significant decrease for both cervical and lumbar IVDs showing statistically significant differences at time points, but not when compared between both anatomical regions (Figure 6). In the cervical IVDs the DHI was decreased showing significant difference when baseline control DHI was compared to 8 weeks (P=0.0088), and baseline compared to 32-week time point (P=0.0264). The lumbar DHI showed a decrease in DHI at 8 weeks (P=0.0029), at 16 weeks (P=0.0014), and at 32 weeks (P=0.0002) compared to baseline. When compared 8 to 32 weeks DHI from lumbar IVD also a significant decreased was noted (P=0.0360).

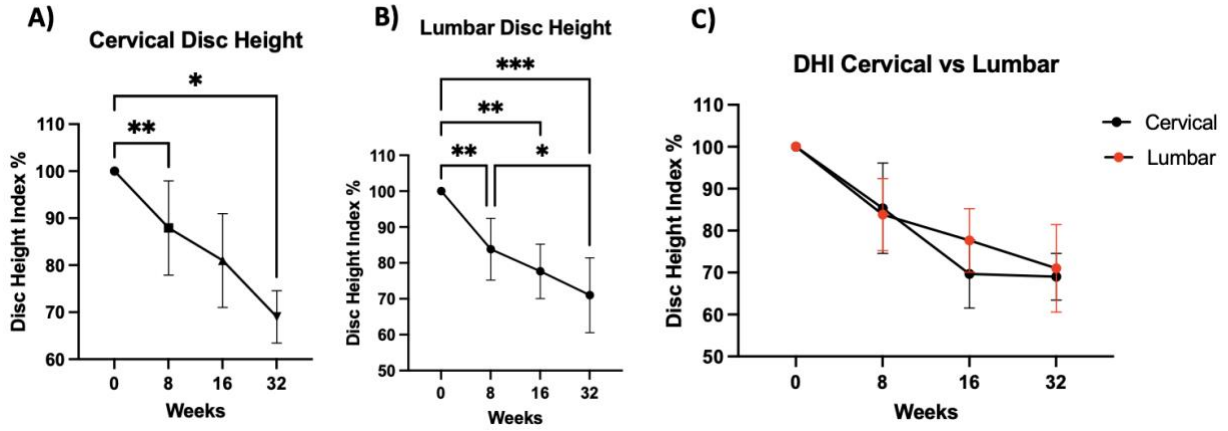

Figure 6: Disc Height Index (DHI) changes were observed in both cervical and lumbar intervertebral discs. (A) Cervical discs exhibited significant reductions in DHI at 8 and 32 weeks compared to baseline (0 weeks). (B) Lumbar discs also showed significant DHI changes, with differences noted between 0 and 8, 16, and 32 weeks, as well as between 8 and 32 weeks. (C) While a similar trend was seen between cervical and lumbar regions, no significant differences were found when comparing these anatomical areas. *P<0.05, **P<0.01, ***P<0.001. DHI: Disc Height Index.

Evaluation of the Pfirrmann grade showed statistically significant differences at time points, but not when compared cervical vs lumbar IVDs (Figure 7). In the cervical IVDs the Pfirrmann grade increased showing significant difference when baseline (0 weeks) was compared to 16 weeks (P=0.0450), and baseline compared to 32-week time point (P=0.0033). When compared 8 to 32 weeks also a significant increase was noted for cervical IVDs (P=0.0348). The lumbar scoring of the MR imaging changes related IVDD showed an increase in Pfirrmann grade at 8 weeks (P=0.0279), at 16 weeks (P=0.0041), and at 32 weeks (P=0.0007) compared to baseline. When compared 8 to 32 weeks also a significant decreased was noted in lumbar IVDs (P=0.0375).

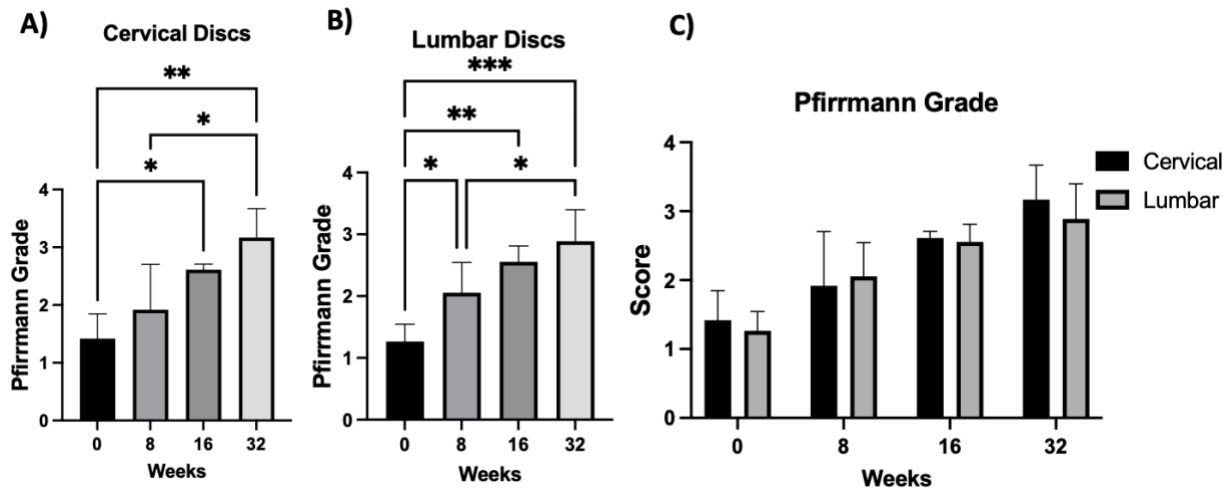

Figure 7: Pfirrmann grades demonstrated significant changes in both cervical and lumbar intervertebral discs. (A) In cervical IVDs, Pfirrmann scores significantly increased at 16 and 32 weeks compared to baseline (0 weeks), with notable differences observed between 8 and 32 weeks as well. (B) Similarly, lumbar IVDs showed significant changes in Pfirrmann scores between 0, 8, 16, and 32 weeks, along with statistical differences between 8 and 32 weeks. (C) Although a similar trend of increasing Pfirrmann scores was seen in both cervical and lumbar regions, no statistically significant differences were observed when comparing these anatomical areas. *P<0.05, **P<0.01, ***P<0.001.

3.4.4 Histological Evaluation

Control naïve, 8- and 32-week groups of animals in the study showed varying signs of IDD development, involving the AF, NP, and endplates. Varying degrees of loss of distinction of structural components of the disc were evident in both cervical and lumbar IVDs at 8 and 32 weeks compared with baseline. Cervical and lumbar IVDs from the control group exhibited normal structure, with clearly defined AF and a centrally positioned nucleus pulposus NP. The CEP was intact, and there was minimal cellular infiltration. The AF was organized into distinct, asymmetrical layers that span the vertebral bodies, with the ventral region showing thicker, longer bands. Vascularization was notable between, and occasionally within, the outer layers, as well as in the fibrocartilage at the vertebral insertion. In the deeper layers, the AF transitioned seamlessly into the NP, which was composed of a homogenous, gelatinous matrix. Viable NP cells were

distributed throughout, alongside occasional apoptotic cell remnants, while the NP itself remained avascular. The CEP was primarily composed of hyaline cartilage, with well-organized columns of chondrocytes that transitioned into a thin layer of mineralized cartilage at the interface with bone. Modest vascularization extended into this junction, resulting in slight interdigitation between the mineralized and non-mineralized cartilage.

At the different time points, IVDs from both cervical and lumbar demonstrated unilateral disruption of the AF, characterized by a loss of lamellar distinction and disorganization of the fibrocartilaginous bands. AF cells were often hyperplastic, with noticeable lacunae, accompanied by vascular and bony proliferation, particularly at the superficial AF insertion site. The nucleus NP exhibited reduced homogeneity, with multifocal and regionally extensive AP cell hyperplasia, occasional hypertrophy, clumping, and areas of cell necrosis. Variations in endplate thickness were observed, with disorganized columnar chondrocyte maturation, and in rare cases, focal NP extrusion through the endplate into the bone. Additionally, a reduction in intervertebral disc height by 20-50% was noted on the affected side.

At 8 weeks, cervical and lumbar IVDs demonstrated early signs of degeneration, including mild fissuring of the AF, reduced proteoglycan content in the NP, and healing responses marked by scar tissue formation. Pronounced bony remodeling and proliferation were observed around the external AF insertion, particularly in cervical IVDs. Notable neovascularization and mild inflammation at the injury site, with cellular infiltration is also increased compared to the healthy disc. These changes were most evident in the external lamellae of the AF, with cervical discs showing more severe alterations compared to lumbar sections.

By 32 weeks, cervical discs displayed severe degeneration, with extensive fissuring of the AF, pronounced deformation of the NP, and significant cellular infiltration concentrated around

the injury site. Robust bone-like formations were also observed, further highlighting the progression of degenerative changes. In both cervical and lumbar IVDs, the mature, dense fibrovascular to fibrocartilaginous tissue replaced the initial injury response. Additionally, hypertrophy of AF cells and a more extensive disruption of the cartilaginous endplates were evident. In the lumbar discs, degeneration was moderate, with deeper fissuring of the AF, a notable decrease in NP volume, and an increase in inflammatory cell infiltration, including neutrophils and lymphocytes.

Histological assessment revealed significant alterations in bone remodeling features, as evaluated through the histological scoring system (**Figure 8)**. However, no significant differences were detected between time points in either the cervical or lumbar intervertebral discs when assessed using the general histological scoring system.

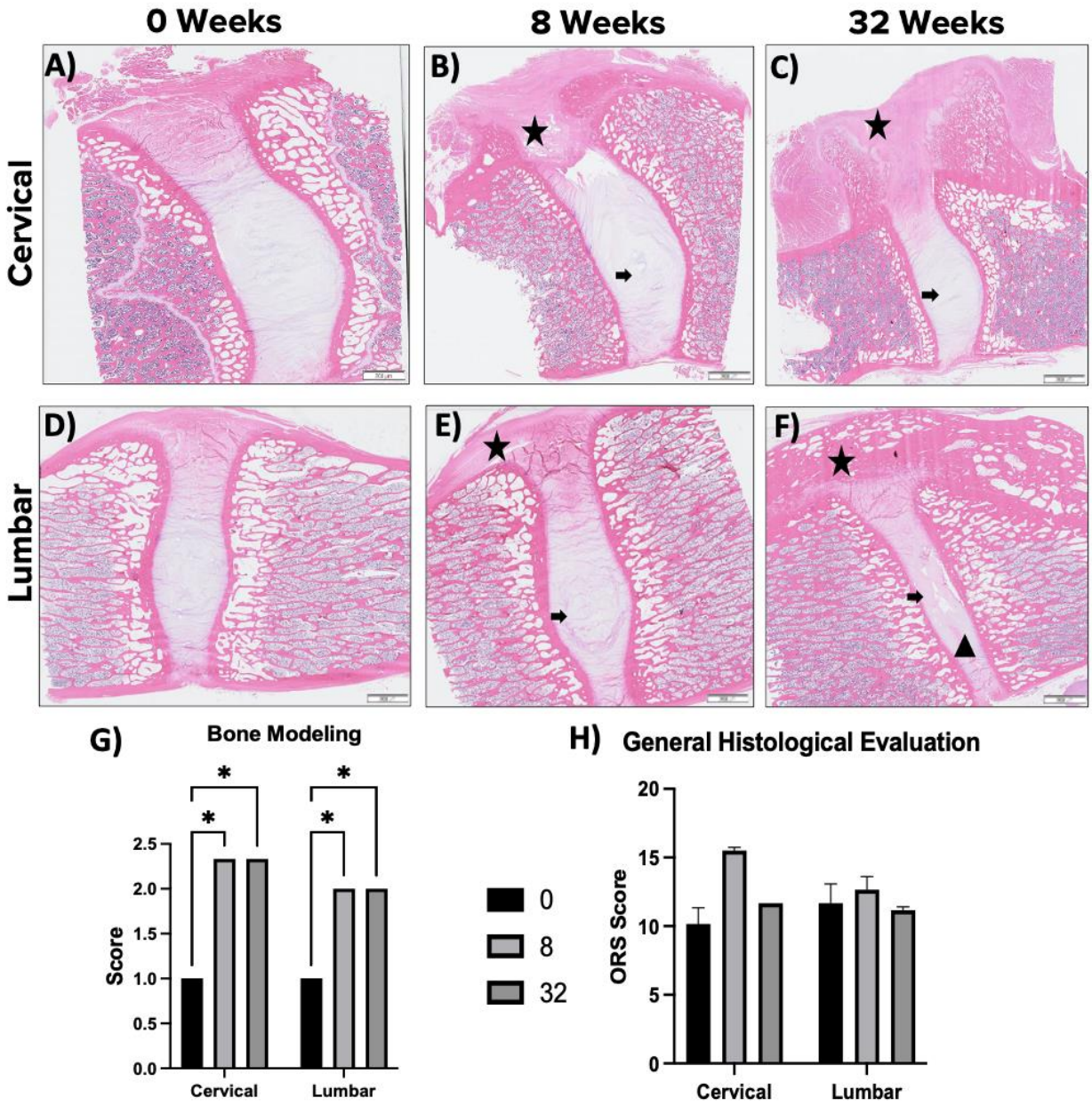

Figure 8: Representative histological images of the cervical and lumbar IVDs and their corresponding histopathological scoring across both anatomical regions are presented. Cervical (A-C) and lumbar (D-E) IVDs exhibited clear differentiation between the NP and AF at the 0-week time point, with an intact structure. By 8 and 32 weeks, distinct signs of degeneration were observed. Specifically, there was a noticeable decrease in NP organization (black arrow), clear decrease in the disc space is noted in the 32 weeks at lumbar IVD (Black arrowhead), and evident disruption of the AF fibers adjacent to the injury site with a pronounced inflammatory bone-healing response (black star). G) A detailed comparison of bone remodeling revealed statistically significant differences between the 0-week time point and both the 8- and 32-week time points for cervical and lumbar regions. However, no significant differences were observed between the cervical and lumbar IVDs. H) Histological scoring evaluation did not reveal significant changes

over time or between anatomical regions. *P<0.05, H&E, scale bar: 200 µm.

3.4.5 Comparative Proteomic profile of Annulus Fibrosus and Nucleus Pulposus

For AF samples, a total of 4,085 proteins and 32,616 peptides were identified, with a false discovery rate (FDR) of ≤1% and at least one peptide per protein. The proportion of contaminant proteins was minimal, at just 0.49%. For abundant comparison analysis only proteins with 66.7% (4/6 per group) of quantitative values were included. A total of 1152 proteins met this criterium. The residual missing values were imputed by using the 0.5 of the minimum value detected in the protein with missing data. Five percent (1086/20736) of the data was replaced. Next, data was log2 transformed before ANOVA testing, 495 proteins had Benjamini-Hochberg corrected p-value <0.05 and were considered statistically different for at least one of the groups. The abundance pairwise comparison of those proteins is shown in Table 2. Heatmaps, volcano plots the list of the top 10 proteins downregulated and upregulated in AF for each time point comparison are presented in Appendix 1.

Annulus Fibrosus Comparison	# Downregulated ↓ Proteins	# Upregulated ↑ Proteins
8 vs. 0 Weeks	97	381
32 vs. 0 Weeks	81	237
32 vs. 8 Weeks	12	3

Table 2. Pairwise comparison of proteins significantly different among times for AF tissue.

For the NP samples, a total of 3567 proteins and 30934 peptides were identified, with a

false discovery rate (FDR) ≤1% and with at least one peptide. The proportion of contaminant proteins was very low 0.50%. For the abundance comparison analysis, only proteins with quantitative values present in at least 66.7% (4 out of 6 per group) were included, resulting in 1,109 proteins meeting this criterion. Missing values (6% of the data; 1,173 out of 19,962) were imputed by assigning them 0.5 of the minimum value detected for the respective protein. Following imputation, the data was log2-transformed before ANOVA testing. A total of 146 proteins had a Benjamini-Hochberg corrected p-value <0.05 and were considered statistically different in at least one of the groups. The results of the pairwise abundance comparison for these proteins is presented in Table 3. Heatmaps, volcano plots the list of the top 10 proteins downregulated and upregulated in NP for each time point comparison are presented in Appendix 2.

Nucleus Pulposus Comparison	# Downregulated ↓ Proteins	# Upregulated ↑ Proteins
8 vs. 0 Weeks	11	104
32 vs. 0 Weeks	33	111
32 vs. 8 Weeks	12	5

Table 3. Pairwise comparison of proteins significantly different among times for NP tissue.

Overall, when comparing the number of DEPs between the AF and NP tissues from cervical and lumbar IVDs, 860 shared proteins were identified. Additionally, AF expressed 289 DEPs that were absent in NP tissue, while NP expressed 242 DEPs not found in AF tissue. Upon cross-evaluation of both tissues at the different time points, 83 DEPs were identified across all

group comparisons. The annotated genes, along with their respective enriched biological processes, are shown in **Figure 9**.

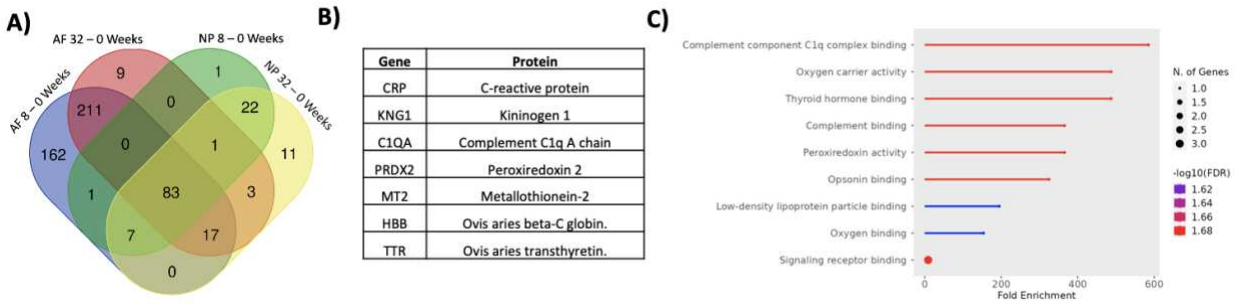

Gene	Protein
CRP	C-reactive protein
KNG1	Kininogen 1
C1QA	Complement C1q A chain
PRDX2	Peroxiredoxin 2
MT2	Metallothionein-2
HBB	Ovis aries beta-C globin.
TTR	Ovis aries transthyretin.

Figure 9: Analysis of DEPs shared between NP and AF. A) Venn diagram of the DEPs from the comparison of AF and NP from both cervical and lumbar IVDs at 0 vs 8 weeks, and 0 vs 32 weeks. B) List of 7 protein and gene identifications for the annotated DEPs shared between NP and AF across various time point comparisons. C) Top 10 enriched Gene Ontology (GO) Biological Processes associated with DEPs identified across all group comparisons.

3.4.6 Comparative Proteomic Profiling of Cervical and Lumbar IVDs

Analysis of DEPs from the AF in cervical compared to lumbar tissue samples revealed 325 proteins across three different time points. At the 32-week time point, 144 proteins were uniquely expressed. Similarly, the 8-week time point showed 37 uniquely expressed DEPs, while the 0-week (naïve) the AF expressed 83 proteins that were not identified at the other time points. Specific comparison of the DEPs from AF at specific 0, 8 and 32 weeks are shown in Table 4 and Figure 10.

Comparison AF Cervical vs Lumbar	# Downregulated ↓ Proteins	# Upregulated ↑ Proteins
0 Weeks	68	567
8 Weeks	142	446

32 Weeks	140	734

Table 4. Pairwise comparison of significantly differentially expressed proteins in AF tissue samples from cervical and lumbar regions across different time points.

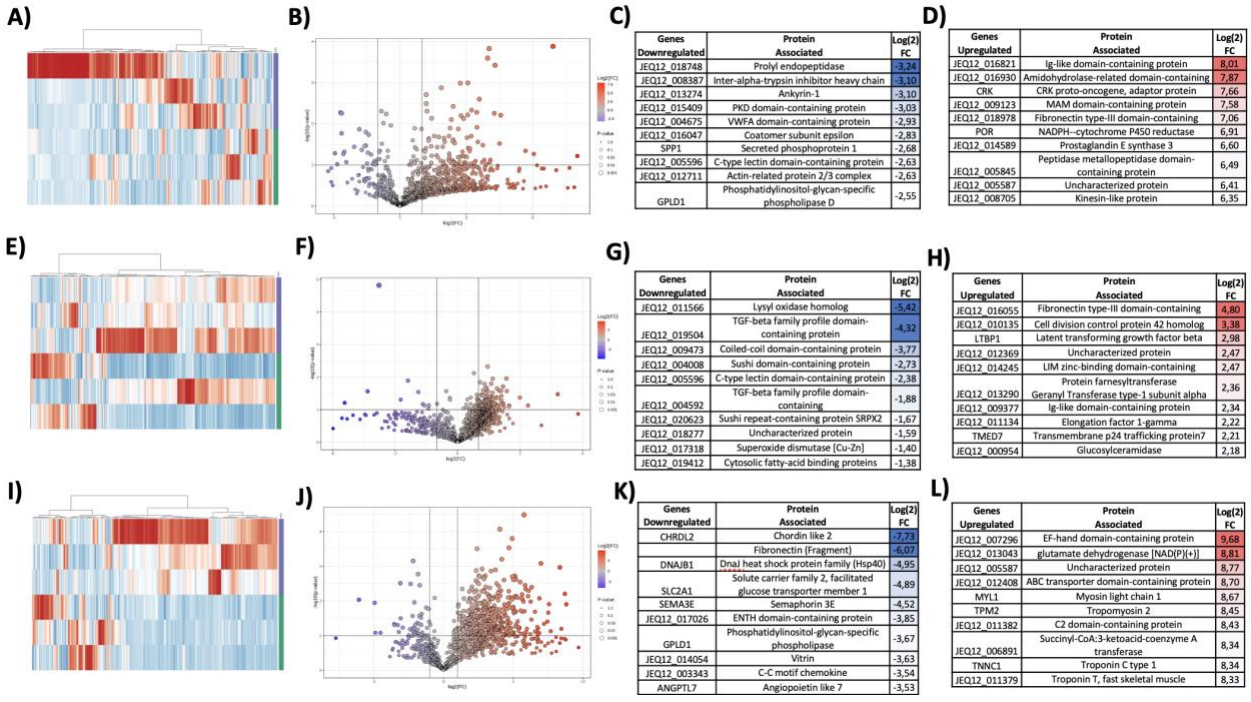

C)

Genes Downregulated	Protein Associated	Log(2) FC
JEQ12_018748	Prolyl endopeptidase	-3,24
JEQ12_008387	Inter-alpha-trypsin inhibitor heavy chain	-3,10
JEQ12_013274	Ankyrin-1	-3,10
JEQ12_015409	PKD domain-containing protein	-3,03
JEQ12_004675	VWFA domain-containing protein	-2,93
JEQ12_016047	Coatomer subunit epsilon	-2,83
SPP1	Secreted phosphoprotein 1	-2,68
JEQ12_005596	C-type lectin domain-containing protein	-2,63
JEQ12_012711	Actin-related protein 2/3 complex	-2,63
GPLD1	Phosphatidylinositol-glycan-specific phospholipase D	-2,55

D)

Genes Upregulated	Protein Associated	Log(2) FC
JEQ12_016821	Ig-like domain-containing protein	8,01
JEQ12_016930	Amidohydrolase-related domain-containing	7,87
CRK	CRK proto-oncogene, adaptor protein	7,66
JEQ12_009123	MAM domain-containing protein	7,58
JEQ12_018978	Fibronectin type-III domain-containing	7,06
POR	NADPH--cytochrome P450 reductase	6,91
JEQ12_014589	Prostaglandin E synthase 3	6,60
JEQ12_005845	Peptidase metallopeptidase domain-containing protein	6,49
JEQ12_005587	Uncharacterized protein	6,41
JEQ12_008705	Kinesin-like protein	6,35

G)

Genes Downregulated	Protein Associated	Log(2) FC
JEQ12_011566	Lysyl oxidase homolog	-5,42
JEQ12_019504	TGF-beta family profile domain-containing protein	-4,32
JEQ12_009473	Coiled-coil domain-containing protein	-3,77
JEQ12_004008	Sushi domain-containing protein	-2,73
JEQ12_005596	C-type lectin domain-containing protein	-2,38
JEQ12_004592	TGF-beta family profile domain-containing	-1,88
JEQ12_020623	Sushi repeat-containing protein SRPX2	-1,67
JEQ12_018277	Uncharacterized protein	-1,59
JEQ12_017318	Superoxide dismutase [Cu-Zn]	-1,40
JEQ12_019412	Cytosolic fatty-acid binding proteins	-1,38

H)

Genes Upregulated	Protein Associated	Log(2) FC
JEQ12_016055	Fibronectin type-III domain-containing	4,80
JEQ12_010135	Cell division control protein 42 homolog	3,38
LTBP1	Latent transforming growth factor beta	2,98
JEQ12_012369	Uncharacterized protein	2,47
JEQ12_014245	LIM zinc-binding domain-containing	2,47
JEQ12_013290	Protein farnesyltransferase Geranyl Transferase type-1 subunit alpha	2,36
JEQ12_009377	Ig-like domain-containing protein	2,34
JEQ12_011134	Elongation factor 1-gamma	2,22
TMED7	Transmembrane p24 trafficking protein7	2,21
JEQ12_000954	Glucosylceramidase	2,18

K)

Genes Downregulated	Protein Associated	Log(2) FC
CHRDL2	Chordin like 2	-7,73
	Fibronectin (Fragment)	-6,07
DNAJB1	DnaJ heat shock protein family (Hsp40)	-4,95
SLC2A1	Solute carrier family 2, facilitated glucose transporter member 1	-4,89
SEMA3E	Semaphorin 3E	-4,52
JEQ12_017026	ENTH domain-containing protein	-3,85
GPLD1	Phosphatidylinositol-glycan-specific phospholipase	-3,67
JEQ12_014054	Vitrin	-3,63
JEQ12_003343	C-C motif chemokine	-3,54
ANGPTL7	Angiopoietin like 7	-3,53

L)

Genes Upregulated	Protein Associated	Log(2) FC
JEQ12_007296	EF-hand domain-containing protein	9,68
JEQ12_013043	glutamate dehydrogenase [NAD(P)(+)]	8,81
JEQ12_005587	Uncharacterized protein	8,77
JEQ12_012408	ABC transporter domain-containing protein	8,70
MYL1	Myosin light chain 1	8,67
TPM2	Tropomyosin 2	8,45
JEQ12_011382	C2 domain-containing protein	8,43
JEQ12_006891	Succinyl-CoA:3-ketoacid-coenzyme A transferase	8,34
TNNC1	Troponin C type 1	8,34
JEQ12_011379	Troponin T, fast skeletal muscle	8,33

Figure 10: Comparison of cervical and lumbar AF proteomic results at different time points. A-D) Heatmap, volcano plot, list of proteins downregulated and upregulated showing the comparison between 8 weeks after induced IVDD and 0 weeks (control). E-H) Heatmap, volcano plot, list of proteins downregulated and upregulated showing the comparison between 32 weeks after induced IVDD and 0 weeks (control). I-L) Heatmap, volcano plot, list of proteins downregulated and upregulated showing the comparison between 32 weeks after induced IVDD and 8 weeks.

Analysis of DEPs from the NP in cervical compared to lumbar tissue samples revealed 176 proteins across three different time points. At the 32-week time point, 181 proteins were uniquely expressed. Similarly, the 8-week time point showed 120 uniquely expressed DEPs, while the 0-week (naïve) the AF expressed 58 proteins that were not identified at the other time points. Specific comparison of the DEPs from AF at specific 0, 8 and 32 weeks are shown in Table 5 and Figure

11 and Figure 12.

Comparison NP Cervical vs Lumbar	# Downregulated ↓ Proteins	# Upregulated ↑ Proteins
0 Weeks	145	205
8 Weeks	447	196
32 Weeks	601	118

Table 5. Pairwise comparison of significantly differentially expressed proteins in NP tissue samples from cervical and lumbar regions across different time points.

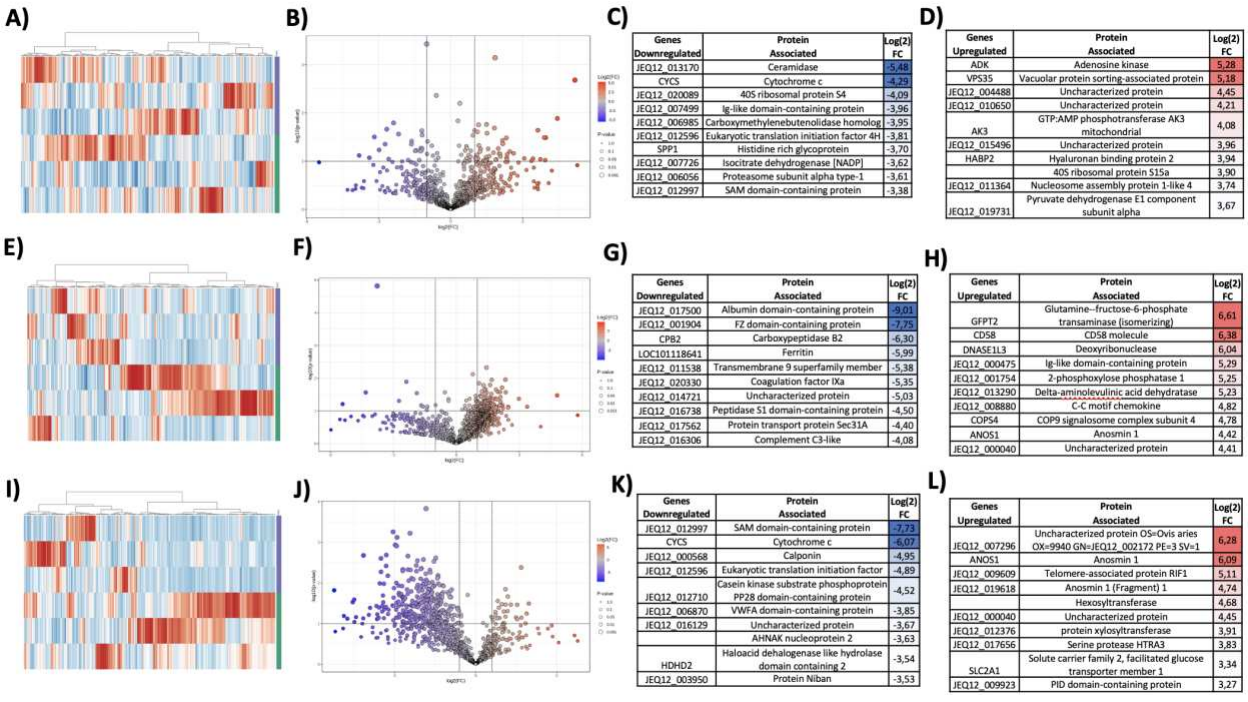

C)

Genes Downregulated	Protein Associated	Log(2) FC
JEQ12_013170	Ceramidase	-5,48
CYCS	Cytochrome c	-4,29
JEQ12_020089	40S ribosomal protein S4	-4,09
JEQ12_007499	Ig-like domain-containing protein	-3,96
JEQ12_006985	Carboxymethylenebutenolidase homolog	-3,95
JEQ12_012596	Eukaryotic translation initiation factor 4H	-3,81
SPP1	Histidine rich glycoprotein	-3,70
JEQ12_007726	Isocitrate dehydrogenase [NADP]	-3,62
JEQ12_006056	Proteasome subunit alpha type-1	-3,61
JEQ12_012997	SAM domain-containing protein	-3,38

D)

Genes Upregulated	Protein Associated	Log(2) FC
ADK	Adenosine kinase	5,28
VPS35	Vacuolar protein sorting-associated protein	5,18
JEQ12_004488	Uncharacterized protein	4,45
JEQ12_010650	Uncharacterized protein	4,21
AK3	GTP:AMP phosphotransferase AK3 mitochondrial	4,08
JEQ12_015496	Uncharacterized protein	3,96
HABP2	Hyaluronan binding protein 2	3,94
	40S ribosomal protein S15a	3,90
JEQ12_011364	Nucleosome assembly protein 1-like 4	3,74
JEQ12_019731	Pyruvate dehydrogenase E1 component subunit alpha	3,67

G)

Genes Downregulated	Protein Associated	Log(2) FC
JEQ12_017500	Albumin domain-containing protein	-9,01
JEQ12_001904	FZ domain-containing protein	-7,75
CPB2	Carboxypeptidase B2	-6,30
LOC101118641	Ferritin	-5,99
JEQ12_011538	Transmembrane 9 superfamily member	-5,38
JEQ12_020330	Coagulation factor IXa	-5,35
JEQ12_014721	Uncharacterized protein	-5,03
JEQ12_016738	Peptidase S1 domain-containing protein	-4,50
JEQ12_017562	Protein transport protein Sec31A	-4,40
JEQ12_016306	Complement C3-like	-4,08

H)

Genes Upregulated	Protein Associated	Log(2) FC
GFPT2	Glutamine--fructose-6-phosphate transaminase (isomerizing)	6,61
CD58	CD58 molecule	6,38
DNASE1L3	Deoxyribonuclease	6,04
JEQ12_000475	Ig-like domain-containing protein	5,29
JEQ12_001754	2-phosphoxylose phosphatase 1	5,25
JEQ12_013290	Delta-aminolevulinic acid dehydratase	5,23
JEQ12_008880	C-C motif chemokine	4,82
COPS4	COP9 signalosome complex subunit 4	4,78
ANOS1	Anosmin 1	4,42
JEQ12_000040	Uncharacterized protein	4,41

K)

Genes Downregulated	Protein Associated	Log(2) FC
JEQ12_012997	SAM domain-containing protein	-7,73
CYCS	Cytochrome c	-6,07
JEQ12_000568	Calponin	-4,95
JEQ12_012596	Eukaryotic translation initiation factor	-4,89
JEQ12_012710	Casein kinase substrate phosphoprotein PP28 domain-containing protein	4,52
JEQ12_006870	VWFA domain-containing protein	-3,85
JEQ12_016129	Uncharacterized protein	-3,67
	AHNAK nucleoprotein 2	-3,63
HDHD2	Haloacid dehalogenase like hydrolase domain containing 2	-3,54
JEQ12_003950	Protein Niban	-3,53

L)

Genes Upregulated	Protein Associated	Log(2) FC
JEQ12_007296	Uncharacterized protein OS=Ovis aries OX=9940 GN=JEQ12_002172 PE=3 SV=1	6,28
ANOS1	Anosmin 1	6,09
JEQ12_009609	Telomere-associated protein RIF1	5,11
JEQ12_019618	Anosmin 1 (Fragment) 1	4,74
	Hexosyltransferase	4,68
JEQ12_000040	Uncharacterized protein	4,45
JEQ12_012376	protein xylosyltransferase	3,91
JEQ12_017656	Serine protease HTRA3	3,83
SLC2A1	Solute carrier family 2, facilitated glucose transporter member 1	3,34
JEQ12_009923	PID domain-containing protein	3,27

Figure 11: Comparison of cervical and lumbar NP proteomic results at different time points. A-D) Heatmap, volcano plot, list of proteins downregulated and upregulated showing the comparison between 8 weeks after induced IVDD and 0 weeks (control). E-H) Heatmap, volcano plot, list of proteins downregulated and upregulated showing the comparison between 32 weeks after induced IVDD and 0 weeks (control). I-L) Heatmap, volcano plot, list of proteins downregulated and upregulated showing the comparison between 32 weeks after induced IVDD and 8 weeks.

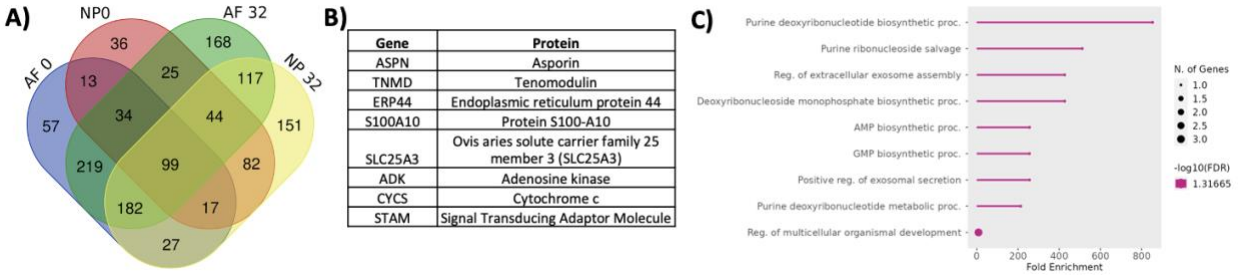

Gene	Protein
ASPN	Asporin
TNMD	Tenomodulin
ERP44	Endoplasmic reticulum protein 44
S100A10	Protein S100-A10
SLC25A3	Ovis aries solute carrier family 25 member 3 (SLC25A3)
ADK	Adenosine kinase
CYCS	Cytochrome c
STAM	Signal Transducing Adaptor Molecule

Figure 12: Analysis of DEPs shared between cervical and Lumbar for both NP and AF. A) Venn diagram of AF and NP differentially expressed proteins (DEPs) at 0 and 32 weeks after induced IVDD. B) List of 8 protein and gene identifications for the annotated DEPs shared between NP and AF across various time point comparisons. C) Top 10 enriched Gene Ontology (GO) Biological Processes associated with DEPs identified across all group comparisons.

3. 5. Discussion

This study, to our knowledge, is the first to provide evidence of the differences between cervical and lumbar AF and NP tissues. Specifically, the proteomic profiling of AF and NP in these two anatomical regions is the first report of such data for ovine IVDs. Key findings reveal a similar progression of IVDD in both cervical and lumbar IVDs, particularly in relation to the surgical approach used. Our results also demonstrate that the cervical ovine model of IVDD is just as valuable as the more commonly studied lumbar model. This cervical model could serve as a crucial tool to explore the specific differences in IVDD and aid in the development of new medical or surgical interventions tailored to each anatomical region, considering the distinct kinematics of the cervical and lumbar spine. Overall, these findings suggest that both cervical and lumbar IVDs exhibit a continuous and comparable progression of disc degeneration in the ovine model.

Gross descriptions of degenerated IVDs in ovine models have been previously reported. However, our study provides clear evidence of IVDD progression at two distinct time points following induction compared with naïve IVDs. While cervical IVDs in large animal models have

often been used to evaluate various scaffolds and suture materials for disc herniation and IVDD, no prior study has reported a gross evaluation of cervical IVDs and compared it with lumbar IVDs at equivalent stages of induced degeneration. We observed gross characteristic changes, particularly the discoloration of the AF and NP, along with a loss of clear distinction between the two tissues, are consistent with the hallmark signs of degeneration in human IVDs.

Imaging evaluations revealed similar results between the cervical and lumbar regions. DHI decreased immediately after the surgical induction of IVDD in both tissues, with statistically significant differences observed. Notably, to our knowledge, DHI has not been previously reported for cervical discs, making the values obtained in this study potential reference points for assessing the progression of disc degeneration. However, further refinement of this measurement method is needed, particularly considering the differences in vertebral body length, a characteristic feature of the cervical spine. Interestingly, when comparing DHI between cervical and lumbar regions, no statistically significant differences were found, indicating a similar and comparable trend in progression of degeneration related to the loss of disc height in cervical and lumbar IVDs.

Regarding MRI, images were obtained using consistent sequence parameters across all animals in the study. These images were of sufficient quality to reliably evaluate the progression of degeneration using the Pfirrmann grading system. This evaluation revealed a similar trend in IVDD progression for both cervical and lumbar IVDs. Interestingly, when comparing Pfirrmann grades between cervical and lumbar regions, no statistically significant differences were found, indicating a comparable progression of IVDD in both areas.

As IDD progresses, the structure of the IVD becomes increasingly disorganized. Histologically, this is characterized by a loss of distinction between the NP and AF, a reduction in cell density, changes in NP shape, and progressive disorganization of the AF. Our findings reveal

similar histological signs of IDD progression in both cervical and lumbar IVDs, consistent with previous reports of IDD in ovine models using various induction methods. However, the histological changes observed in this study highlight the need for a more refined model to accurately capture the specific alterations that occur in ovine IVDs following traumatic injury. Notably, changes related to bone tissue formation at the injury site are not adequately addressed by current scoring systems, potentially leading to misinterpretations when compared to baseline features. Another factor to consider is spontaneous, age-related IDD, which has been documented in skeletally mature ovine, such as those used in this study. This may result in higher initial scores for naïve IVDs compared to naïve, healthy discs in other species. Additionally, the histological processing could affect the proper visualization of the respective induced degeneration changes, especially considering the differences in the surgical approaches for the cervical and lumbar regions. A customized histological section needs also considered depending on or the type and direction of the lesion. The histological characterization of cervical IVDs in this study provides valuable insights for future researchers aiming to understand the progression of IDD and evaluate potential treatments, particularly their effects on the histological features of these tissues. Our findings further support the notion that cervical and lumbar IVDs exhibit similar signs of degeneration, even at different time points.

This is the first study to assess proteomic profile and protein changes in the cervical and lumbar IVDs in the same subjects over time using proteomic analysis in a longitudinal sheep model of IVDD. Our initial exploration of the sheep IVDs proteome resulted in the identification of a vast number of proteins. Particularly, 495 and 146 DEPs were identified for AF and NP respectively. When cross comparison was achieved between both IVD tissues at different time points, 83 were observed to be shared between each time point. Seven of these proteins were

annotated (CRP, KNG1, C1QA, PRDX2, MT2, HBB, TTR, HRG, TAGLN2, SERPINF2) and are therefore speculated to be key in IVDD progression in the sheep.

These results will enhance the established proteomic data comparisons between species, particularly those used as animal models for IVDD (263,264). For instance, the proteomic profile of the canine model of IVDD has been published, demonstrating how these models are valuable for studying IVD degeneration and evaluating potential biological therapies (264). Our findings now allow the inclusion of the proteomic profile from the ovine model at different stages of induced IVDD. Similar studies in small animal models have provided reference datasets of normal, healthy rats and the proteomic changes associated with degeneration (265). Identifying the similarities and differences between DEP at various stages of degeneration will help determine the most appropriate animal models for IVDD research. Furthermore, comparative proteomic profiling could be conducted with human IVDD profiles to translate findings and identify potential proteins and metabolic pathways that may serve as therapeutic targets (266–269).

Notably, C-reactive protein (CRP), an acute-phase protein commonly used as a biomarker to assess the severity and progression of infectious and inflammatory diseases (270). Given its significance in inflammatory processes, studies have explored its potential as a biomarker for IVD injuries or to predict post-surgical treatment of IVD pathologies in dogs (271,272). Recently, has been identified in its monomeric form in human AF and NP tissues. Its presence was shown to upregulate the expression of nitric oxide synthase 2 (NOS2), cyclooxygenase 2 (COX2), matrix metalloproteinase 13 (MMP13), vascular cell adhesion molecule 1 (VCAM1), interleukin (IL)-6, IL-8, and lipocalin 2 (LCN2) in human AF and NP cells (273). Similarly, the relevance of Kininogen 1 (KNG1) in the human disc has been reported. This gene has been determinate as one of the critical genes in NP cells isolated from degenerated human IVDs using bioinformatics

analysis. Expression of KNG1 has been linked to the progression of IVDD, particularly associated with several key functions in degenerated human NP cells, including defense response, vasodilation, and cation homeostasis (274).

Another key gene identified was Complement C1q A chain (C1QA). Recent studies have highlighted the crucial role of the complement system in IVDD, and C1QA, along with other complement components, has been well documented in human IVD samples. Specifically, elevated levels of C1Q have been observed in IVDs with Modic changes, which involve alterations in the bone and cartilage endplates (275,276). The repeated detection of complement proteins strongly suggests the consistent activation of the coagulation and complement cascade pathways, as indicated by KEGG enrichment analyses. This approach provided valuable insights into the biological pathways enriched among the DEPs, offering a more comprehensive understanding of their functional significance in the context of IVDD progression. The identification of complement proteins and their associated pathways in the ovine cervical and lumbar models of IVDD underscores critical inflammatory mechanisms driving disc degeneration, potentially revealing novel therapeutic targets for intervention (277).

The comparison of DEPs between NP and AF in cervical and lumbar IVDs across different time points revealed distinct patterns. Specifically, AF exhibited a trend of having more upregulated than downregulated DEPs at various time points. A similar trend was observed in NP at 0 weeks; however, at 8 and 32 weeks, NP showed more downregulated than upregulated proteins. In a cross-comparison of DEPs from the 0 vs 8 weeks and 0 vs 32 weeks groups for both cervical and lumbar regions, 99 DEPs were identified as shared across all comparisons. Of these shared proteins, 8 genes (ASPN, TNMD, ERP44, S100A10, SLC25A3, ADK, CYCS, and STAM) were annotated, suggesting their key roles in IVDD progression, with notable presence without

distinction of the anatomical region.

Among these genes, highlight the presence of Asporin (ASPN), this encoding for an ECM protein belonging to a small leucine rich proteoglycan, with recognized elevated expression during IVDD and osteoarthritis (278,279). This protein binds collagen and calcium, thus inducing collagen mineralization (280). Additionally, Asporin is known for the regulation of chondrogenesis by inhibiting transforming growth factor-β (TGF-β) gene expression that is commonly expressed in cartilaginous tissues (281). Asporin, has been shown to be upregulated with age and in degenerative disc conditions (282,283). Studies indicate an association between carrying the D14 allele of ASPN and the development of IVDD. This link is particularly significant in Asian populations, with research showing a strong correlation between ASPN variations and lumbar disc degeneration (279). The presence of specific ASPN polymorphisms suggests a genetic predisposition to disc degeneration, emphasizing its role in the etiology of spinal disorders.

In vivo studies have explored the role of Asporin in LBP by generating mouse models that overexpress the human ASPN gene in the IVD. These studies demonstrated that overexpression of ASPN induces degenerative changes in the IVD (284). Given that Asporin levels increase during IVDD, it suggests a possible positive feedback mechanism, positioning ASPN as a genetic risk factor for IVDD. Further detailed analyses are necessary, but current evidence suggests that the signaling pathways associated with Asporin regulation present promising potential for therapeutic interventions. Different studies have reviewed Asporin as a candidate protein for IVDD treatment, suggesting that manipulating these pathways could help modulate ASPN involvement in the progression of disc degeneration (285,286). Such therapeutic approaches could address the underlying mechanisms of disc degeneration, providing new avenues for treatment and disease management.

The small sample size is a limitation of this study and may have contributed to the lack of statistically significant differences in the histological evaluation. However, this finding is consistent with previous research on the ovine model of IVDD, where histological scores showed no significant differences following induced AF defects (216). These results suggest that both the cervical and lumbar regions behave similarly in terms of histological degeneration and tissue repair. This similarity highlights the challenges in detecting certain degenerative changes using histological scoring methods alone and suggests the need for complementary evaluation techniques to capture subtle differences. Additionally, the lack of correlation between histological findings, gross morphological, and MRI changes suggests that the histological scoring system may lack the sensitivity needed to detect subtle degenerative changes. Future studies should consider utilizing a modified or alternative histological scoring system to capture subtle changes that were apparent in the gross and imaging assessments but were not reflected in the histological analysis. Addressing this gap could enhance the evaluation of tissue degeneration and provide a more comprehensive understanding of the observed structural alterations. Despite the relatively small number of animals, the study was able to provide compelling evidence of IVDD following ventral and lateral induction methods in the cervical and lumbar IVDs, respectively. Gross morphological changes, reductions in DHI, and elevated Pfirrmann grades provided robust indicators of IVDD in both regions.

The proteomic evaluation revealed several DEPs, especially inflammatory molecules specific to AF and NP during disc degeneration, highlighting their potential as biomarkers for early diagnosis. These biomarkers could serve as crucial evidence-based tools to guide preventive measures, potentially reducing reliance on surgical interventions. Furthermore, they could enable the ongoing monitoring of disease progression, significantly improving the management and

treatment of disc degeneration (287). Especially, these results could be used to increase the knowledge about similarities with human IDD. Comparison of proteomic databases could help to understand the similarities and differences in the progression of IDD, and the specific translational proteomic profile of the ovine model of IDD. To strengthen these findings, future studies should focus on larger sample sizes and include adjacent control IVDs for comparison. This would offer deeper insights into the specific differences between cervical and lumbar IVDD, ultimately improving our understanding of their relevance as models for IVDD treatment. By identifying distinct molecular and structural variations, researchers could develop more targeted therapeutic interventions tailored to each anatomical region.

3.6. References

1. Lotz JC. Animal Models of Intervertebral Disc Degeneration. Spine (Phila Pa 1976). 2004 Dec 1;29(23):2742–50.
2. Jin L, Balian G, Li XJ. Animal models for disc degeneration-an update. Vol. 33, Histology and Histopathology. Histology and Histopathology; 2018. p. 543–54.
3. Lotz JC. Animal models of intervertebral disc degeneration: Lessons learned. Spine (Phila Pa 1976). 2004;29(23):2742–50.
4. Alini M, Eisenstein SM, Ito K, Little C, Kettler AA, Masuda K, et al. Are animal models useful for studying human disc disorders/degeneration? European Spine Journal [Internet]. 2008 Jan 14;17(1):2–19. Available from: http://link.springer.com/10.1007/s00586-007-0414-y
5. Shi C, Qiu S, Riester SM, Das V, Zhu B, Wallace AA, et al. Animal models for studying the etiology and treatment of low back pain. Vol. 36, Journal of Orthopaedic Research. John

Wiley and Sons Inc.; 2018. p. 1305–12.

6. Daly C, Ghosh P, Jenkin G, Oehme D, Goldschlager T. A Review of Animal Models of Intervertebral Disc Degeneration: Pathophysiology, Regeneration, and Translation to the Clinic. Biomed Res Int. 2016;2016:1–14.

7. Reitmaier S, Graichen F, Shirazi-Adl A, Schmidt H. Separate the Sheep from the Goats: Use and Limitations of Large Animal Models in Intervertebral Disc Research. Journal of Bone and Joint Surgery - American Volume. 2017;99(19):e102.

8. Lim KZ, Daly CD, Ghosh P, Jenkin G, Oehme D, Cooper-White J, et al. Ovine Lumbar Intervertebral Disc Degeneration Model Utilizing a Lateral Retroperitoneal Drill Bit Injury. J Vis Exp. 2017;(123):55753.

9. Martini L, Fini M, Giavaresi G, Giardino R. Sheep model in orthopedic research: a literature review. Comp Med [Internet]. 2001 Aug;51(4):292–9. Available from: http://www.ncbi.nlm.nih.gov/pubmed/11924786

10. Reid JE, Meakin JR, Robins SP, Skakle JMS, Hukins DWL. Sheep lumbar intervertebral discs as models for human discs. Clinical Biomechanics. 2002 May 1;17(4):312–4.

11. Constant C, Hom WW, Nehrbass D, Carmel EN, Albers CE, Deml MC, et al. Comparison and optimization of sheep in vivo intervertebral disc injury model. JOR Spine. 2022 Jun 1;5(2).

12. Nisolle JF, Bihin B, Kirschvink N, Neveu F, Clegg P, Dugdale A, et al. Prevalence of age-related changes in ovine lumbar intervertebral discs during computed tomography and magnetic resonance imaging. Comp Med [Internet]. 2016 Aug 1 [cited 2022 Dec 13];66(4):300–7. Available from: /pmc/articles/PMC4983172/

13. Bouhsina N, Decante C, Hardel JB, Madec S, Abadie J, Hamel A, et al. Correlation between

magnetic resonance, x-ray imaging alterations and histological changes in an ovine model of age-related disc degeneration. Eur Cell Mater. 2021 Jul 1;42:166–78.

14. Borem R, Walters J, Madeline A, Madeline L, Gill S, Easley J, et al. Characterization of chondroitinase-induced lumbar intervertebral disc degeneration in a sheep model intended for assessing biomaterials. J Biomed Mater Res A. 2020;109(7):1–15.

15. Easley NE, Wang M, McGrady LM, Toth JM. Biomechanical and radiographic evaluation of an ovine model for the human lumbar spine. Proc Inst Mech Eng H [Internet]. 2008 Jun 1;222(6):915–22. Available from: http://journals.sagepub.com/doi/10.1243/09544119JEIM345

16. Yu CC, Hao DJ, Huang DG, Qian LX, Feng H, Li HK, et al. Biomechanical Analysis of a Novel Prosthesis Based on the Physiological Curvature of Endplate for Cervical Disc Replacement. Zhao C, editor. PLoS One [Internet]. 2016 Jun 29;11(6):e0158234. Available from: https://dx.plos.org/10.1371/journal.pone.0158234

17. Daentzer D, Willbold E, Kalla K, Bartsch I, Masalha W, Hallbaum M, et al. Bioabsorbable Interbody Magnesium-Polymer Cage: degradation kinetics, biomechanical stiffness, and histological findings from an ovine cervical spine fusion model. Spine (Phila Pa 1976). 2014 Sep;39(20):E1220–7.

18. Lee NN, Salzer E, Bach FC, Bonilla AF, Cook JL, Gazit Z, et al. A comprehensive tool box for large animal studies of intervertebral disc degeneration. JOR Spine. 2021;(July 2020):1–36.

19. Masuda K, Aota Y, Muehleman C, Imai Y, Okuma M, Thonar EJ, et al. A novel rabbit model of mild, reproducible disc degeneration by an anulus needle puncture: Correlation between the degree of disc injury and radiological and histological appearances of disc

degeneration. Spine (Phila Pa 1976). 2005;30(1):5–14.

20. Pfirrmann CWA, Metzdorf A, Zanetti M, Hodler J, Boos N. Magnetic resonance classification of lumbar intervertebral disc degeneration. Spine (Phila Pa 1976). 2001;26(17):1873–8.

21. Lee NN, Salzer E, Bach FC, Bonilla AF, Cook JL, Gazit Z, et al. A comprehensive tool box for large animal studies of intervertebral disc degeneration. JOR Spine. 2021;(July 2020):1–36.

22. Chong J, Xia J. MetaboAnalystR: an R package for flexible and reproducible analysis of metabolomics data. Bioinformatics. 2018 Dec 15;34(24):4313–4.

23. Ge SX, Jung D, Yao R. ShinyGO: a graphical gene-set enrichment tool for animals and plants. Bioinformatics. 2020 Apr 15;36(8):2628–9.

24. McCann MR, Patel P, Frimpong A, Xiao Y, Siqueira WL, Séguin CA. Proteomic Signature of the Murine Intervertebral Disc. PLoS One. 2015 Feb 17;10(2):e0117807.

25. Erwin WM, DeSouza L, Funabashi M, Kawchuk G, Karim MZ, Kim S, et al. The biological basis of degenerative disc disease: proteomic and biomechanical analysis of the canine intervertebral disc. Arthritis Res Ther. 2015 Dec 5;17(1):240.

26. He S, Zhou X, Yang G, Zhou Z, Zhang Y, Shao X, et al. Proteomic comparison between physiological degeneration and needle puncture model of disc generation disease. European Spine Journal [Internet]. 2022 Nov 16;31(11):2920–34. Available from: https://link.springer.com/10.1007/s00586-022-07284-x

27. Tam V, Chen P, Yee A, Solis N, Klein T, Kudelko M, et al. DIPPER, a spatiotemporal proteomics atlas of human intervertebral discs for exploring ageing and degeneration dynamics. Elife. 2020 Dec 31;9.

28. Ye D, Liang W, Dai L, Zhou L, Yao Y, Zhong X, et al. Comparative and quantitative proteomic analysis of normal and degenerated human annulus fibrosus cells. Clin Exp Pharmacol Physiol. 2015 May 23;42(5):530–6.

29. Qiu C, Wu X, Bian J, Ma X, Zhang G, Guo Z, et al. Differential proteomic analysis of fetal and geriatric lumbar nucleus pulposus: immunoinflammation and age-related intervertebral disc degeneration. BMC Musculoskelet Disord. 2020 Dec 2;21(1):339.

30. Sarath Babu N, Krishnan S, Brahmendra Swamy C V., Venkata Subbaiah GP, Gurava Reddy A V., Idris MM. Quantitative proteomic analysis of normal and degenerated human intervertebral disc. The Spine Journal. 2016 Aug;16(8):989–1000.

31. Jha R, Bernstock JD, Chalif JI, Hoffman SE, Gupta S, Guo H, et al. Updates on Pathophysiology of Discogenic Back Pain. J Clin Med. 2023 Nov 2;12(21):6907.

32. Foreman M, Vettorato E, Caine A, Monti P, Cherubini GB, Eminaga S. Serum C-reactive protein in dogs with paraplegia secondary to acute intervertebral disc extrusion. J Vet Intern Med. 2021 Jul 3;35(4):1857–64.

33. Trub SA, Bush WW, Paek M, Cuff DE. Use of C-reactive protein concentration in evaluation of diskospondylitis in dogs. J Vet Intern Med. 2021 Jan 14;35(1):209–16.

34. Ruiz-Fernández C, Ait Eldjoudi D, González-Rodríguez M, Cordero Barreal A, Farrag Y, García-Caballero L, et al. Monomeric CRP regulates inflammatory responses in human intervertebral disc cells. Bone Joint Res. 2023 Mar 8;12(3):189–98.

35. Zhu Z, Chen G, Jiao W, Wang D, Cao Y, Zhang Q, et al. Identification of critical genes in nucleus pulposus cells isolated from degenerated intervertebral discs using bioinformatics analysis. Mol Med Rep. 2017 Jan;16(1):553–64.

36. Heggli I, Laux CJ, Mengis T, Karol A, Cornaz F, Herger N, et al. Modic type 2 changes are

fibroinflammatory changes with complement system involvement adjacent to degenerated vertebral endplates. JOR Spine. 2023 Mar 23;6(1).

37. Rajasekaran S, Soundararajan DCR, Nayagam SM, Tangavel C, Raveendran M, Thippeswamy PB, et al. Modic changes are associated with activation of intense inflammatory and host defense response pathways – molecular insights from proteomic analysis of human intervertebral discs. The Spine Journal. 2022 Jan;22(1):19–38.

38. Heggli I, Teixeira GQ, Iatridis JC, Neidlinger-Wilke C, Dudli S. The role of the complement system in disc degeneration and <scp>Modic</scp> changes. JOR Spine. 2024 Mar 2;7(1).

39. Eskola PJ, Lemmelä S, Kjaer P, Solovieva S, Männikkö M, Tommerup N, et al. Genetic Association Studies in Lumbar Disc Degeneration: A Systematic Review. PLoS One. 2012 Nov 21;7(11):e49995.

40. Song YQ, Cheung KMC, Ho DWH, Poon SCS, Chiba K, Kawaguchi Y, et al. Association of the Asporin D14 Allele with Lumbar-Disc Degeneration in Asians. The American Journal of Human Genetics. 2008 Mar;82(3):744–7.

41. Boskey AL, Robey PG. The Regulatory Role of Matrix Proteins in Mineralization of Bone. In: Osteoporosis. Elsevier; 2013. p. 235–55.

42. Fiani B, Covarrubias C, Jarrah R. Genetic Predictors of Early-Onset Spinal Intervertebral Disc Degeneration: Part Two of Two. Cureus. 2021 May 22;

43. Ohnishi T, Novais EJ, Risbud M V. Alterations in ECM signature underscore multiple sub-phenotypes of intervertebral disc degeneration. Matrix Biol Plus. 2020 May;6–7:100036.

44. Näkki A, Battié MC, Kaprio J. Genetics of disc-related disorders: current findings and lessons from other complex diseases. European Spine Journal. 2014 Jun 10;23(S3):354–63.

45. Ma S, Lee AK, Yip SM, Cynthia C, Kudelko M, Zhang JY, et al. Asporin Alters Tgf-B

Signaling And Ecm Biology As A Genetic Risk Factor For Intervertebral Disc Degeneration. Osteoarthritis Cartilage. 2022 Apr;30:S184.

46. TIAN W, ZHENG S, JIANG X zhou, WU C ai, WANG N, ZHAO D hui. Asporin, a candidate protein for treatment of disc degenerative disease. Chin Med J (Engl). 2013 Jan 20;126(2):369–72.

47. Rajasekaran S, Soundararajan DCR, Tangavel C, Nayagam SM, K S SV, R S, et al. Uncovering molecular targets for regenerative therapy in degenerative disc disease: do small leucine-rich proteoglycans hold the key? The Spine Journal. 2021 Jan;21(1):5–19.

48. Rajasekaran S, Tangavel C, K.S. SVA, Soundararajan DCR, Nayagam SM, Matchado MS, et al. Inflammaging determines health and disease in lumbar discs—evidence from differing proteomic signatures of healthy, aging, and degenerating discs. The Spine Journal. 2020 Jan;20(1):48–59.

Appendix 1.

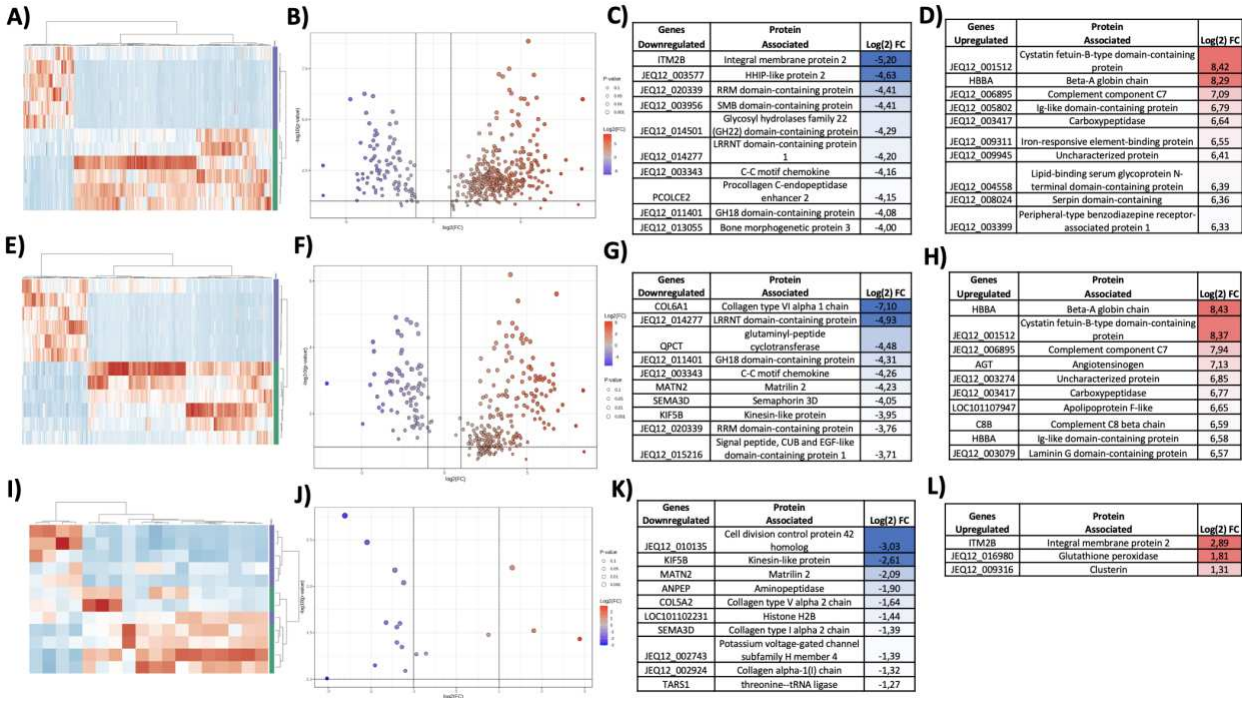

C)

Genes Downregulated	Protein Associated	Log(2) FC
ITM2B	Integral membrane protein 2	-5,20
JEQ12_003577	HHIP-like protein 2	-4,63
JEQ12_020339	RRM domain-containing protein	-4,41
JEQ12_003956	SMB domain-containing protein	-4,41
JEQ12_014501	Glycosyl hydrolases family 22 (GH22) domain-containing protein	-4,29
JEQ12_014277	LRRNT domain-containing protein 1	-4,20
JEQ12_003343	C-C motif chemokine	-4,16
PCOLCE2	Procollagen C-endopeptidase enhancer 2	-4,15
JEQ12_011401	GH18 domain-containing protein	-4,08
JEQ12_013055	Bone morphogenetic protein 3	-4,00

D)

Genes Upregulated	Protein Associated	Log(2) FC
JEQ12_001512	Cystatin fetuin-B-type domain-containing protein	8,42
HBBA	Beta-A globin chain	8,29
JEQ12_006895	Complement component C7	7,09
JEQ12_005802	Ig-like domain-containing protein	6,79
JEQ12_003417	Carboxypeptidase	6,64
JEQ12_009311	Iron-responsive element-binding protein	6,55
JEQ12_009945	Uncharacterized protein	6,41
JEQ12_004558	Lipid-binding serum glycoprotein N-terminal domain-containing protein	6,39
JEQ12_008024	Serpin domain-containing	6,36
JEQ12_003399	Peripheral-type benzodiazepine receptor-associated protein 1	6,33

G)

Genes Downregulated	Protein Associated	Log(2) FC
COL6A1	Collagen type VI alpha 1 chain	-7,10
JEQ12_014277	LRRNT domain-containing protein	-4,93
QPCT	glutaminyl-peptide cyclotransferase	-4,48
JEQ12_011401	GH18 domain-containing protein	-4,31
JEQ12_003343	C-C motif chemokine	-4,26
MATN2	Matrilin 2	-4,23
SEMA3D	Semaphorin 3D	-4,05
KIF5B	Kinesin-like protein	-3,95
JEQ12_020339	RRM domain-containing protein	-3,76
JEQ12_015216	Signal peptide, CUB and EGF-like domain-containing protein 1	-3,71

H)

Genes Upregulated	Protein Associated	Log(2) FC
HBBA	Beta-A globin chain	8,43
JEQ12_001512	Cystatin fetuin-B-type domain-containing protein	8,37
JEQ12_006895	Complement component C7	7,94
AGT	Angiotensinogen	7,13
JEQ12_003274	Uncharacterized protein	6,85
JEQ12_003417	Carboxypeptidase	6,77
LOC101107947	Apolipoprotein F-like	6,65
C8B	Complement C8 beta chain	6,59
HBBA	Ig-like domain-containing protein	6,58
JEQ12_003079	Laminin G domain-containing protein	6,57

K)

Genes Downregulated	Protein Associated	Log(2) FC
JEQ12_010135	Cell division control protein 42 homolog	-3,03
KIF5B	Kinesin-like protein	-2,61
MATN2	Matrilin 2	-2,09
ANPEP	Aminopeptidase	-1,90
COL5A2	Collagen type V alpha 2 chain	-1,64
LOC101102231	Histone H2B	-1,44
SEMA3D	Collagen type I alpha 2 chain	-1,39
JEQ12_002743	Potassium voltage-gated channel subfamily H member 4	-1,39
JEQ12_002924	Collagen alpha-1(I) chain	-1,32
TARS1	threonine--tRNA ligase	-1,27

L)

Genes Upregulated	Protein Associated	Log(2) FC
ITM2B	Integral membrane protein 2	2,89
JEQ12_016980	Glutathione peroxidase	1,81
JEQ12_009316	Clusterin	1,31

Figure S1: Comparative analysis of the upregulated and downregulated AF proteins at different time points. A- D) Heatmap, volcano plot, list of proteins downregulated and upregulated showing the comparison between 8 weeks after induced IVDD and 0 weeks (control). E-H) Heatmap, volcano plot, list of proteins downregulated and upregulated showing the comparison between 32 weeks after induced IVDD and 0 weeks (control). I-L) Heatmap, volcano plot, list of proteins downregulated and upregulated showing the comparison between 32 weeks after induced IVDD and 8 weeks.

Appendix 2.

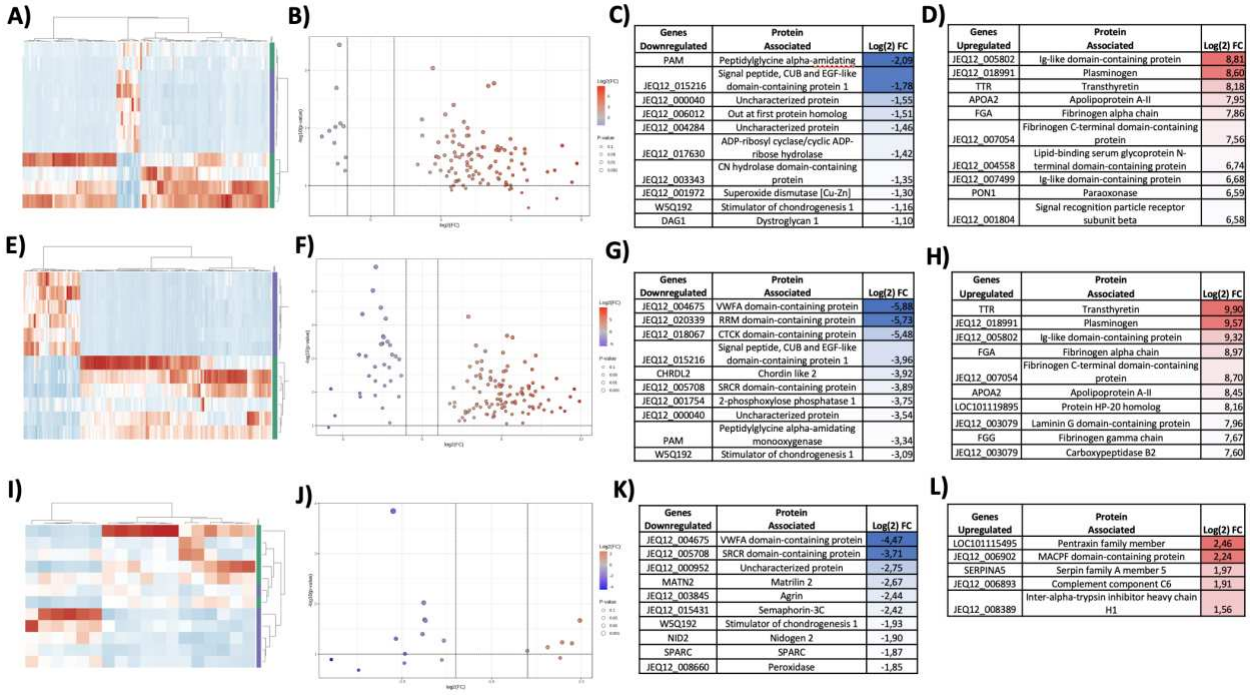

C)

Genes Downregulated	Protein Associated	Log(2) FC
PAM	Peptidylglycine alpha-amidating	-2,09
JEQ12_015216	Signal peptide, CUB and EGF-like domain-containing protein 1	-1,78
JEQ12_000040	Uncharacterized protein	-1,55
JEQ12_006012	Out at first protein homolog	-1,51
JEQ12_004284	Uncharacterized protein	-1,46
JEQ12_017630	ADP-ribosyl cyclase/cyclic ADP-ribose hydrolase	-1,42
JEQ12_003343	CN hydrolase domain-containing protein	-1,35
JEQ12_001972	Superoxide dismutase [Cu-Zn]	-1,30
WSQ192	Stimulator of chondrogenesis 1	-1,16
DAG1	Dystroglycan 1	-1,10

D)

Genes Upregulated	Protein Associated	Log(2) FC
JEQ12_005802	Ig-like domain-containing protein	8,81
JEQ12_018991	Plasminogen	8,60
TTR	Transthyretin	8,18
APOA2	Apolipoprotein A-II	7,95
FGA	Fibrinogen alpha chain	7,86
JEQ12_007054	Fibrinogen C-terminal domain-containing protein	7,56
JEQ12_004558	Lipid-binding serum glycoprotein N-terminal domain-containing protein	6,74
JEQ12_007499	Ig-like domain-containing protein	6,68
PON1	Paraoxonase	6,59
JEQ12_001804	Signal recognition particle receptor subunit beta	6,58

G)

Genes Downregulated	Protein Associated	Log(2) FC
JEQ12_004675	VWFA domain-containing protein	-5,88
JEQ12_020339	RRM domain-containing protein	-5,73
JEQ12_018067	CTCK domain-containing protein	-5,48
JEQ12_015216	Signal peptide, CUB and EGF-like domain-containing protein 1	-3,96
CHRDL2	Chordin like 2	-3,92
JEQ12_005708	SRCR domain-containing protein	-3,89
JEQ12_001754	2-phosphoxylose phosphatase 1	-3,75
JEQ12_000040	Uncharacterized protein	-3,54
PAM	Peptidylglycine alpha-amidating monooxygenase	-3,34
WSQ192	Stimulator of chondrogenesis 1	-3,09

H)

Genes Upregulated	Protein Associated	Log(2) FC
TTR	Transthyretin	9,90
JEQ12_018991	Plasminogen	9,57
JEQ12_005802	Ig-like domain-containing protein	9,32
FGA	Fibrinogen alpha chain	8,97
JEQ12_007054	Fibrinogen C-terminal domain-containing protein	8,70
APOA2	Apolipoprotein A-II	8,45
LOC101119895	Protein HP-20 homolog	8,16
JEQ12_003079	Laminin G domain-containing protein	7,96
FGG	Fibrinogen gamma chain	7,67
JEQ12_003079	Carboxypeptidase B2	7,60

K)

Genes Downregulated	Protein Associated	Log(2) FC
JEQ12_004675	VWFA domain-containing protein	-4,47
JEQ12_005708	SRCR domain-containing protein	-3,71
JEQ12_000952	Uncharacterized protein	-2,75
MATN2	Matrilin 2	-2,67
JEQ12_003845	Agrin	-2,44
JEQ12_015431	Semaphorin-3C	-2,42
WSQ192	Stimulator of chondrogenesis 1	-1,93
NID2	Nidogen 2	-1,90
SPARC	SPARC	-1,87
JEQ12_008660	Peroxidase	-1,85

L)

Genes Upregulated	Protein Associated	Log(2) FC
LOC101115495	Pentraxin family member	2,46
JEQ12_006902	MACPF domain-containing protein	2,24
SERPINA5	Serpin family A member 5	1,97
JEQ12_006893	Complement component C6	1,91
JEQ12_008389	Inter-alpha-trypsin inhibitor heavy chain H1	1,56

Figure S2: Comparative analysis of the upregulated and downregulated NP proteins at different time points. A- D) Heatmap, volcano plot, list of proteins downregulated and upregulated showing the comparison between 8 weeks after induced IVDD and 0 weeks (control). E-H) Heatmap, volcano plot, list of proteins downregulated and upregulated showing the comparison between 32 weeks after induced IVDD and 0 weeks (control). I-L) Heatmap, volcano plot, list of proteins downregulated and upregulated showing the comparison between 32 weeks after induced IVDD and 8 weeks.

Appendix 3.

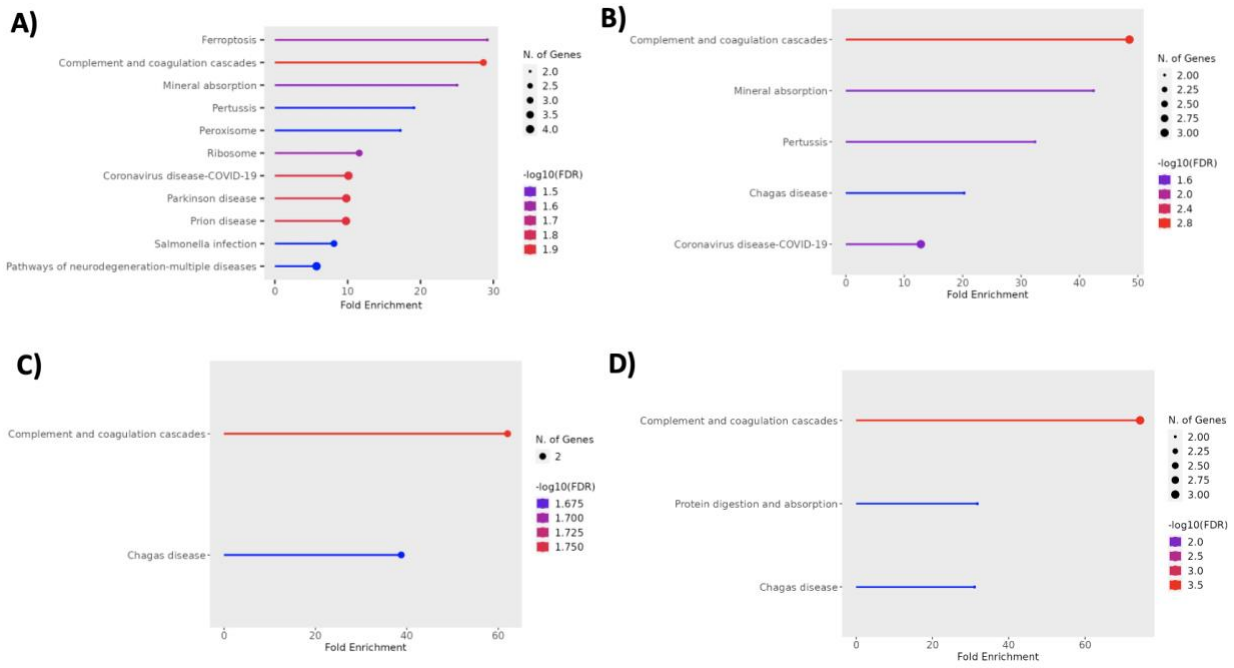

Figure S3: Representation of enriched KEGG pathways for different comparison at different time points for AF and NP. A) Comparison of AF DEPs at 8 weeks vs 0 weeks (control). B) Comparison of AF DEPs at 32 weeks vs 0 weeks of IVDD. C) Comparison of NP DEPs at 8 weeks vs 0 weeks (control). D) Comparison of NP DEPs at 32 weeks vs 0 weeks (control).

CHAPTER 4 EVALUATION OF A NOVEL SHOCKWAVE METHOD FOR INDUCING INDIRECT TRAUMA TO THE INTERVERTEBRAL DISC

4.1 Summary

Current models often fail to adequately mimic the complexities of human IVDD, highlighting the need for improved experimental systems. This study aimed to establish and validate a novel large animal model of IVDD using extracorporeal shock wave therapy (ESWT) on the ovine lumbar spine. Six skeletally mature Rambouillet cross sheep underwent random assignment to either a control group or an ESWT treatment group. The ESWT was administered to the L2-3 and L4-5 intervertebral discs, with comprehensive evaluations performed pre- and post-treatment using radiographs and magnetic resonance imaging (MRI) at 6 and 12 weeks. Results indicated no significant radiographic or MRI changes indicative of IVDD in the treated discs when compared to the control group. However, despite the lack of observable degenerative changes through conventional imaging, gross macroscopic evaluations revealed new bone formation at the treatment sites. This finding was corroborated by histological assessments, which showed localized effects of ESWT on surrounding tissues. Importantly, classical signs of degeneration, such as annulus fibrosus disruption or alterations in nucleus pulposus morphology, were not observed, further underscoring the absence of widespread degenerative changes. Biomechanical analysis also indicated no significant differences between control and treated discs in terms of kinematic range of motion, and biochemical evaluations revealed no differences in glycosaminoglycan content among the groups.

This chapter includes the information published manuscript: Bonilla AF, Burton LH, Page M, Von Stade D, Reagan D, Puttlitz C, Dow SW,Johnstone B, and Easley JT (2023) Development of a clinically-relevant large animal model of intervertebral disc disease. The Spine Journal. Volume 23, Issue 9, DOI: 10.1016/j.spinee.2023.06.404

Biomechanical analysis also indicated no significant differences between control and treated discs in terms of kinematic range of motion, and biochemical evaluations revealed no differences in glycosaminoglycan content among the groups.

Additionally, serum cytokine measurements indicated no significant variations in inflammatory markers between treated and control discs. In conclusion, while ESWT was well-tolerated and resulted in localized bone formation, it did not induce significant degenerative changes within the 12-week observation period. This study establishes a foundation for further research to explore optimal shock parameters and longer evaluation periods, ultimately aiming to enhance our understanding of IVDD and develop effective therapeutic strategies for managing low back pain.

4. 2 Introduction

There is scientific consensus around the need for improved animal models for enhanced assessment of therapies and accurate elucidation of potential novel targets to treat IVDD (241,288). Various methods and models have been established to induce IVDD without causing direct trauma to the structural components of the IVD. One promising approach is the use of shock waves, which can induce non-traumatic, indirect damage to the IVD, closely mimicking the natural progression of IVDD seen in aging human patients. This method offers the potential to replicate the gradual degenerative process, making it a valuable tool for studying disease mechanisms and testing potential treatments.

Shock waves are high-energy acoustic waves produced underwater through high-voltage explosions and vaporization (289,290). In urology, shock waves are primarily utilized for

lithotripsy to break down urolithiasis (291), and in orthopedics, shock waves (orthotripsy) are mostly used to promote neovascularization, enhance blood supply, and facilitate tissue regeneration (289,292,293). Extracorporeal shock wave therapy (ESWT) has been shown to induce localized biological effects, such as new bone formation and changes in tissue remodeling, which can mimic the degenerative processes observed in human IVDD (294). The ovine model is advantageous due to the anatomical and physiological similarities of sheep spines to human spines, allowing for more relevant translational research (146,253,295–297). Here we used ESWT on the ovine lumbar spine to establish and validate a novel large animal model of IVDD. By applying ESWT, we aimed to assess the varying effects of this technique in inducing IVDD. Additionally, this model could offer valuable insights into the pathophysiology of IVDD, facilitating the development of effective treatments and bridging the gap between preclinical research and clinical applications.

4.3 Materials and Methods

Animals – This study was conducted with the approval of the Institutional Animal Care and Use Committee at Colorado State University (protocol#: 1052). A total of six skeletally mature Rambouillet cross sheep (age range 4–5 years, weight range 90–110 kg) were enrolled (Figure 1). Before the study, all animals underwent thorough health evaluations to confirm they were in good condition at the time of enrollment. Additionally, the sheep were given an acclimation period to ensure they were well adjusted to their environment before the experimental procedures. The animals were randomly divided into two groups: the control group (n=3) and the ESWT (treatment) group (n=3).

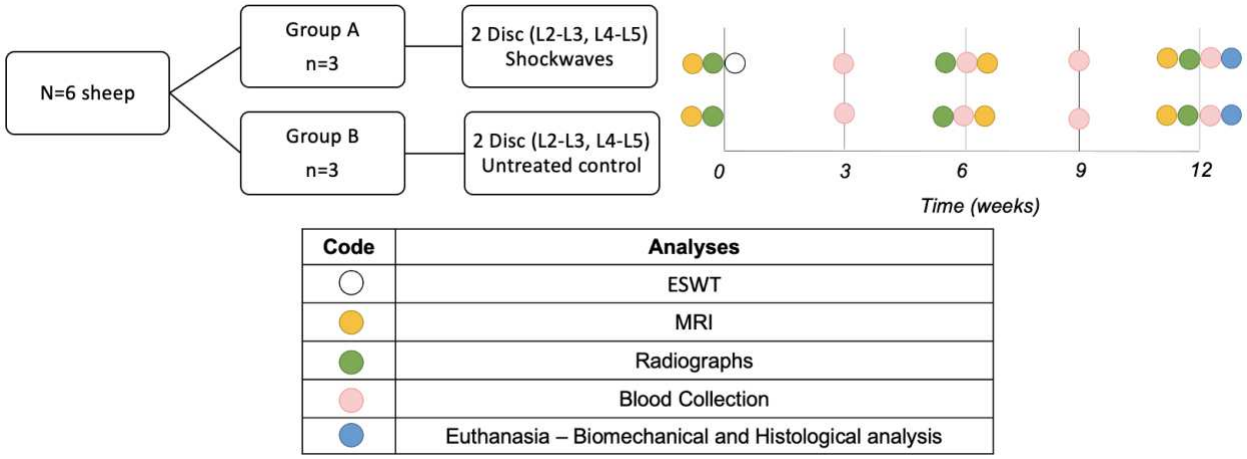

Code	Analyses
○	ESWT
●	MRI
●	Radiographs
●	Blood Collection
●	Euthanasia – Biomechanical and Histological analysis

Figure 1: Diagram illustrating the study design to evaluate the effects of ESWT on ovine lumbar intervertebral discs, detailing the various outcomes and time points used to assess the progression IVDD.

ESWT administration – Three animals from treatment group surgically received ESWT. All surgical procedures were conducted under aseptic conditions. The auricular vein and artery were accessed for catheter placement. A combination of ketamine (3.3 mg/kg, IV) and diazepam (0.1 mg/kg, IV) was used to initiate anesthesia. After achieving the anesthetic state, the sheep were intubated using a cuffed endotracheal tube. They were then positioned in right lateral recumbency and maintained on isoflurane (1.5%-3%) combined with 100% oxygen. Through a left lateral retroperitoneal method, the intervertebral spaces from L2 to L5 were made visible by dissecting through the oblique abdominal muscles, leading to the muscle layer in front of the transverse processes. The L2-L3 and L4-L5 intervertebral discs were identified. Then 10,000 shocks were applied to L2-3 level using 5.0 bar 12 Hertz and the probe "DI15 deep impact" (Duolith SD1 Vet, Storz Medical), and 10.000 shocks at the L4-5 using 5.0 bar 12 Hertz using the probe "D20-T D-Actor" (Duolith SD1 Vet, Storz Medical) (Figure 2). After the ESWT administration, routine

closure was performed of the epaxial musculature and dorsal fascia with absorbable suture, subcutaneous tissue with absorbable suture, and skin with non-absorbable suture.

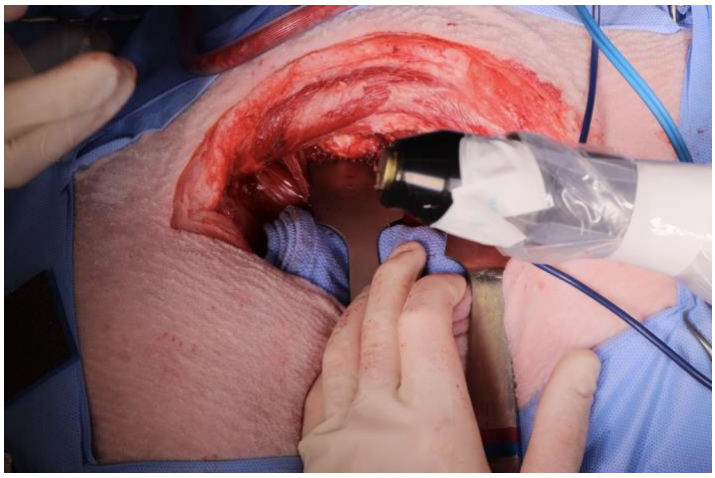

Figure 2: Representative photograph showing the open left retroperitoneal surgical approach used for the application of ESWT to the ovine lumbar intervertebral discs.

In vivo Imaging – Radiographs and magnetic resonance (MR) imaging of the lumbar spine was conducted for both groups before ESWT administration, as well as at 6 and 12 weeks post-treatment. Animals were pre-medicated and anesthetized with an initial induction of 4% isoflurane, followed by maintenance at 1–3%, and placed in the prone position during the procedures. Digital radiographic views of the lumbar spine, including lateral and dorsoventral projections, were obtained for each animal. The MR imaging protocol included T1 and T2 sagittal views (1.5 mm slices), T2 axial views (1.5 mm slices), all acquired using a 3T MR scanner (Philips Medical Systems, Intera) with a sense-body imaging coil. Two independent, blinded observers evaluated the radiographs and MR images to assess the Disc Height Index (DHI) (258), and Pfirrmann grade (260) of the intervertebral discs, ensuring objective measurements for both groups.

Blood collection – Prior to the administration of ESWT and at specific intervals—24 hours, 48 hours, 3 days, 7 days, 3 weeks, 6 weeks, 9 weeks, and 12 weeks—blood samples were collected via venipuncture of the jugular vein while the sheep were under minimal physical restraint to minimize stress. Once collected, each whole blood sample was immediately centrifuged using a Thermo XTR centrifuge at 2500 RPM for 15 minutes to separate the serum. The isolated serum was then stored and later used to evaluate the levels of pro-inflammatory cytokines TNF-alpha, IL-1ß, IL-6, and IL-17A, as well as the anti-inflammatory cytokine IL-10. These cytokine levels were measured using a Luminex multiplex assay system, a highly sensitive platform that allows for the simultaneous detection of multiple cytokines in a single sample, following the manufacturer's specific protocol for optimal accuracy (298).

Euthanasia and Sample Harvest – At the conclusion of the 12-week study period, the sheep were humanely euthanized following AVMA (American Veterinary Medical Association) guidelines. Euthanasia was carried out through the intravenous administration of an overdose of pentobarbitone sodium at a dose of 88mg/kg, ensuring a painless and ethical procedure. After euthanasia, the lumbar spines were carefully dissected and removed to facilitate an extensive ex vivo evaluation. This comprehensive evaluation included biomechanical testing to assess the functional properties of the spine, biochemical analysis to measure molecular changes in disc composition, and histopathological analysis to investigate tissue-level alterations. Additionally, high-resolution digital photographs were taken of the dissected lumbar spines to document and evaluate any gross morphological changes that occurred following the administration of ESWT. These images allowed for a thorough assessment of any visible anatomical differences between treated and control groups, complementing the microscopic and mechanical analyses.

Biomechanical Evaluation – Non-destructive biomechanical testing was performed to determine the kinematic Range of Motion (ROM). The lumbar spines will be harvested *en bloc* and fine dissection of all lumbar Functional Spinal Units (FSUs) from treated or control animals (L2-L3 and L4-5) were performed. Samples were kept hydrated via physiological saline spray at 10-minute intervals during the preparation and testing protocols. Following dissection, FSUs were potted in a strong two-part hard cast resin (SmoothCast 321; Smooth-On, Macungie, PA, USA) to ensure proper mechanical fixation between the sample and the testing system previously reported (299). A custom-built testing system was used to apply pure moments in the right-left axial rotation. All spines underwent three cycles of non-destructive loading with loads of 0.2 Nm. The parameters of interest were range of motion (ROM; degrees (deg)); construct stiffness (N-m/deg); and neutral zone (NZ, deg). Marker triads were placed at the tips of Kirschner wires, drilled into the vertebral bodies, and tracked by the three high-resolution cameras. Three dimensional coordinates of the marker sets were recorded, and the related Euler angles for the relative motion at the implanted levels were calculated.

Biochemical Assays – The Dimethyl Methylene Blue (DMMB) technique was employed to quantify the proteoglycan content in the NP and AF derived from the right halves of the IVDs at the L2-L3 and L4-5 levels. Initially, approximately 10 ± 5 mg of NP and AF were aseptically isolated from the IVDs and subjected to digestion with papain to release the proteoglycans for analysis. Following digestion, diluted samples of the tissue extracts, at a dilution factor ranging from 1 to 100, were combined with the DMMB reagent, which selectively binds to the sulfated glycosaminoglycans found in proteoglycans. To ensure accurate quantification, chondroitin sulfate

(Sigma, St. Louis, MO) was utilized to establish a standard curve, facilitating the comparison of sample absorbance values. The resulting colorimetric change was then measured at a wavelength of 530 nm (Molecular Devices, Softmax Pro, USA).

Histopathological analysis- Two functional spinal units (FSUs) per sheep (specifically L2-L3 and L4-L5) were collected, and the left halves of these FSUs were bisected along the sagittal plane for decalcified histological analysis. After the initial fixation, the specimens underwent a decalcification process using 10% ethylenediaminetetraacetic acid (EDTA) to remove any mineral content, facilitating detailed tissue examination. Once decalcified, the samples were processed using standard histological techniques (Tissue-Tek VIP, Sakura, Torrance, CA), ensuring proper tissue preservation and consistency. The tissues were then embedded in paraffin to prepare them for sectioning. Two histological slides were generated from each specimen, which were stained using Hematoxylin and Eosin (H&E) to highlight cellular and structural details of the intervertebral discs. These stained sections were subsequently evaluated by two blinded observers, including a board-certified veterinary pathologist, ensuring an unbiased and expert assessment. A specialized scoring system designed for evaluating IVDD in large animal models was employed to quantify the extent of disc degeneration (146).

Statistical analysis - Following the processing and organization of the collected data, comprehensive statistical analyses were performed on all the measured outcome parameters to assess the effects of the treatments. A standard two-way analysis of variance (ANOVA) was conducted to evaluate whether there were statistically significant differences (with a threshold of $p \leq 0.05$) both within the treatment groups over time and across the different groups (control and

ESWT-treated). This approach allowed for the examination of interactions between treatment and time, determining if the treatment had a consistent effect at different time points or if changes occurred differently over time between the groups (GraphPad Software, San Diego, CA). The results of the analyses—specifically regarding changes in disc height, Pfirrmann grade, kinematic evaluation, biochemical markers, and histological grading—are all presented as mean ± standard deviation (SD) to convey the average outcomes and the variability within each group.

4 .4 Results

All treated animals recovered from surgery without complications. Radiographic evaluations were performed at baseline, 6, and 12 weeks, allowing for a comprehensive assessment of the lumbar spine and corresponding bone structures. No radiographic differences were observed compared to the control group (Figure 3). Similarly, MR imaging at baseline, 6 weeks, and 12 weeks revealed no changes in intervertebral disc signal intensity or Pfirrmann grade (Figure 4).

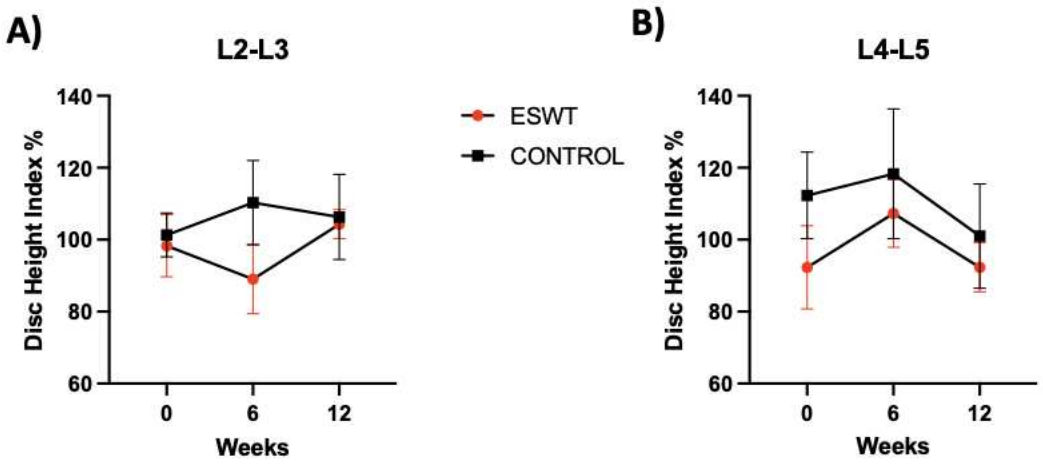

Figure 3. Graph comparing DHI for L2-L3 and L4-L5 intervertebral discs between treated and control animals. Measurements were taken from radiographic lateral views using an imaging analyzer (Horos®). No significant differences were observed between IVDS of the groups or across time points.

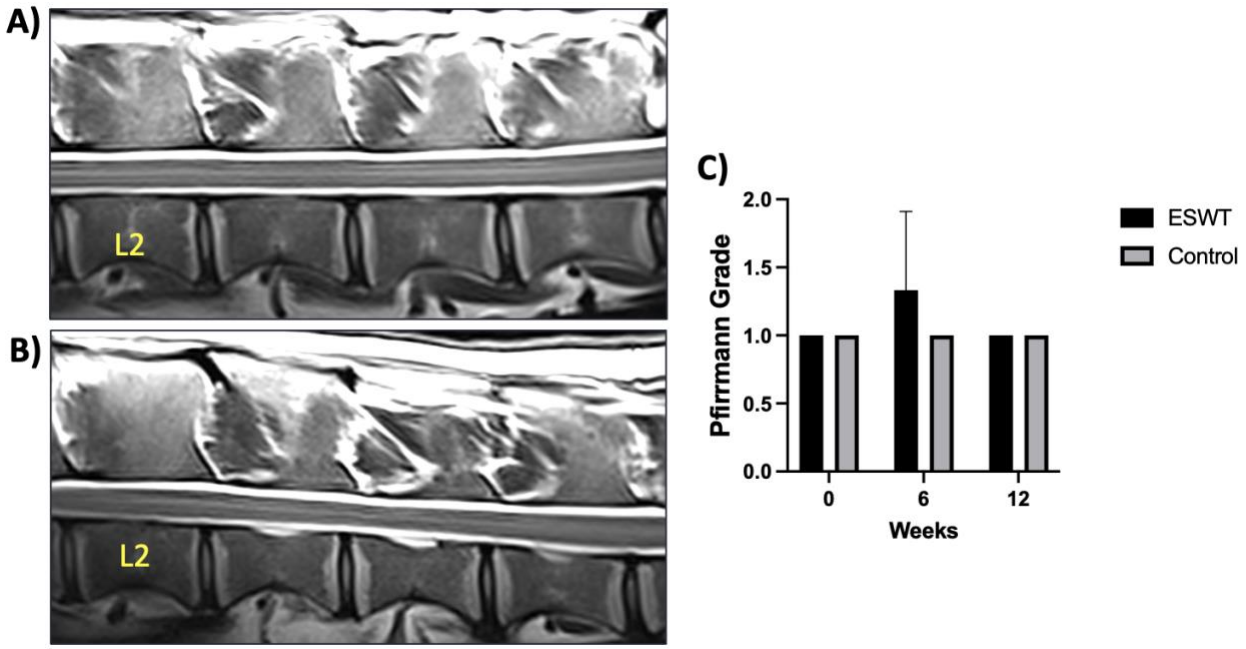

Figure 4. Representative lumbar T2-weighted MR images of L2-3, L3-4, and L4-5 from animals treated with ESWT at 0 weeks (A) and 12 weeks (B). No MR imaging changes indicative of IVDD were observed in the discs at L2-3 or L4-5 following ESWT treatment. L2 vertebral bodies are labeled in each image for anatomic location. C) Graph illustrating Pfirrmann scores at baseline, 6 weeks, and 12 weeks. No significant changes in Pfirrmann grades were observed in the ESWT-treated discs over the 12-week period compared to the naïve control discs.

Gross macroscopic evaluation of the lumbar spines, conducted 12 weeks after the application of ESWT, revealed new bone formation laterally at the sites of treatment in both the L2-3 and L4-5 intervertebral discs. This finding was further confirmed by histological evaluation. (Figure 5). No significant differences were observed using the histological grading score for large animal models of intervertebral disc degeneration (Figure 6). However, notable changes in bone formation were identified at the locations where ESWT was applied, indicating localized effects of the treatment on the surrounding tissue. Importantly, no classical histological signs of degeneration, such as AF disruption or alterations in the shape of the NP, extracellular matrix composition, or cellularity, were noted when compared to control naïve discs.

Biomechanical analysis revealed no significant differences between the control and ESWT-treated discs in terms of flexion, axial rotation, or lateral bending. Luminex assay measurements of TNF-alpha, IL-1ß, IL-6, IL-10, IL-17A did not show statistical differences between groups or time points (Figure 7). Biochemical evaluation of *glycosaminoglycans (GAG) content* using *DMMB evaluation did not show differences in GAG in NP or AF in animals treated with ESWT and control animals (Figure 8).*

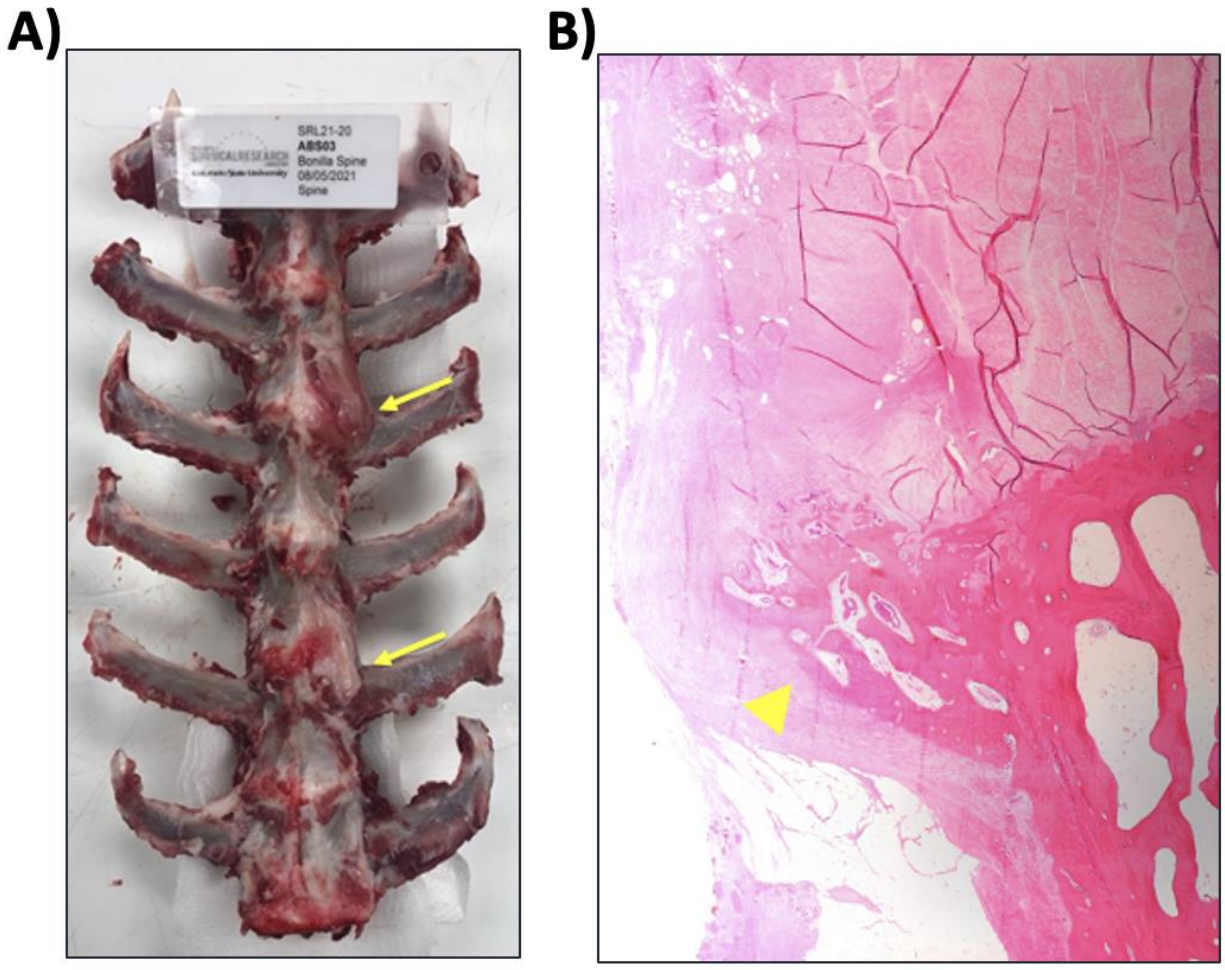

Figure 5. Structural changes were observed precisely at the sites where ESWT was applied to the intervertebral discs (IVDs). A) Macroscopic evaluation of the lumbar spines revealed new bone growth at these specific locations (yellow arrows) where shock waves were administered. B) Histological evaluation of these areas confirmed new bone formation adjacent to the endplates and

annulus fibrosus (yellow arrowheads) at the L2-3 and L4-5-disc levels.

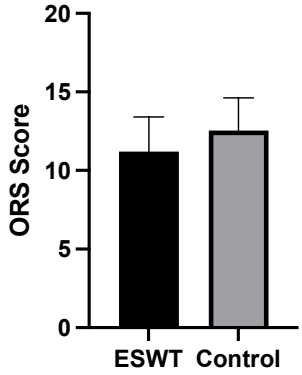

Figure 6. Graph illustrating the histological scoring of treated and control discs. Histological evaluation of the L2-3 and L4-5-disc levels treated with ESWT revealed no significant differences when compared to control discs. Data are presented as median ± SD.

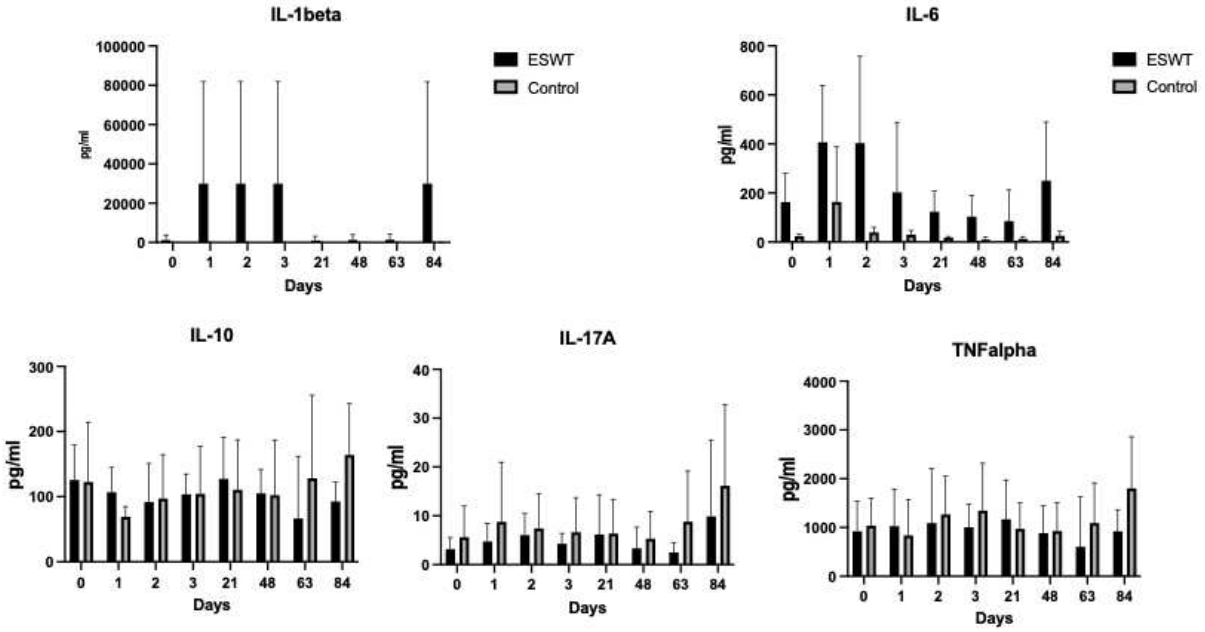

Figure 7. The graphs illustrate serum cytokine measurements obtained via Luminex assay at baseline and at 1, 2, 3 days, as well as at 6, 9, and 12 weeks. Although some cytokines exhibited visual trends, no significant differences were observed in the concentrations of IL-1beta, IL-6, IL-10, IL-17A, and TNF-alpha between the treated with ESWT and control intervertebral discs. Data are presented as median ± SD.

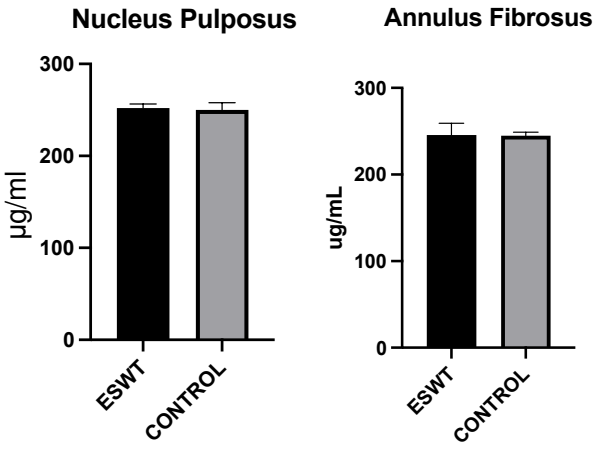

Figure 8. The graph presents glycosaminoglycan measurements obtained via the DMMB assay at the 12-week time point. No significant differences were observed between the IVDs after ESWT application and the control IVDs. Data are presented as median ± SD.

4. 5 Discussion

Low back pain, a common multifactorial condition, imposes significant economic burdens through lost productivity and healthcare costs, with IVDD being a major contributor. The need for effective animal models to elucidate the pathophysiological mechanisms underlying IVDD and to test new therapeutic interventions is critical, as existing models often fall short in their ability to mimic the complexities of human disease. This study aimed to establish and validate a novel large animal model of IVDD in the ovine lumbar spine through the application of ESWT, a technique known to induce biological changes such as neovascularization and tissue remodeling (300).

The successful development of a clinically relevant ovine model is underpinned by the anatomical and physiological similarities between ovine and human spines, facilitating translational research that could lead to better understanding and treatment of IVDD. Our findings indicate that the administration of ESWT was well tolerated by the animals, with no observed clinical signs of pain throughout the study duration. This is consistent with previous literature suggesting the safety of ESWT in clinical and experimental settings (293,301,302)

However, despite the well-tolerated nature of the treatment, our results demonstrated that the application of ESWT did not result in significant radiographic or MR Imaging changes associated with IVDD. Specifically, there were no notable differences in IVD signal intensity or Pfirrmann grades between the treated and control groups at any of the evaluated time points. This lack of significant findings may suggest that while ESWT promotes localized biological effects, it does not induce systemic degenerative changes observable through conventional imaging techniques within the study timeframe.

The establishment of significant timeframes and optimal shock parameters for inducing pathophysiological changes associated with IVDD remains a pivotal area for future exploration (300,302). Previous research in rabbits has indicated that ESWT induces dose-dependent changes in the IVD, specifically in the endplate, suggesting the need for further investigation into its broader impact on disc degeneration (303). As this proof-of-concept study did not yield significant results regarding IVDD induction, it suggests that the model may not be optimal in its current form. Key factors such as longer evaluation periods, varying the number of shock waves, and exploring different energy levels were not addressed in this study and should be considered in future research. Investigating these parameters is essential to better understand the relationship between ESWT and IVDD progression, and to improve the relevance of the model and predictive capacity in capturing the pathophysiological mechanisms of IVDD.

Results demonstrated that ESWT could induce anatomical changes related to new bone formation in the lumbar intervertebral disc, as observed both macroscopically and histologically. Similar results have been observed in other animal models of IVDD, where osteophyte formation occurred following injury to the intervertebral disc (167,304). Formation of severe disc osteophytes have been reported in small animal models after traumatic induction of IVDD (305).

However, the noted lateral new bone formation observed at the treatment sites is intriguing, but it remains unclear whether these changes directly correlate with ESWT application or are part of the natural healing processes occurring in response to the surgical intervention. Future studies should build upon these findings by investigating the molecular mechanisms underlying the observed bone changes and assessing the long-term implications of ESWT in the context of IVDD treatment.

In conclusion, our results provide a foundational understanding of the effects of ESWT on the ovine lumbar spine. Although no significant changes indicating the induction of IVDD were observed in this study, these findings contribute valuable insights into the potential of this technique for developing effective therapeutic strategies for IVDD. Continued research in this area could bridge the gap between preclinical models and clinical applications, ultimately contributing to improved outcomes for individuals suffering from low back pain due to intervertebral disc degeneration.

4.6 References

1. Poletto DL, Crowley JD, Tanglay O, Walsh WR, Pelletier MH. Preclinical in vivo animal models of intervertebral disc degeneration. Part 1: A systematic review. JOR Spine. 2022;(October 2022):1–20.
2. Fusellier M, Clouet J, Gauthier O, Tryfonidou M, Le Visage C, Guicheux J. Degenerative lumbar disc disease: In vivo data support the rationale for the selection of appropriate animal models. Eur Cell Mater. 2020;39:18–47.
3. Wang CJ. An overview of shock wave therapy in musculoskeletal disorders. Chang Gung Med J. 2003 Apr;26(4):220–32.
4. Ogden JA, T??th-Kischkat A, Schultheiss R. Principles of Shock Wave Therapy. Clin

Orthop Relat Res. 2001 Jun;387:8–17.

5. Lingeman JE, McAteer JA, Gnessin E, Evan AP. Shock wave lithotripsy: advances in technology and technique. Nat Rev Urol. 2009 Dec;6(12):660–70.

6. Ogden JA, Alvarez RG, Levitt R, Marlow M. Shock Wave Therapy (Orthotripsy) in Musculoskeletal Disorders. Clin Orthop Relat Res. 2001 Jun;387:22–40.

7. Che YJ, Hou JJ, Guo JB, Liang T, Zhang W, Lu Y, et al. Low energy extracorporeal shock wave therapy combined with low tension traction can better reshape the microenvironment in degenerated intervertebral disc regeneration and repair. The Spine Journal. 2021 Jan;21(1):160–77.

8. Gadomski BC, McGilvray KC, Easley JT, Palmer RH, Jiao J, Li X, et al. An investigation of shock wave therapy and low-intensity pulsed ultrasound on fracture healing under reduced loading conditions in an ovine model. Journal of Orthopaedic Research. 2018;36(3):921–9.

9. Lee NN, Salzer E, Bach FC, Bonilla AF, Cook JL, Gazit Z, et al. A comprehensive tool box for large animal studies of intervertebral disc degeneration. JOR Spine. 2021;(July 2020):1–36.

10. Daly CD, Ghosh P, Badal T, Shimmon R, Jenkin G, Oehme D, et al. A Comparison of Two Ovine Lumbar Intervertebral Disc Injury Models for the Evaluation and Development of Novel Regenerative Therapies. Global Spine J. 2018 Dec 1;8(8):847–59.

11. Oehme D, Goldschlager T, Rosenfeld J, Danks A, Ghosh P, Gibbon A, et al. Lateral Surgical Approach to Lumbar Intervertebral Discs in an Ovine Model. The Scientific World Journal. 2012;2012.

12. Lim KZ, Daly CD, Ghosh P, Jenkin G, Oehme D, Cooper-White J, et al. Ovine lumbar

intervertebral disc degeneration model utilizing a lateral retroperitoneal drill bit injury. Journal of Visualized Experiments. 2017 May 25;2017(123).

13. Bouhsina N, Decante C, Hardel JB, Madec S, Abadie J, Hamel A, et al. Correlation between magnetic resonance, x-ray imaging alterations and histological changes in an ovine model of age-related disc degeneration. Eur Cell Mater. 2021 Jul 1;42:166–78.

14. Lee NN, Salzer E, Bach FC, Bonilla AF, Cook JL, Gazit Z, et al. A comprehensive tool box for large animal studies of intervertebral disc degeneration. JOR Spine. 2021;(July 2020):1–36.

15. Pfirrmann CWA, Metzdorf A, Zanetti M, Hodler J, Boos N. Magnetic resonance classification of lumbar intervertebral disc degeneration. Spine (Phila Pa 1976). 2001;26(17):1873–8.

16. Naylor D, Sharma A, Li Z, Monteith G, Sullivan T, Canovas A, et al. Short communication: Characterizing ovine serum stress biomarkers during endotoxemia. J Dairy Sci. 2020 Jun;103(6):5501–8.

17. Easley J, Puttlitz C, Seim H, Ramo N, Abjornson C, Cammisa F, et al. Biomechanical and histologic assessment of a novel screw retention technology in an ovine lumbar fusion model. Spine Journal. 2018;18:2302–15.

18. Fiani B, Davati C, Griepp DW, Lee J, Pennington E, Moawad CM. Enhanced Spinal Therapy: Extracorporeal Shock Wave Therapy for the Spine. Cureus. 2020 Oct 27;

19. Gadomski BC, McGilvray KC, Easley JT, Palmer RH, Jiao J, Li X, et al. An investigation of shock wave therapy and low-intensity pulsed ultrasound on fracture healing under reduced loading conditions in an ovine model. Journal of Orthopaedic Research. 2018 Mar 1;36(3):921–9.

20. Mokhtar M, Elhosary E, Said M, Hamoda I, Elsebahy S, Abdelaleem R. Comparative study between shock wave therapy and electromagnetic waves on pain and function in patients with lumbar disc prolapse A randomized controlled trial: NILES journal for Geriatric and Gerontology. 2023 Jan 1;6(1):133–47.

21. Ertürk C, Altay MA, Özardali I, Altay N, Çeçe H, Işikan UE. The effect of extracorporeal shockwaves on cartilage end-plates in rabbits: A preliminary MRI and histopathological study. Acta Orthop Traumatol Turc. 2012;46(6):449–54.

22. Lipson SJ, Muir H. Vertebral osteophyte formation in experimental disc degeneration. Arthritis Rheum. 1980 Mar 23;23(3):319–24.

23. Liang T, Gao B, Zhou J, Qiu X, Qiu J, Chen T, et al. Constructing intervertebral disc degeneration animal model: A review of current models. Front Surg. 2023 Mar 10;9.

24. Fainor M, Orozco BS, Muir VG, Mahindroo S, Gupta S, Mauck RL, et al. Mechanical crosstalk between the intervertebral disc, facet joints, and vertebral endplate following acute disc injury in a rabbit model. JOR Spine. 2023 Dec 24;6(4).

CHAPTER 5. DESIGN, IMPLEMENT, AND EVALUATE THE EFFICACY OF A MECHANICAL ALTERATIONS USING A COMPRESSION DEVICE TO INDUCE DISC DEGENERATION

5.1 Summary

The development of animal models to mimic IVDD is critical for advancing our understanding of its pathophysiology and for evaluating therapeutic interventions. However, current models face limitations in accurately reproducing the mechanical and biochemical aspects of human disc degeneration. This study aimed to develop a novel mechanical compression model of IVDD with MRI-compatible materials, allowing for longitudinal imaging assessment. Six skeletally mature Rambouillet cross sheep were randomly assigned to either a control group (n=3) or a treatment group (n=3). In the treatment group, mechanical compression was applied to the lumbar spine using a custom apparatus comprising titanium pins and a bronze compression spring. Dynamic compression was applied at the L2-L3 disc, while L4-L5 remained stabilized without compression. Radiographic and magnetic resonance imaging were performed pre-operatively, immediately post-surgery, and at 6 and 12 weeks to monitor disc height and degeneration, with Pfirrmann grading used to assess degenerative changes. Biomechanical, biochemical, and histopathological evaluations were also conducted at study endpoint. Serum samples were collected for inflammatory cytokine analysis via Luminex assay.

This chapter includes the information published manuscript: Bonilla AF, Burton LH, Page M, Von Stade D, Reagan D, Puttlitz C, Dow SW,Johnstone B, and Easley JT (2023) Development of a clinically-relevant large animal model of intervertebral disc disease. The Spine Journal. Volume 23, Issue 9, DOI: 10.1016/j.spinee.2023.06.404

The mechanical compression device successfully reduced disc height at the L2-L3 level, with significant dorsal compression and ventral distraction observed throughout the study period. MRI evaluation was hindered by signal artifacts from the titanium pins, though disc changes were still identifiable. No significant differences in Pfirrmann grades were detected between compressed and control discs at any time point. Additionally, the Luminex assay did not reveal significant changes in pro-inflammatory cytokines (TNF-alpha, IL-1ß, IL-6, IL-10, IL-17A) across groups. Biomechanical testing showed a significant Increase in lateral neutral zone In the compressed discs at 12 weeks ($P = 0.0424$), but no other biomechanical differences were observed. Histological and biochemical analysis using glycosaminoglycan content also showed no significant alterations between groups. In conclusion, this study demonstrated the feasibility of using MRI-compatible materials for mechanical induction of IVDD in a large animal model, allowing for real-time imaging of disc changes. While significant biomechanical alterations were detected, no substantial histological, biochemical, or inflammatory changes were observed in this model. These findings suggest that further optimization of mechanical induction methods may be required to replicate the complex degenerative processes observed in human IVDD.

5. 2 Introduction

Mechanical destabilization is known to be a contributing factor to disc degeneration (221,306). Specifically, mechanical forces that alter the normal biomechanics of the spine can lead to such destabilization (307,308). Considering this, various surgical-mechanical approaches have been employed to destabilize the spine and induce disc degeneration in animal models (212,309–311). Most of these mechanical destabilization techniques have been performed in small animal models, which complicates their translation to human applications (312–314). Among these

techniques are the stabilization of specific spinal segments and the application of excessive mechanical forces to the spine (315,316). These excessive mechanical forces are applied to specific segments of the spine in order to compress the intervertebral disc and recreate mechanical forces that induce disc degeneration, for instance caused by overweight or bad posture.

Magnetic Resonance Imaging (MRI) is one of the most valuable and reliable techniques for diagnosing IVDD. In addition to its diagnostic utility, MRI is crucial for modeling this condition as it allows for the confirmation and monitoring of induced IVDD progression (217,311,317–319). Traditional mechanical induction models often employ metal artifacts to alter mechanical forces, rendering MRI tracking impractical due to image distortion. In this study, we employed a novel approach by using MRI-compatible materials for mechanical compression in a large animal model.

5.3 Materials and Methods

Animals – This study was performed with approval from the Institutional Animal Care and Use Committee at Colorado State University (protocol#: 1052). A total of 6 skeletally mature Rambouillet cross sheep (age range 4–5 years, weight range 90–110 kg) were enrolled in this study. Animals were randomly assigned to control group or mechanical compression (treatment) group (n = 3 sheep per group).

Mechanical compression – Three animals from treatment group were under surgically implantation of 15 cm titanium pins in the left pedicles of L2 and L3, and right pedicles of L4 and L5 (Figure 1). For the implantation, surgical procedures were conducted under aseptic conditions. Initially, the auricular vein and artery were accessed for catheter placement. A combination of ketamine (3.3 mg/kg, IV) and diazepam (0.1 mg/kg, IV) was used to initiate anesthesia. After

achieving the anesthetic state, the sheep were intubated using a cuffed endotracheal tube. They were then positioned in right lateral recumbency and maintained on isoflurane (1.5%-3%) combined with 100% oxygen. Through a left lateral retroperitoneal method, the intervertebral spaces from L2 to L5 were made visible by dissecting through the oblique abdominal muscles, leading to the muscle layer in front of the transverse processes. The L2-L3 and L4-L5 intervertebral discs were identified. The distal threaded portion of each titanium pin (150 mm in length and 5.5 mm in diameter) was drilled into the respective vertebral body using a variable-speed electric drill. The pins were inserted until they traversed the complete thickness of the bone structure, parallel to the adjacent study disc. After implanting the titanium pins, routine closure of the epaxial musculature and dorsal fascia was performed using absorbable sutures, followed by closure of the subcutaneous tissue with absorbable sutures and the skin with non-absorbable sutures. The proximal portions of the pins exited the skin posteriorly. Immediately after skin closure, a mechanical disc compression apparatus, composed of two titanium pins, one compression bronze spring, and two aluminum compression box connectors, was set up for each intervertebral disc compression (Figure 2). For the compression device at the L2-L3 level, 147.6 N of compression was applied (dynamic compression). At the L4-L5 level, no acute compression was applied, resulting in static stabilization.

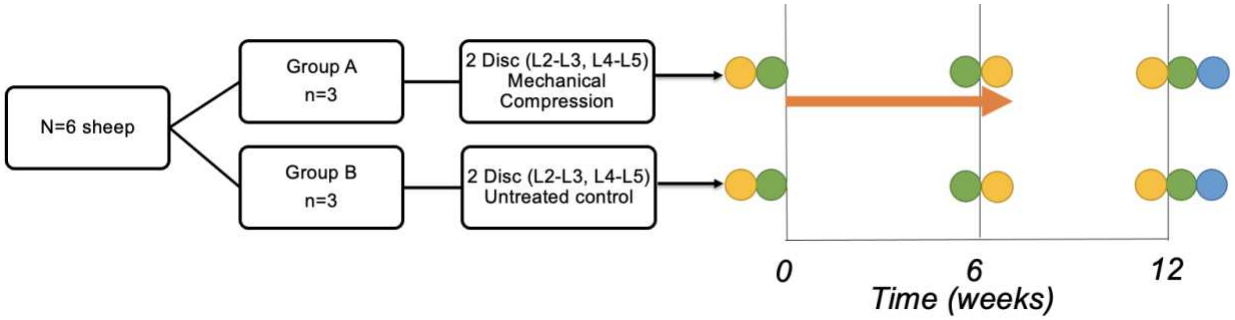

Code	Analyses
→	Mechanical Compression
●	MRI
●	Radiographs
●	Euthanasia – Biomechanical, Biochemical and Histological analysis

Figure 1: Diagram illustrating the study design to induce mechanical compression at the ovine lumbar levels, detailing the various outcomes used to assess the progression of IVDD.

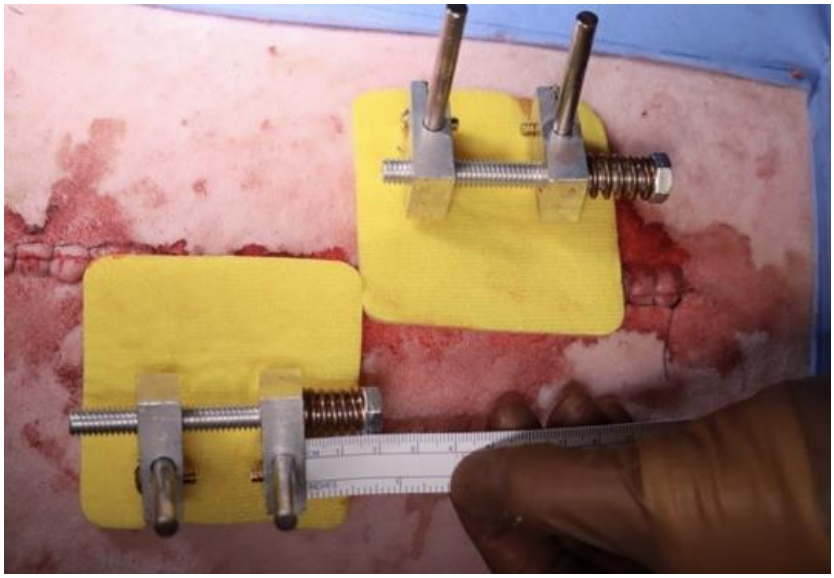

Figure 2: Photograph depicting the mechanical compression apparatus, consisting of two titanium pins, a bronze compression spring, and two aluminum box connectors. A ruler is included as a reference to measure the change in spring length before and after compression is applied.

In vivo Imaging - Radiographs and MR (Magnetic Resonance) imaging of the lumbar spine was performed for both group prior to compression administration, immediately after surgery and at 6,

and 12 weeks. Animals were pre-medicated and anesthetized by initial induction of 4% isoflurane, with maintenance at 1 – 3%, and placed in the prone position. Lateral and dorsoventral digital radiographic views of the lumbar spines were acquired for each animal. The MR imaging protocol consisted of T1 and T2 sagittal views (1.5mm slices), T2 axial views (1.5mm slices) through a 3 T MR scanner (Philips Medical Systems, Intera) using a sense- body imaging coil. Evaluation of radiographic and MR images were completed two blinded observers to determine disc height changes (258), and Pfirrmann grade (260).

Blood collection - Prior to mechanical compression, and at intervals of 24 hours, 48 hours, 3 days, 7 days, 3 weeks, 6 weeks, 9 weeks, and 12 weeks, blood samples were collected via venipuncture of the jugular vein under minimal physical restraint. Each whole blood sample was then centrifuged (Thermo, XTR) for 15 minutes at 2500 RPM to collect serum. The serum was used to evaluate TNF-alpha, IL-1ß, IL-6, IL-10, and IL-17A levels using a Luminex assay, following the manufacturer's instructions (298).

Euthanasia and Sample Harvest - The sheep were humanely euthanized at week 12 by intravenous overdose of pentobarbitone sodium (88mg/kg), in accordance with the American Veterinary Medical Association (AVMA) guidelines. The lumbar spines were removed to complete the *ex vivo* evaluation which included biomechanical, biochemical and histopathological analysis.

Biomechanical Evaluation - Non-destructive biomechanical testing was performed to determine the kinematic Range of Motion (ROM). The lumbar spines will be harvested *en bloc* and fine

dissection of all lumbar Functional Spinal Units (FSUs) from treated or control animals (L2-L3 and L4-5) were performed. Samples were kept hydrated via physiological saline spray at 10-minute intervals during the preparation and testing protocols. Following dissection, FSUs were potted in a strong two-part hard cast resin (SmoothCast 321; Smooth-On, Macungie, PA, USA) to ensure proper mechanical fixation between the sample and the testing system previously reported (299). A custom-built testing system was used to apply pure moments in the right-left axial rotation. All spines underwent three cycles of non-destructive loading with loads of 0.2 Nm. The parameters of interest were range of motion (ROM; degrees (deg)); construct stiffness (N-m/deg); and neutral zone (NZ, deg). Marker triads were placed at the tips of Kirschner wires, drilled into the vertebral bodies, and tracked by the three high-resolution cameras. Three dimensional coordinates of the marker sets were recorded, and the related Euler angles for the relative motion at the implanted levels were calculated.

Biochemical Assays - Dimethyl methylene blue (DMMB) technique was used to measure proteoglycan content in the NP and AF from L2-L3, and L4-5 right half of the IVDs. Briefly, 10 ± 5 mg of NP and AF were separately and aseptically isolated and digested using papain. Diluted samples from digested tissue (1-100) were mixed with the DMMB reagent. Chondroitin sulfate (Sigma, St. Louis, MO) was used to create a standard curve, and results were measured at 530 nm wavelength (Molecular Devices, Softmax Pro, USA).

Histopathological analysis- Two FSUs per sheep (L2-L3, and L4-5) left halves were bisected in the sagittal plane and processed for decalcified histological analysis. Following fixation, specimens were decalcified using EDTA 10%. Then, specimens were processed using standard

techniques (Tissue-Tek VIP, Sakura, Torrance, CA) and embedded in paraffin. Two slides were produced from each sample and stained with Hematoxylin Eosin. Stained histology sections were evaluated by two blinded observers including a certified veterinary pathologist, using a specific scoring system for IVDD in large animal models (146).

Statistical analysis - Following data processing, statistical analyses were performed on all outcome parameters. Standard two-way analyses of variance were performed to determine statistically significant differences ($p \leq 0.05$) within and across treatment groups (GraphPad Prism 8.3.0, San Diego, CA). Differences in the disc height, Pfirrmann grade, kinematic evaluation, biochemical analysis, and histological grading are presented as mean ± SD.

5.4 Results

All treated animals recovered from surgery without complications. Clinical monitoring, including cleaning of the surgical wound and the mechanical compression apparatus using chlorhexidine swabs, was conducted until 50 days post-surgery. However, pin tract infections were observed in all treated animals. In consideration of animal welfare, the devices were promptly removed to control the infections. Daily lavages with 5% diluted povidone-iodine solution were administered. The infections appeared to resolve following pin removal and antibiotic treatment. The animals remained under clinical observation, displaying normal behavior and recovery from infection throughout the 12-week study period.

Radiographic evaluation performed before and immediately after surgical implantation and compression of the mechanical apparatus demonstrated significant changes in disc height at the compressed level (L2-L3) and preservation of disc height at the non-compressed level (L4-L5).

Specifically, compression caused a marked reduction in disc height at the dorsal aspect of L2-L3, along with a reflexive distraction at the ventral aspect of the IVD (Figure 3). The average disc height at the compressed L2-L3 level prior to surgery was (mean ± SD) 2.647 ± 0.34 mm dorsally and 3.658 ± 0.57 mm ventrally. Immediately after surgery, the average disc height at L2-L3 measured 1.342 ± 0.55 mm dorsally and 5.558 ± 1.82 mm ventrally. In contrast, the non-compressed intervertebral disc (L4-L5) showed no significant changes in disc height in either the dorsal or ventral aspects.

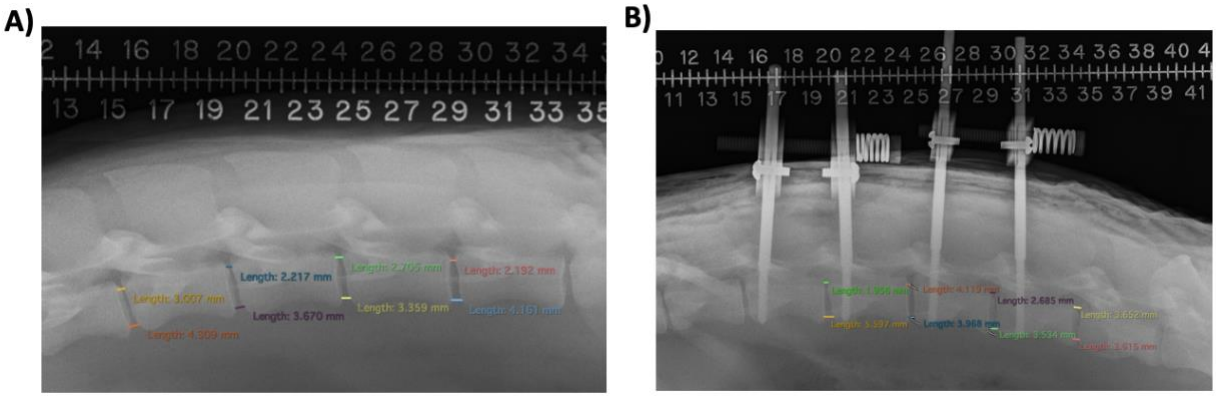

Figure 3. Representation of the changes in the disc height of the IVDs treated before and immediately post mechanical compression. A) Representative lateral lumbar radiographic image pre surgery from animal before the mechanical compression apparatus was implanted. B) Representative lateral lumbar radiographic image post-surgery showing evident changes in disc height at the cranial compressed device (L2-L3).

Subsequent imaging time points allowed for regular assessment of dorsal and ventral disc height. Statistically significant changes were observed at 6 and 12 weeks between the dorsal and ventral aspects of the compressed IVD level (L2-L3). In contrast, the non-compressed static stabilized IVD level (L4-L5) showed no significant changes throughout the 6- or 12-week study period (Figure 4).

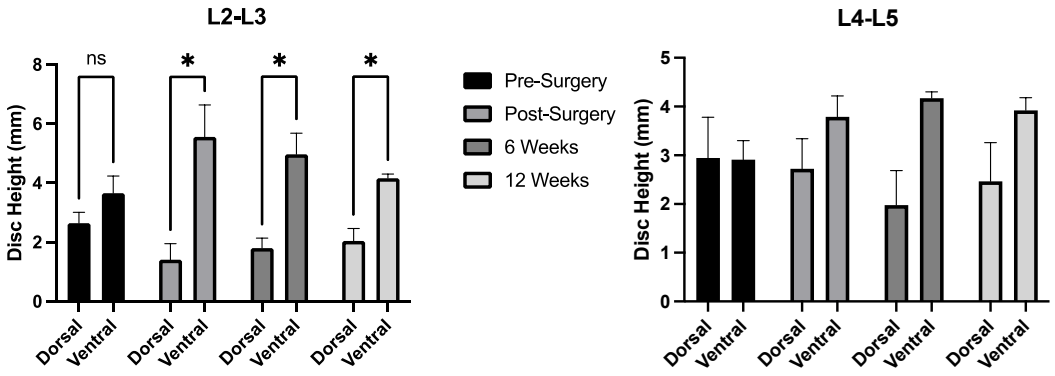

Figure 4. Graphs displaying disc height measurements at the L2-L3 and L4-L5 levels demonstrate that the compression device successfully altered disc height immediately following application. Significant difference in disc height was observed at the L2-L3 IVD immediately after compression and throughout the 12-week study period, resulting in dorsal compression (decreased disc height) and ventral distraction (increased disc height). No significant changes in disc height were observed at the L4-L5 level. Data are presented as median ± SD. *P < 0.05.

Analysis of the MR images revealed noticeable artifacts caused by the materials used in the implanted mechanical compression apparatus. Nevertheless, a comprehensive evaluation of the IVDs was successfully achieved. Even after the removal of the titanium pins due to infection, pin tracks were still evident in the MR images at 12 weeks post-implantation in animals from the treatment group. (Figure 5). Pfirrmann evaluation of L2-L3 and L4-L5 levels in the animals from the treatment group, and animals from control group showed not significant changes related to the degree of degeneration (Figure 6).

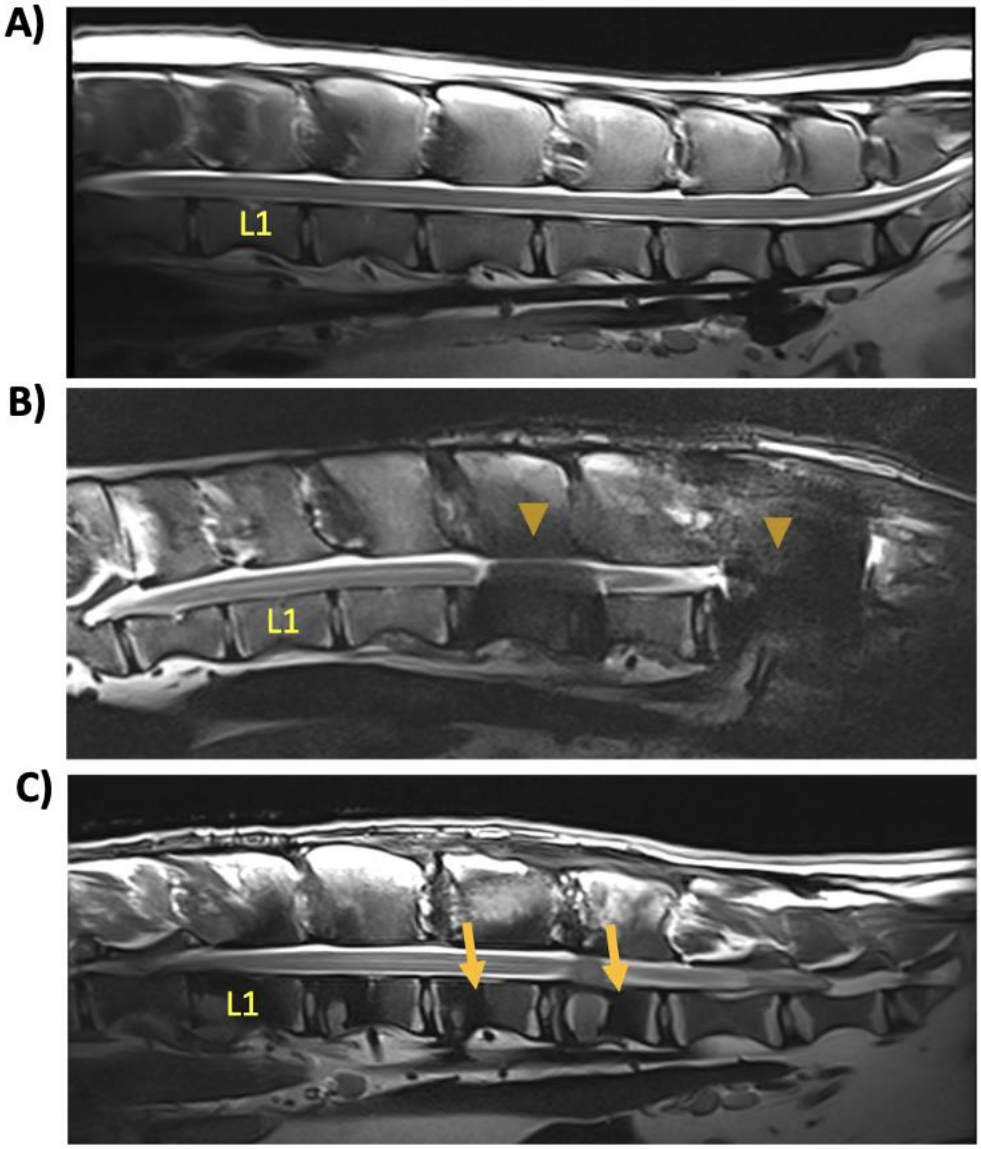

Figure 5. Representative sagittal lumbar T2-weighted MR images of the L2-3, L3-4, and L4-5 discs from animals subjected to compression at 0 weeks (A), 6 weeks (B), and 12 weeks (C). Signal interference caused by the titanium pins is evident at 6 weeks (arrowheads). Pin tracks are visible after pin removal at 12 weeks (arrows). No significant Pfirrmann changes were observed in the MRI assessments of the L2-3 or L4-5 discs throughout the 12-week study period following mechanical compression.

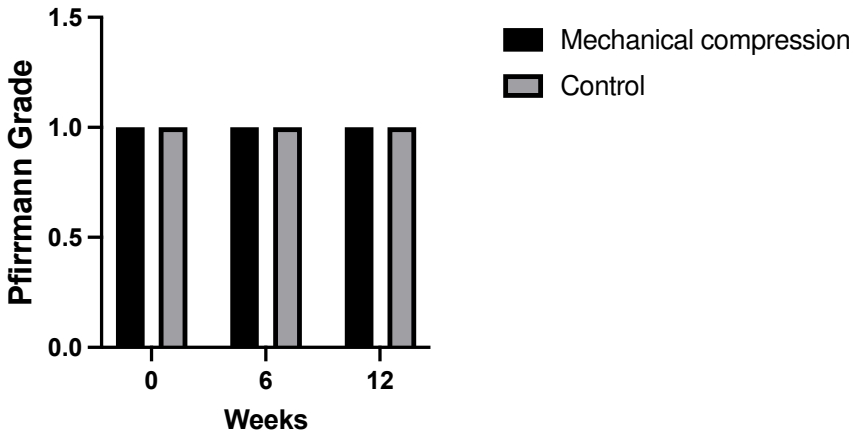

Figure 6. The graph illustrates Pfirrmann scores at baseline, 6 weeks, and 12 weeks for control IVDs and discs subjected to mechanical compression. No significant changes in Pfirrmann scores were observed on MRI assessment in the compressed discs compared to the naïve control discs at any time point.

Luminex assay measurements of TNF-alpha, IL-1ß, IL-6, IL-10, and IL-17A revealed no statistically significant differences between groups or time points (Figure 7). Similarly, biochemical analysis using the DMMB technique showed no differences in the Nucleus pulposus or Annulus Fibrosus tissues among the groups (Figure 8). Additionally, no significant differences were observed in the histological grading scores for large animal models of intervertebral disc degeneration (Figure 9).

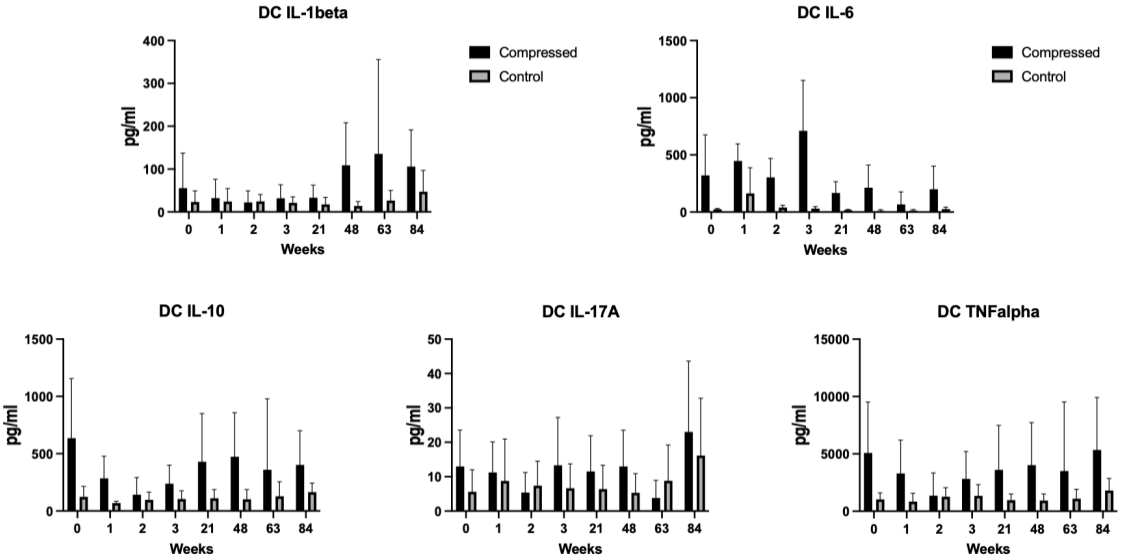

Figure 7. The graphs illustrate serum cytokine measurements obtained via Luminex assay at baseline and at 1, 2, 3 days, as well as at 6, 9, and 12 weeks. Although some cytokines exhibited visual trends, no significant differences were observed in the concentrations of IL-1beta, IL-6, IL-10, IL-17A, and TNF-alpha between the treated and control intervertebral discs. Data are presented as median ± SD

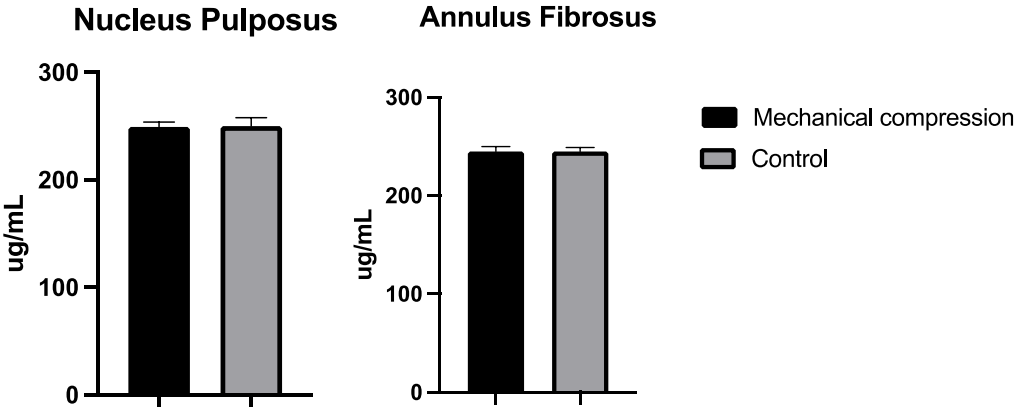

Figure 8. The graph presents glycosaminoglycan measurements obtained via the DMMB assay at the 12-week time point. No significant differences were observed between the mechanically compressed discs and the control discs. Data are presented as median ± SD.

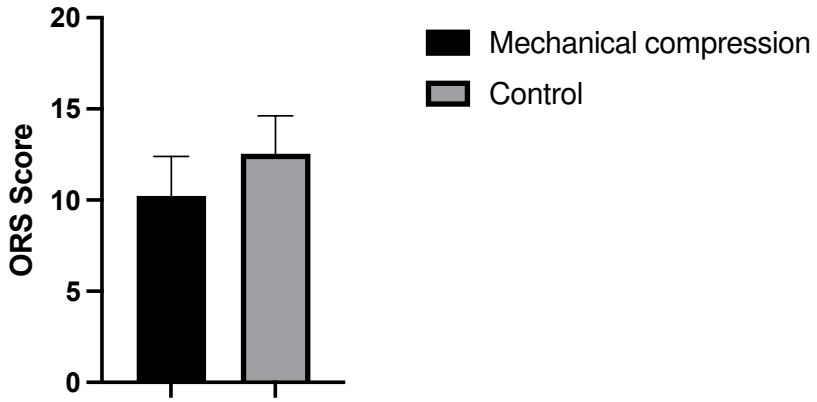

Figure 9. The graph outlines the histological scoring of treated and control discs. Histological evaluation of the L2-L3 and L4-L5 disc levels subjected to mechanical compression, compared to the control discs, revealed no significant differences. Data are presented as median ± SD.

Biomechanical evaluation was successfully completed for all control and treated functional spinal units (FSUs) across flexion, lateral, and axial movements. For each type of movement, the range of motion, neutral zone, and neutral zone stiffness were assessed. Significant differences were observed in the lateral neutral zone between control and compressed IVDs at 12 weeks following the removal of the compression device ($P = 0.0424$) (Figure 10). No statistically significant differences were found in the other parameters evaluated.

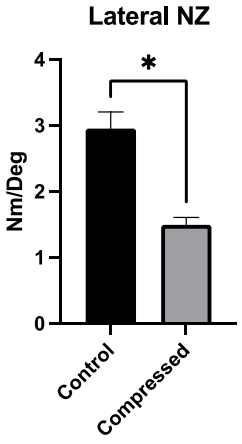

Figure 10. The graph highlights significant differences in neutral zone measurements between control and treated IVDs. NZ: Neutral zone. Data are presented as median ± SD. *P < 0.05.

5. 5 Discussion

The present study successfully developed a novel large animal model IVDD through mechanical compression using MRI-compatible materials in sheep. Despite the unexpected infection compromising the mechanical compression device, this model offers valuable insights into the biomechanical and imaging changes associated with IVDD, with significant translational potential for understanding human disc degeneration and for evaluating therapeutic interventions.

The mechanical compression device applied to the L2-L3 IVD resulted in significant alterations in disc height, as confirmed by radiographic imaging immediately post-surgery and throughout the 12-week study period. The significant reduction in dorsal portion disc height, coupled with ventral distraction, provides evidence that the compression apparatus effectively induced mechanical stress on the IVD. These results align with previous studies suggesting that mechanical destabilization contributes to the progression of disc degeneration by disrupting disc height and altering load distribution across the vertebral column (307,310). Importantly, the non-compressed static stabilized L4-L5 disc levels showed no significant changes, underscoring the specificity of the model to targeted disc compression. These results also align with the changes related to unisegmental disc compression and the non-affection to adjacent segments reported in other animal models (320).

The MR imaging allowed for non-invasive monitoring of disc changes, though the presence of titanium pins introduced artifacts that interfered with image quality. Despite these artifacts, the study successfully demonstrated that MRI can still be used to track disc degeneration progression, which is crucial for future applications of this model (252,321). Notably, the Pfirrmann grading, commonly used to evaluate disc degeneration on MRI, did not reveal significant changes between

compressed and control discs. This could suggest that while biomechanical changes were evident, the progression of disc degeneration at the morphological level might require longer observation periods or more refined imaging techniques that minimize metal-related artifacts. This also emphasizes the need for improving non-metallic compression devices to enhance MRI clarity.

The biochemical analysis of proteoglycan content and cytokine profiling through Luminex assays revealed no significant differences between compressed and control discs. These findings suggest that the mechanical compression applied in this study did not induce substantial biochemical degradation of the disc matrix over the 12-week period. Previous research has suggested that prolonged or more intense mechanical loading may be necessary to observe biochemical shifts in the extracellular matrix (322–324). The absence of inflammatory cytokine elevation further suggests that mechanical compression alone, in the absence of acute traumatic injury, may not be sufficient to elicit a pronounced systemic inflammatory response in this timeframe. However, the trends observed in some cytokines warrant further investigation over longer durations or with different loading intensities.

The most notable biomechanical outcome of this study was the significant alteration observed in the lateral neutral zone of compressed IVDs. The neutral zone, which represents the flexibility of the spine under low loads, is a key biomechanical parameter in assessing disc function (325–327). The significant decrease in the lateral neutral zone in compressed discs at 12 weeks suggests that mechanical destabilization impairs the normal flexibility and stability of the disc, potentially predisposing the spine to further degeneration or injury. This finding is particularly relevant, as lateral movement is a common contributor to disc injury in both animal models and humans (326,328). While no significant differences were found in other biomechanical parameters, the lateral neutral zone outcome highlights the effectiveness of the model in replicating

mechanical alterations associated with early disc degeneration.

This study represents the first use of MRI-compatible materials for mechanical disc compression in a large animal model, which overcomes a major limitation in prior research using metal devices that cause significant imaging artifacts. The ability to monitor disc degeneration through MRI provides an essential tool for longitudinal studies, allowing researchers to track the progression of degeneration and evaluate therapeutic interventions (146,252). However, future studies should aim to refine the compression apparatus to further reduce imaging interference and extend observation periods to capture more advanced stages of degeneration. Additionally, it may be beneficial to explore variations in mechanical loading to assess dose-dependent effects on biochemical, histological, and biomechanical parameters.

One of the challenges encountered in this study was the development of pin tract infections, leading to the early removal of the compression devices. While these infections were controlled through device removal and antibiotic treatment, future studies should consider alternative device designs or the use of antimicrobial coatings to reduce the risk of infection, or mechanical compression without external exposure of the device. Furthermore, longer follow-up periods could provide valuable insights into the long-term effects of mechanical compression on both the IVD and surrounding tissues.

Finally, this study successfully established a novel large animal model for intervertebral disc degeneration using MRI-compatible mechanical compression in sheep. The model effectively induced biomechanical alterations, particularly in the lateral neutral zone, without significant biochemical or inflammatory changes within the 12-week period. While the study faced challenges related to pin tract infections and MRI artifacts, the findings support the utility of this model for studying the early stages of disc degeneration and evaluating potential therapeutic interventions.

Future refinements to the compression apparatus and longer-term studies will be crucial for further enhancing the clinical relevance of this model.

5.6 References

1. Hartvigsen J, Hancock MJ, Kongsted A, Louw Q, Ferreira ML, Genevay S, et al. What low back pain is and why we need to pay attention. The Lancet. 2018 Jun 1;391(10137):2356–67.
2. Oichi T, Taniguchi Y, Oshima Y, Tanaka S, Saito T. Pathomechanism of intervertebral disc degeneration. JOR Spine. 2020;3(1):1–9.
3. Alini M, Diwan AD, Erwin WM, Little CB, Melrose J. An update on animal models of intervertebral disc degeneration and low back pain: Exploring the potential of artificial intelligence to improve research analysis and development of prospective therapeutics. JOR Spine. 2023;(August 2022):1–29.
4. Jin L, Balian G, Li XJ. Animal models for disc degeneration-an update. Histol Histopathol. 2018;33(6):543–54.
5. Poletto DL, Crowley JD, Tanglay O, Walsh WR, Pelletier MH. Preclinical in vivo animal models of intervertebral disc degeneration. Part 1: A systematic review. JOR Spine. 2022;(October 2022):1–20.
6. Fusellier M, Clouet J, Gauthier O, Tryfonidou M, Le Visage C, Guicheux J. Degenerative lumbar disc disease: In vivo data support the rationale for the selection of appropriate animal models. Eur Cell Mater. 2020;39:18–47.
7. Melrose J, Shu C, Young C, Ho R, Smith MM, Young AA, et al. Mechanical destabilization induced by controlled annular incision of the intervertebral disc dysregulates metalloproteinase expression and induces disc degeneration. Spine (Phila Pa 1976). 2012

Jan 1;37(1):18–25.

8. Schollum ML, Appleyard RC, Little CB, Melrose J. A detailed microscopic examination of alterations in normal anular structure induced by mechanical destabilization in an ovine model of disc degeneration. Spine (Phila Pa 1976). 2010 Oct 15;35(22):1965–73.

9. Cunningham BW, Kotani Y, McNulty PS, Cappuccino A, McAfee PC. The Effect of Spinal Destabilization and Instrumentation on Lumbar Intradiscal Pressure. Spine (Phila Pa 1976). 1997 Nov;22(22):2655–63.

10. Desmoulin GT, Pradhan V, Milner TE. Mechanical Aspects of Intervertebral Disc Injury and Implications on Biomechanics. Spine (Phila Pa 1976). 2020 Apr 15;45(8):E457–64.

11. Desmoulin GT, Pradhan V, Milner TE. Mechanical Aspects of Intervertebral Disc Injury and Implications on Biomechanics. Spine (Phila Pa 1976). 2020 Apr 15;45(8):E457–64.

12. Drew SC, Silva P, Crozier S, Pearcy MJ. A diffusion and T2 relaxation MRI study of the ovine lumbar intervertebral disc under compression in vitro. Phys Med Biol. 2004 Aug 21;49(16):3585–92.

13. Beckstein JC, Sen S, Schaer TP, Vresilovic EJ, Elliott DM. Comparison of Animal Discs Used in Disc Research to Human Lumbar Disc. Spine (Phila Pa 1976). 2008 Mar;33(6):E166–73.

14. Kroeber MW, Unglaub F, Wang H, Schmid C, Thomsen M, Nerlich A, et al. New in vivo animal model to create intervertebral disc degeneration and to investigate the effects of therapeutic strategies to stimulate disc regeneration. Spine (Phila Pa 1976). 2002;27(23):2684–90.

15. Oichi T, Taniguchi Y, Soma K, Chang SH, Yano F, Tanaka S, et al. A Mouse Intervertebral Disc Degeneration Model by Surgically Induced Instability. Spine (Phila Pa 1976). 2018

May 15;43(10):E557–64.

16. Guehring T, Unglaub F, Lorenz H, Omlor G, Wilke HJ, Kroeber MW. Intradiscal pressure measurements in normal discs, compressed discs and compressed discs treated with axial posterior disc distraction: An experimental study on the rabbit lumbar spine model. European Spine Journal. 2006 May;15(5):597–604.

17. LePage EC, Stoker AM, Kuroki K, Cook JL. Effects of cyclic compression on intervertebral disc metabolism using a whole-organ rat tail model. Journal of Orthopaedic Research. 2020;(May):1–10.

18. Zhu S, Yang X, Luan Y, Liu Q, Zhang C. [Experiments study on mechanical behavior of porcine lumbar intervertebral disc after nucleotomy under compression]. Sheng Wu Yi Xue Gong Cheng Xue Za Zhi. 2019 Aug;36(4):590–5.

19. Yao T, Gao J, You C, Xu Y, Qiao D, Shen S, et al. A new animal model of lumbar disc degeneration in rabbits. The Spine Journal. 2024 Aug;24(8):1519–26.

20. Lappalainen AK, Kääpä E, Lamminen A, Laitinen OM, Grönblad M. The Diagnostic Value of Contrast-Enhanced Magnetic Resonance Imaging in the Detection of Experimentally Induced Anular Tears in Sheep. Spine (Phila Pa 1976). 2002 Dec;27(24):2806–10.

21. Bouhsina N, Decante C, Hardel JB, Rouleau D, Abadie J, Hamel A, et al. Comparison of MRI T1, T2, and T2* mapping with histology for assessment of intervertebral disc degeneration in an ovine model. Sci Rep. 2022 Dec 1;12(1).

22. Alisauskaite N, Bitterli T, Kircher PR, Pozzi A, Grinwis GCM, Steffen F, et al. Evaluation of agreement and correlation of results obtained with mri-based and macroscopic observation– based grading schemes when used to assess intervertebral disk degeneration in cats. Am J Vet Res. 2020 Apr 1;81(4):309–16.

23. Wang L, Han M, Wong J, Zheng P, Lazar AA, Krug R, et al. Evaluation of human cartilage endplate composition using MRI: Spatial variation, association with adjacent disc degeneration, and in vivo repeatability. Journal of Orthopaedic Research. 2021 Jul 1;39(7):1470–8.

24. Lee NN, Salzer E, Bach FC, Bonilla AF, Cook JL, Gazit Z, et al. A comprehensive tool box for large animal studies of intervertebral disc degeneration. JOR Spine. 2021;(July 2020):1–36.

25. Pfirrmann CWA, Metzdorf A, Zanetti M, Hodler J, Boos N. Magnetic resonance classification of lumbar intervertebral disc degeneration. Spine (Phila Pa 1976). 2001;26(17):1873–8.

26. Naylor D, Sharma A, Li Z, Monteith G, Sullivan T, Canovas A, et al. Short communication: Characterizing ovine serum stress biomarkers during endotoxemia. J Dairy Sci. 2020 Jun;103(6):5501–8.

27. Easley J, Puttlitz C, Seim H, Ramo N, Abjornson C, Cammisa F, et al. Biomechanical and histologic assessment of a novel screw retention technology in an ovine lumbar fusion model. Spine Journal. 2018;18:2302–15.

28. Lee NN, Salzer E, Bach FC, Bonilla AF, Cook JL, Gazit Z, et al. A comprehensive tool box for large animal studies of intervertebral disc degeneration. JOR Spine. 2021;(July 2020):1–36.

29. Unglaub F, Guehring T, Lorenz H, Carstens C, Kroeber MW. Effects of unisegmental disc compression on adjacent segments: an in vivo animal model. European Spine Journal. 2005 Dec 17;14(10):949–55.

30. Nisolle JF, Wang XQ, Squélart M, Hontoir F, Kirschvink N, Clegg P, et al. Magnetic

Resonance Imaging (MRI) Anatomy of the Ovine Lumbar Spine. Anat Histol Embryol. 2014 Jun;43(3):203–9.

31. Nisolle JF, Bihin B, Kirschvink N, Neveu F, Clegg P, Dugdale A, et al. Prevalence of age-related changes in ovine lumbar intervertebral discs during computed tomography and magnetic resonance imaging. Comp Med [Internet]. 2016 Aug 1 [cited 2022 Dec 13];66(4):300–7. Available from: /pmc/articles/PMC4983172/

32. Lotz JC. Animal Models of Intervertebral Disc Degeneration. Spine (Phila Pa 1976). 2004 Dec;29(23):2742–50.

33. Ching CTS, Chow DHK, Yao FYD, Holmes AD. The effect of cyclic compression on the mechanical properties of the inter-vertebral disc: An in vivo study in a rat tail model. Clinical Biomechanics. 2003 Mar;18(3):182–9.

34. Kroeber M, Unglaub F, Guehring T, Nerlich A, Hadi T, Lotz J, et al. Effects of Controlled Dynamic Disc Distraction on Degenerated Intervertebral Discs. Spine (Phila Pa 1976) [Internet]. 2005 Jan;30(2):181–7. Available from: https://insights.ovid.com/crossref?an=00007632-200501150-00004

35. Cannella M, Arthur A, Allen S, Keane M, Joshi A, Vresilovic E, et al. The role of the nucleus pulposus in neutral zone human lumbar intervertebral disc mechanics. J Biomech. 2008 Jul;41(10):2104–11.

36. Di Pauli von Treuheim T, Torre OM, Mosley GE, Nasser P, Iatridis JC. Measuring the neutral zone of spinal motion segments: Comparison of multiple analysis methods to quantify spinal instability. JOR Spine. 2020 Jun 25;3(2).

37. Smit TH, van Tunen MS, van der Veen AJ, Kingma I, van Dieën JH. Quantifying intervertebral disc mechanics: a new definition of the neutral zone. BMC Musculoskelet

Disord. 2011 Dec 7;12(1):38.

38. Mimura M, Panjabi MM, Oxland TR, Crisco JJ, Yamamoto I, Vasavada A. Disc Degeneration Affects the Multidirectional Flexibility of the Lumbar Spine. Spine (Phila Pa 1976). 1994 Jun;19(12):1371–80.

CHAPTER 6. DEVELOPMENT AND EVALUATION OF AN IMMUNOLOGICAL APPROACH TO NOVEL DISC DEGENERATION MODEL

6. 1 Summary

Low back pain poses a significant societal burden, with progressive intervertebral disc degeneration (IDD) emerging as a pivotal contributor to chronic pain. Improved animal models of progressive IDD are needed to comprehensively investigate new diagnostic and therapeutic approaches to managing IDD. Recent studies underscore the immune system's involvement in IDD, particularly with regards to the role of immune privileged tissues such as the nucleus pulposus (NP) becoming an immune targeting following initial disc injury. We therefore hypothesized that generating an active immune response against NP antigens with an NP vaccine could significantly accelerate and refine an IDD animal model triggered by mechanical puncture of the disc. To address this question, rabbits were immunized against NP antigens following disc puncture, and the impact on development of progressive IDD was assessed radiographically, functionally, and histologically compared between vaccinated and non-vaccinated animals over a 12-week period. Immune responses to NP antigens were assessed by ELISA and Western blot. We found that the vaccine elicited strong immune responses against NP antigens, including a dominant ~37 kD antigen. Histologic evaluation revealed increases IDD in animals that received the NP vaccine plus disc puncture, compared to disc puncture and vaccine only animals. Imaging evaluation evidenced a decrease in disc height index and higher scores of disc degeneration in animals after disc punctures and in those animals that received the NP vaccine in addition to disc puncture.

This chapter includes the complete published manuscript: Bonilla AF, Sikes KJ, Burton LH, Chow L, Kurihara J, Santangelo K, Dow SW and Easley JT (2024) Immunization against nucleus pulposus antigens to accelerate degenerative disc disease in a rabbit model. Front. Vet. Sci. 11:1382652. doi: 10.3389/fvets.2024.1382652

These findings therefore indicate that it is possible to elicit immune responses against NP antigens in adult animals, and that these immune responses may contribute to accelerated development of IDD in a novel immune-induced and accelerated IDD model.

6. 2. Introduction

Low back pain is a common multifactorial condition in the general population, causing a great economic impact due to loss of productivity and increased health care costs (329). Intervertebral disc degeneration (IDD) has been identified as one of the main causes of low back pain (330). Several animal models have been developed to understand the pathophysiology and evaluate new therapeutic strategies for low back pain caused by IDD (158,331). However, there is scientific consensus around the need for improved animal models for elucidation of potential novel targets and approaches to treat IDD (241,288).

The intervertebral disc (IVD) is the largest avascular structure in the human body. It is composed of an outer Annulus Fibrosus (AF), made up of concentric lamellae rich in collagen type I, and a central gelatinous nucleus pulposus (NP), rich in proteoglycans and collagen type II. With increasing age and degeneration, the disc tissue becomes disorganized (330). Specifically, irregularities and loss of hydration to the AF through aggrecan degradation occurs, which leads to progressive loss of space between vertebrae, and fissures of the AF fibers often leading to disc herniation and exposure of NP to the vascular system and subsequently to the immune system (203,332,333).

An immune component in the development of IDD has recently attracted the attention of several researchers (334–336). There are differing theories on the role that immunologically privileged features of certain tissues of intervertebral disc, most notably the NP antigens, play in

the pathogenesis of the IDD (336–338). In healthy IVD, the NP is avascular and isolated from the immune system by the AF (339,340). As IDD progresses, the vascularization process and fissures within the AF results in exposure of the NP antigens to cells and antibodies of the immune system. Degradation products of disc proteins can trigger an immune reaction experimentally, and there is evidence from clinical studies that IVD injury can induce the production of anti-NP antibodies (339,341). Common techniques used to induce IDD in preclinical models involve disrupting the AF and exposing the NP antigens to the peripheral immune system. This exposure could trigger inflammatory responses within the IVD, thereby promoting further IVD injury (342). Several previous studies have reported finding anti-NP antibody and cellular responses in humans with IDD, as well as in animal models (341,343–345). We hypothesized that administering a vaccine containing NP material would increase disc degeneration signs in an animal model compared to animals solely subjected to disc puncture without the vaccine. Our study is, to our knowledge, the first to combine inducing anti-NP immunity with mechanical IVD injury to accelerate IDD in an animal model. In this report, we present the results of our efforts to replicate and refine IDD in a rabbit model through vaccination against NP antigens combined with surgical IVD injury.

6. 3 Materials and methods

Animals - This study was performed with approval from the Institutional Animal Care and Use Committee at Colorado State University (protocol#: 20-9762A). A total of 12 female New Zealand White rabbits (age range 12–16 months, weight range 4.3–5.2 kg) were acclimated at least two weeks prior study initiation. Animals were randomly assigned to NP-Vaccine group (NP-Vac), NP-Exposure group (NP-Exp) or NP-Vaccine + NP Exposure group (NP-Vac+NP-Exp) (n = 4

rabbits per group).

Vaccine preparation - Nucleus pulposus material was collected from two healthy sheep to prepare the NP antigens. Sheep were selected as a source of NP material because injected rabbits would likely have a higher chance of developing an immune reaction to NP proteins due to the species cross-reactivity. The NP tissue was then processed following the protocol proposed by Capossela (346). Briefly, the NP tissue samples were pulverized on dry ice in a stainless-steel mortar. Collagenase (Type 2, ThermoFisher Scientific) was added to cause digestion of the tissue, and lysates were homogenized using a Sonicator ultrasonic device. After 15 min of incubation at room temperature, lysates were centrifuged at 17,000 g for 15 min at 4 °C to remove debris. Protein concentrations of supernatants were measured by BCA protein assay (Axonlab). To prepare the NP vaccine, NP proteins were mixed with a liposome-TLR agonist vaccine adjuvant, previously been reported to elicit high levels of both antibody and cellular immunity to a number of different protein and peptide antigens (347–349). The vaccine was developed under stringent conditions in a dedicated BSL2 laboratory. Each batch of the vaccine was uniquely derived from ovine nucleus pulposus extraction, ensuring consistency and uniformity across administrations. The rabbits were immunized with 250ug NP protein via the subcutaneous route, administered once every two weeks for a total of three immunizations, with the first dose being administered immediately before surgery.

Surgical intervention - All surgical procedures were conducted under aseptic conditions. Animals were pre-medicated with glycopyrrolate and buprenorphine. Once initially sedated using ketamine/dexmedetomidine, animals were placed on Isoflurane face mask at 4-5% until they

reached a surgical plane of anesthesia, then maintained on 2-3% Isoflurane and 100% oxygen. Prior to surgery, each rabbit was placed in right lateral recumbency, and the posterolateral aspect (over the lumbar spine) was shaved and prepped using an alternating combination of 70% alcohol and chlorhexidine. For NP-Exp and NP-Vac+NP-Exp groups the lumbar spine was approached from the left side and the technique described by Luo *et al.,*(350) was performed. Briefly, a minimally invasive transcutaneous needle puncture technique, guided by fluoroscopy, was employed using a 16G spinal needle to puncture the L2-3, L3-4, L4-5, and L5-6 intervertebral discs. Needle placement was confirmed through fluoroscopic images until it passed through the full diameter of the intervertebral disc without puncturing the contralateral annulus fibrosus.

Detection of anti-NP antibody responses by ELISA - Blood serum was collected prior to surgery and NP vaccine injection, and at 0, 2, 4, 8 and 12 weeks after these procedures to detect the presence of anti-NP antibody responses using an NP ELISA custom created for this study. Briefly, a 96-well Immulon plate (ThermoFisher) was coated with 100 µl of NP protein isolated from pooled sheep NP material collected at necropsy. The NP protein was diluted to a concentration of 20ug/mL in carbonate buffer. After incubation overnight at 4 °C, wells were washed with PBS Tween using a plate washer, and non-specific binding sites were blocked for 2 h at room temperature with PBS+10% BSA. After washing with PBS, 100 µl of rabbit serum (diluted 1:100 in 1%BSA/PBS) were added to the plates and incubated for 2 h at room temperature. After a second plate wash, 100 µl of 1:3000 dilution (in PBS + 1% BSA) of peroxidase conjugated donkey anti rabbit IgG (Jackson Immuno Research) was added and incubated for 1 h at room temperature. Following washing with PBS, TMB-ELISA Substrate Solution (ThermoFisher) was added and incubated for 10 min. Finally, 50 µL TMB stop solution was added and the optical density (OD)

was measured at an absorbance at 450 nm. Optical density values were plotted, and pre-vaccination serum ODs were compared to post-vaccination ODs.

Western Blot - The sheep NP proteins used to prepare the vaccine were also used in the Western blotting procedure. The NP proteins were prepared under reducing, denaturing conditions, and 20ug total protein was loaded into a 4–20% Mini-PROTEAN TGX gel (Bio-Rad) and transferred to PVDF membrane (Bio-Rad). After blocking the membrane with 5% BSA in Tris-buffered saline with 0.1% Tween (TBST) for 1 hr, the membranes were then incubated with blood serum samples from 0 weeks and 12 weeks. Serums were diluted 1:100,000 using 5% BSA in TBST and incubated overnight at 4°C. The membranes were incubated 1 hr at room temperature with Peroxidase AffiniPure™ Goat Anti-Rabbit IgG (H+L) (Jackson Immunoresearch, USA), followed by washing, the blots were developed using Clarity Western ECL Substrate (Bio-Rad) and imaged on ChemiDoc XRS+ with Image Lab Software (Bio-Rad). Bands of gel that showed robust antibody response were isolated and submitted for proteomic evaluation using Mass spectrometry analysis (Orbitrap Eclipse, Thermo Scientific). Raw data was evaluated using Proteome Discoverer 3.0 (Thermo Scientific) and interrogated against the FASTA reference proteome of *Oryctolagus cuniculus* (rabbit, taxon ID 9986) from Uniprot. Additionally, the cRAP proteome was included (The common Repository of Adventitious Proteins -cRAP- contains commonly found contaminant proteins in proteomics experiments).

***In vivo* Imaging -** Radiographs and MR (Magnetic Resonance) imaging of the lumbar spines was performed prior to injury, 8 weeks post-injury, and immediately pre-mortem at 12 weeks (**Figure 1**). Animals were pre-medicated and anesthetized by initial induction of 4% isoflurane, with

maintenance at 1 – 3%, and placed in the prone position. Lateral and dorsoventral digital radiographic views of the lumbar spines were acquired for each animal and use to evaluated significant bone abnormalities. The MR imaging was performed using a 3T MR scanner (Siemens 3T MAGNETOM Skyra MR Scanner) to obtain 2-dimensional T1 and T2-weighted sequences in sagittal orientation, and axial views with a T2-weighted sequence. The following basic protocol parameters were used for image acquisition: RT 3010 ms, ET 97 ms, 1.5 mm slices, acquisition matrix 384 x 288, Flip Angle of 260 degrees, and bandwidth of 480 Hz. Evaluation of MR images was completed by two blinded observers (AB, JE) and used to determine disc height index (DHI) (258,259), and Pfirrmann grade (260). MRI was chosen to assess DHI due to its superior resolution, which enables precise evaluation of disc height changes within the same slice or plane, enhancing the accuracy of measurements and analysis.

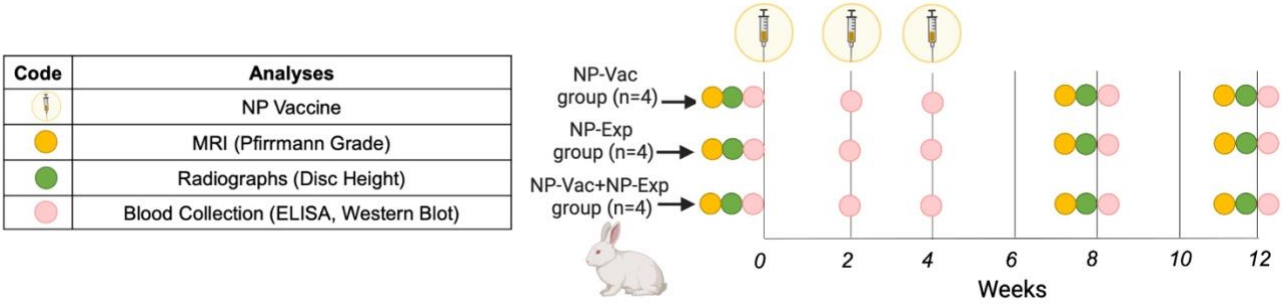

Figure 1: Schematic representation of the study design. Rabbits were allocated into three groups, NP-Vaccine group (NP-Vac), NP-Exposure group (NP-Exp) or NP-Vaccine + NP Exposure group (NP-Vac+NP-Exp). NP vaccine (syringe) was administered at 0, 2, and 4 weeks for NP-Vac and NP-Vac+NP-Exp groups. Imaging, comprising radiographs and MRI, was conducted at 0, 8, and 12 weeks (Yellow and green circles, respectively). Subsequent blood collection for ELISA and Western Blot evaluation took place at 0, 2, 4, 8, and 12 weeks (Pink circles).

Euthanasia and sample harvest - The rabbits were humanely euthanized 12 weeks after surgery and/or first vaccination by intravenous overdose of pentobarbitone sodium (88mg/kg), in accordance with the American Veterinary Medical Association (AVMA) guidelines. The lumbar spines were removed to complete the *ex vivo* evaluation. Additional evaluation methods, including

Micro-CT, biomechanical testing, biochemical assays (L3-4, L5-6), and histomorphometry, along with corresponding results, are detailed in the supplemental material.

Histopathological analysis - Two functional spinal units (L_{2-3}, L_{4-5}) were bisected in the sagittal plane and processed for decalcified histological analysis. Following fixation, specimens were decalcified using EDTA 10%. Then, specimens were processed using standard techniques (Tissue-Tek VIP, Sakura, Torrance, CA) and embedded in paraffin. Two slides were produced from each sample. One was stained with Hematoxylin Eosin and the other with Alcian blue for evaluation of glycosaminoglycans (GAG) (30). Histology sections stained for analysis underwent meticulous evaluation by two blinded observers, one being a certified veterinary pathologist. Utilizing a specific scoring system tailored for IDD in rabbit models (351), various parameters including nucleus pulposus (NP) morphology (shape and area), NP matrix integrity, NP cellularity, distinction of annulus fibrosus (AF) and NP border, AF morphology, and endplate (EP) thickening were assessed.

Statistical analysis - Following data processing, statistical analyses were performed on all outcome parameters. Standard two-way ANOVA test, followed by Tukey's multiple comparison test, was performed to determine statistically significant differences ($p \leq 0.05$) within and across treatment groups (GraphPad Prism 8.3.0, San Diego, CA). Data for ELISA, histological grading, Pfirrmann grade, and disc height are presented as mean ± SD.

6. 4. Results

Assessment of anti-NP immunity using ELISA screening - We assessed the impact of NP

vaccination on induction of anti-NP antibody responses to determine the effectiveness of the NP vaccine. Serum samples from animals in all three study groups were evaluated for the presence of anti-NP antibodies using an NP ELISA (see Methods). In both groups receiving the NP vaccine, strong IgG antibody responses to NP antigens developed and were detectable after the first immunization, increasing further by weeks 8 and 12 (**Figure 2**). Conversely, anti-NP antibody responses were not detected in the control or disc puncture only groups of animals. Notably, antibody responses were detected at numerically higher in the NP vaccine plus disc puncture group of animals, though the differences in antibody responses between the vaccine only group and the vaccine plus disc puncture groups did not reach the level of statistical significance. These findings indicate, therefore, that the NP vaccine effectively elicited rabbit humoral immune responses against NP.

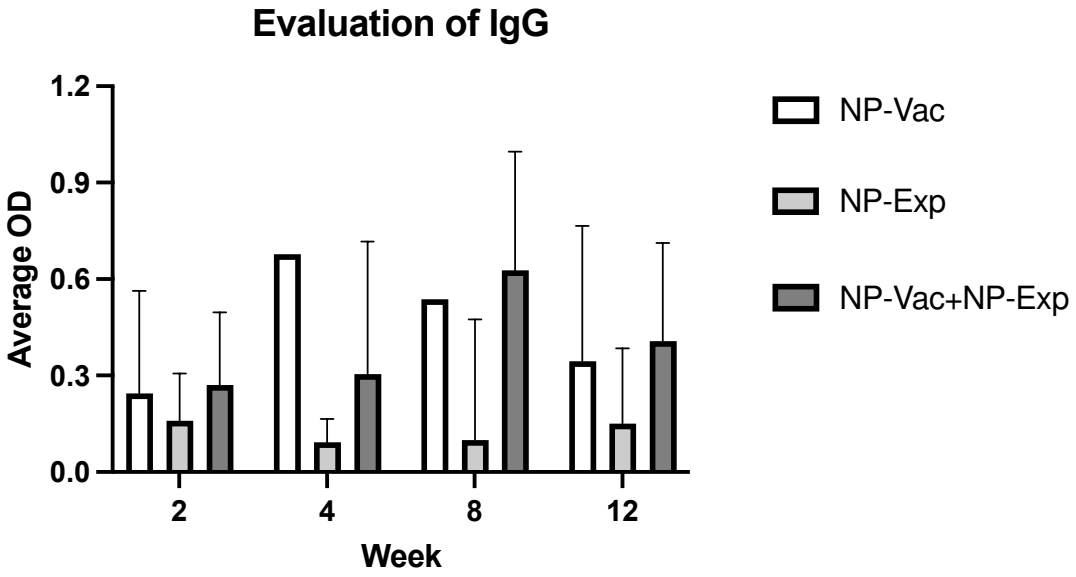

Figure 2: Evaluation of IgG in animals after induction of IVD degeneration. Animals from NP-Vac+NP-Exp group showed higher levels of IgG at 2-weeks, 4-weeks, 8-weeks, and 12-weeks compared with animals from NP-Vac and NP-Exp groups. An increase trend in IgG in the NP-Exp in time is also evident after exposure of the NP for NP-Exp group. Data are presented as mean with SD for each group with values normalized to 0 and excluding negative values. OD: Optical

density.

Western Blot - Next, we used Western blotting to identify dominant NP antigens being recognized by the anti-NP antibody responses. Intriguingly, in both groups of NP vaccinated animals, there was strong antibody recognition (**Figure 3**). Proteomic analysis of the bands exhibiting strong antibody response revealed the presence of 193 proteins and 958 peptides. Table 1 presents the most abundant proteins identified, which correlate with the molecular weights observed in the Western blot results. Therefore, evidence from this study suggests that few highly immunogenic NP proteins may be targets for immune recognition in cases of naturally occurring IDD. Identifying the nature of these antigens is important for better understanding IDD pathogenesis and designing potential therapeutic interventions in patients with IDD.

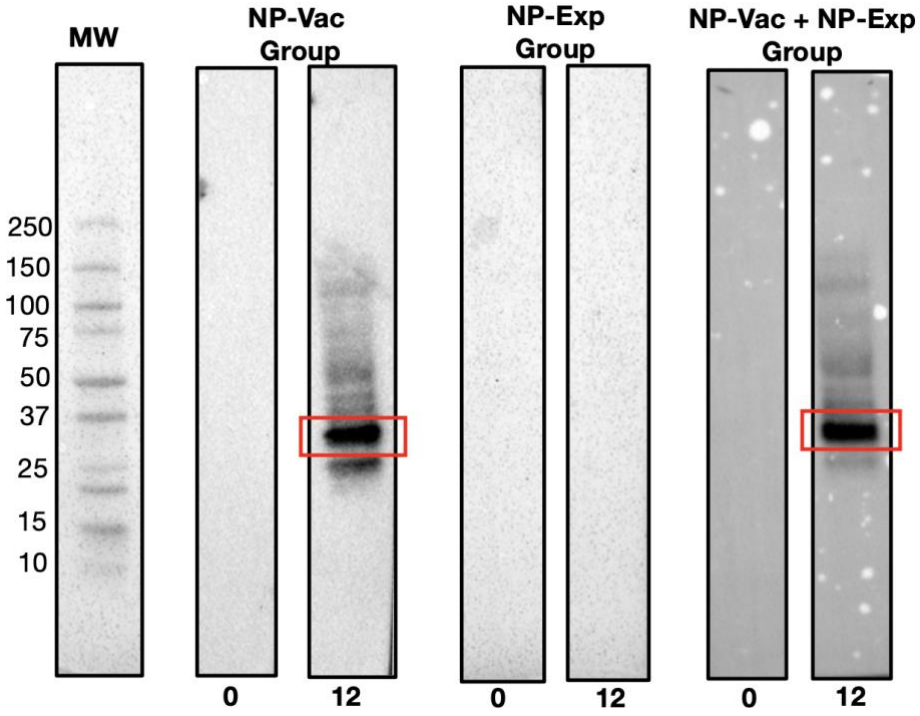

Figure 3: Representative Western Blot results demonstrating distinct immunoreactivity patterns among experimental groups. Clear bands at the 12-week time point in lanes corresponding to the NP-Vac group and the NP-Vac+NP-Exp group indicate a robust antibody response post-vaccination (Red squares). In contrast, no observable bands are seen in the lane representing NP-

Exp group, emphasizing the lack of immunoreactivity in this group. Results of all groups are presented in the supplemental material. MW: Molecular weight.

Accession	Description	Molecular Weight (kDa)
G1SHY5	Hyaluronan and proteoglycan link protein 1	40,2
A0A5F9DKI8	Actin, cytoplasmic 2	40
G1T5H0	HtrA serine peptidase 1	36,4

Table 1. Most abundant proteins with similar molecular weights to those observed in western blot results.

Histopathological analysis of IVD tissues and impact of NP vaccination - All three groups of animals in the study showed varying signs of IDD development, involving the AF, NP, and endplates, compared to healthy control reference values (351). Varying degrees of loss of distinction of structural components of the disc were evident in all three groups over the 12-week study period. Animals from NP-Vac group showed clear NP shape and evident integrity of the AF area but sclerosis of the endplates, compared with NP-Exp and NP-Vac+NP-Exp groups. In contrast, these latter two groups exhibited irregular NP shape and area, loss of distinction between NP and AF, and sclerosis of the endplates. Histological assessment showed increased severity of IDD in the NP-Vac+NP-Exp group compared with both the NP-Vac or NP-Exp groups, as well as with healthy control references (351). Histological scoring for rabbit IVDs showed a significantly higher degree of IDD, specifically for NP-Vac+NP-Exp animals compared with NP-Vac group (p=0,339) (**Figure 4**).

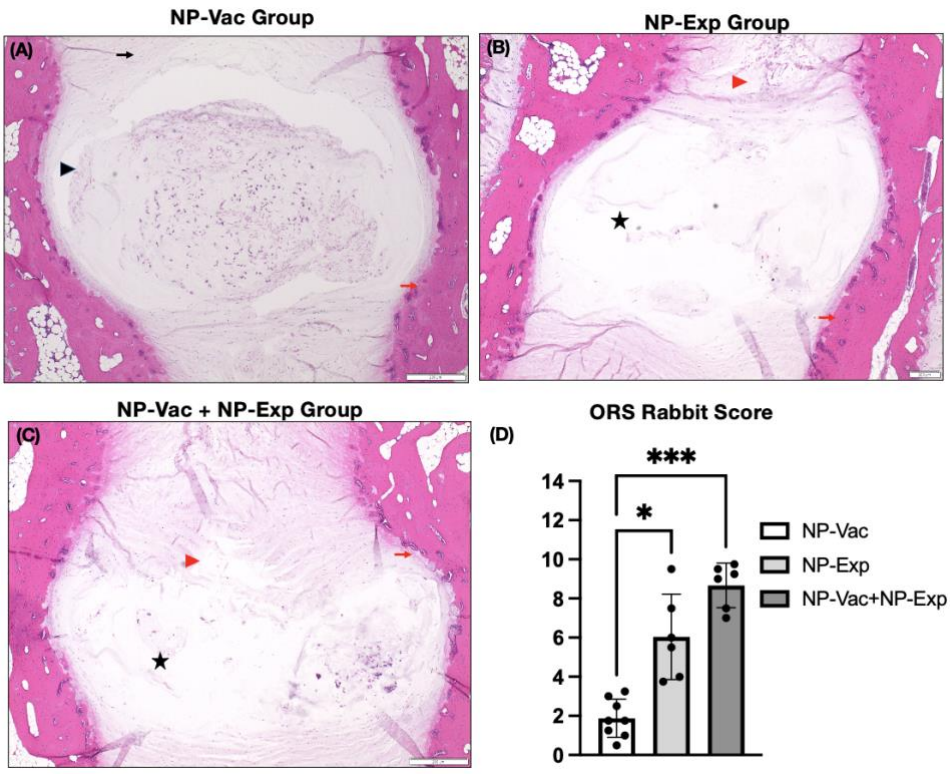

Figure 4: Representative histological images of the IVD and histopathological scoring from NP-Vac, NP-Exp, and NP-Vac+NP-Exp groups. A) Animals from NP-Vac group showed clear NP shape (Black arrowhead) and good integrity of the AF area (Black arrow), and sclerosis of the endplates (Red arrows). Conversely, NP-Exp (B) and NP-Vac+NP-Exp (C) groups showed irregular NP shape area, and less cellularity (Black star), and loss of distinction between NP and AF (Red arrowhead). Subjective histological assessment showed increased IVD degeneration in NP-Vac+NP-Exp animals compared with NP-Vac group or NP-Exp animals. D) Objective blinded histological scoring showed a significantly higher degree of IDD for NP-Vac+NP-Exp group animals compared with NP-Vac group ($p<0,05$). NP: Nucleus pulposus, AF: Annulus Fibrosus. H&E, scale bar: 200 µm.

Imaging of IVD injury sites following surgery and NP vaccination - Evaluation of the DHI showed a significant decrease for all groups after surgical intervention (disc puncture). The NP-Vac group showed a decrease in DHI at 8 weeks (P=0.0255) and 12 weeks (P=0.0119) compared to baseline. Animals from the NP-Exp group exhibited a decrease in DHI between 0 and 12 weeks (P=0.0254) and between 8 and 12 weeks (P=0.0076). Animals from NP-Vac+NP-Exp showed a decrease in DHI at 8 weeks (P=0.0420) and 12 weeks (P=0.0398) compared to baseline. The

comparison of DHI between groups showed a decrease in DHI across all groups, although no significant differences were observed between them (**Figure 5**). Four animals (two from NP-Vac group, one from NP-Exp group, and one from NP-Vac+NP-Exp group) showed signs of IDD in the MR images at baseline (Average of Pfirrmann grade of the 4 lumbar disc levels = 1.5, 2.625, 1.367 and 2.875 respectively).

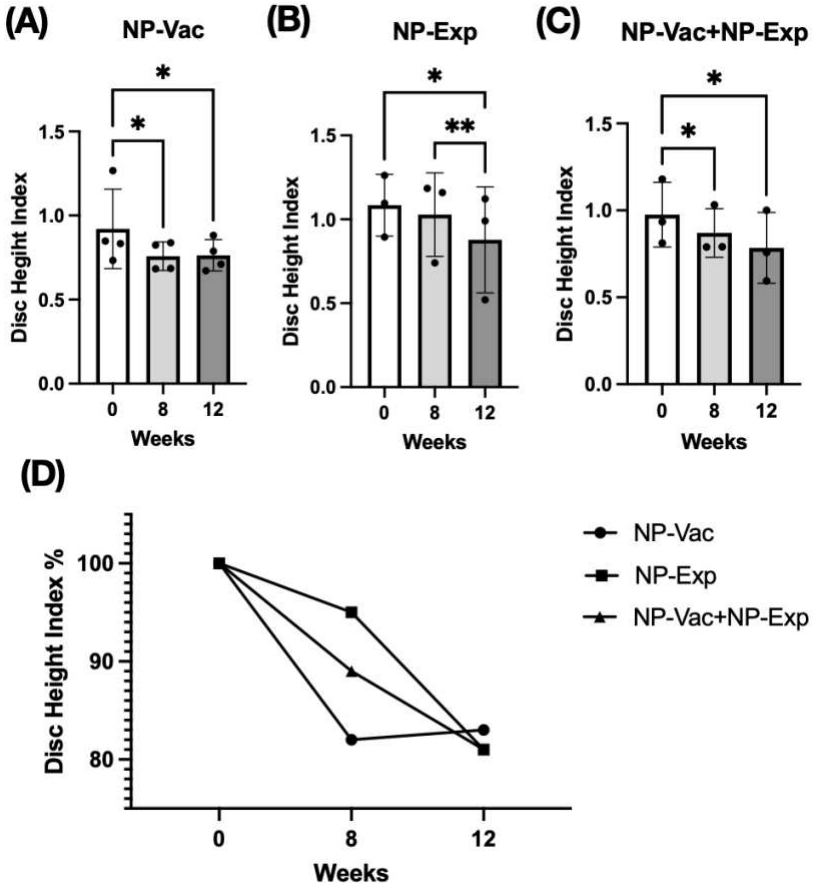

Figure 5: Changes in Disc height index (DHI) for all experimental groups. **A**) NP-Vac group showed significant changes between baseline (0 weeks), 8 and 12 weeks. **B**) NP-Exp group showed significant differences in the DHI between 0 and 12 weeks, and between 8 and 12 weeks. **C**) NP-Vac+NP-Exp group showed significant differences in the DHI between 0 and 8 weeks, and between 0 and 12 weeks. **D**) Noticeable reduction in DHI is evident across all experimental groups, indicating a consistent trend of disc height decrease over time. *= P<0.05, **=P<0.01, DHI; Disc height index.

Magnetic resonance imaging was also used to evaluate the impact of surgical disc

disruption alone or in combination with an NP vaccine in the rabbit model. We found that MR and radiograph imaging did not detect evidence of new bone formation (osteophytes) or abnormalities after NP vaccination or vaccination plus disc puncture in any of the injured disc spaces from any of the three groups of animals. MR images from NP-Vac group of animals showed consistent homogeneous high-signal intensity within the central region of the IVD over the 12-week study period, indicative of healthy IVD. In contrast, MR images from the NP-Exp and NP-Vac+NP-Exp groups showed a significant decrease in signal intensity within the central region of the IVD, indicative of moderate IDD. No significant differences were noted in Pfirrmann grades at either 8 or 12 weeks between NP-Vac and NP-Exp groups. However, Pfirrmann grades were significantly higher in the NP-Vac+NP-Exp group compared to the NP-Vac group at 8 weeks (P=0.0114) and 12 weeks (P=0.0241) (**Figure 6**). These findings are consistent with the acceleration of disc injury in the animals that received the NP vaccine plus disc puncture surgery.

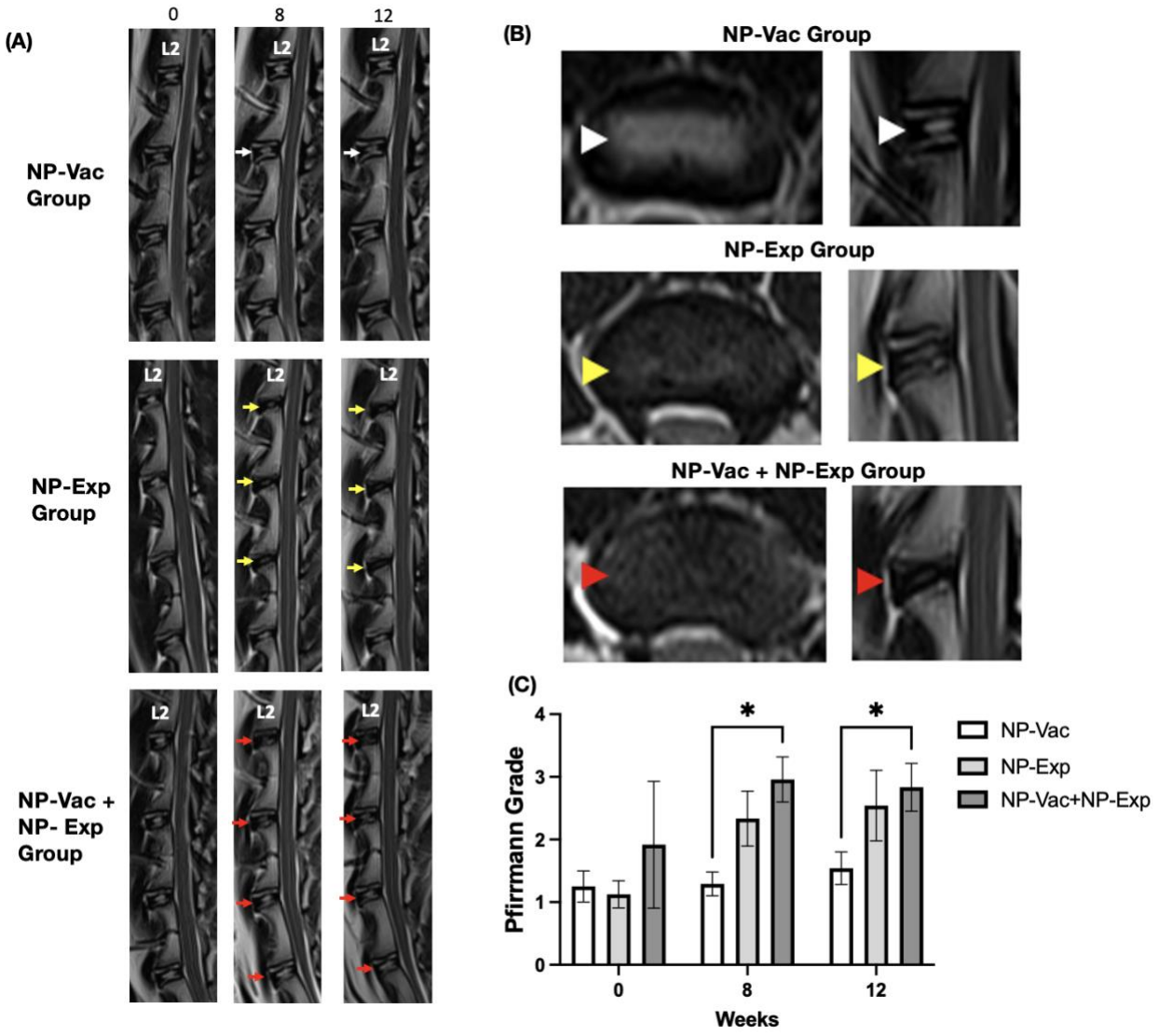

Figure 6: Magnetic resonance (MR) imaging evaluation showed higher degeneration grade for animals from NP-Exp group and NP-Vac+NP-Exp compared to NP-Vac. A) Representative T2-weighted MR images from each group. NP-Exp and NP-Vac+NP-Exp groups showed more drastic decreases in signal intensity and increases in Pfirrmann grade defect types (Yellow and red arrows respectively) compared to NP-Vac group (White arrows) at 8 or 12-weeks. B) Comparison of Axial and Sagittal T2-weighted MR views from the same disc in representative animals from each group at 12-week time point. Normal signal intensity of the NP is evident in NP-Vac group (white arrow heads) but decreased in NP-Exp group (Yellow arrow heads) and even more in NP-Vac+NP-Exp group (Red arrow heads). C) Evaluation of the Pfirrmann grade showed significant differences with a higher degree of degeneration in animals from NP-Vac+NP-Exp group compared with NP-Vac group, after 8 and 12 weeks of intervention. *= $P<0.05$. Data are presented as mean and SD.

6. 5 Discussion

This study, to our knowledge, is the first to provide evidence that immunization against NP antigens can refine and/or accelerate IDD in an animal model. Key findings from this study were induction of strong immune responses against a dominant NP antigen by NP vaccination and the progression of disc degeneration parameters in animals that received the NP vaccine plus surgical disc puncture. Our findings also indicate that this new animal model of accelerated IVD damage by immune processes could be an important new tool to elucidate the role of immune responses in human IDD and to develop new medical or surgical interventions to ameliorate anti-NP immunity (352). These new findings suggest that indeed anti-NP immune responses may be an important part of the progressive nature of IDD in animal models and that immune interventions designed to blunt these immune responses may be one strategy to slow or reverse IVD progressive damage.

The potential role of the immune system in the development and progression of IDD was introduced several decades ago (340,353). *In vitro* studies support the notion that both degenerated and normal NP proteins can elicit detectable immune responses (341). Additionally, clinical findings by Kim *et al.* demonstrated increased anti-NP antibodies in patients with spontaneous disc herniation (353). Satoh *et al.* also identified antigen-antibody complexes in herniated NP tissue compared to non-herniated NP tissue (345). Capossela *et al.* detected antibody responses against specific proteins in the NP in patients with IVD, confirming an immune reaction against the immune-privileged NP antigens (346).

In this study, we offer an insight into the proteins recognized by the NP vaccine. HtrA serine peptidase and Hyaluronan and proteoglycan link protein 1 (HAPLN1) proteins may serve as potential targets as they were both abundantly detected in the Western blots reacting to NP vaccine serums. HAPLN1 has been implicated in the degradation of the extracellular matrix and

the process of intervertebral disc degeneration in both humans and animals (22)(354–356) Similarly, HtrA serine peptidase is recognized for its involvement in osteoarthritic pathology and intervertebral disc degradation. Notably, elevated HTRA1 mRNA expression in degenerated disc tissue has been associated with the promotion of IVD degeneration through the proteolytic cleavage of fibronectin and subsequent activation of resident disc cells (357).

We found that animals that received the NP vaccine and then underwent disc puncture developed stronger antibody responses than animals that only received the NP vaccine. This finding would therefore be consistent with exposure of NP proteins to the immune system by virtue of physical barrier disruption (AF/disc puncture), which would serve to accelerate anti-NP immunity induced by the NP vaccine. While the literature primarily focuses on anti-NP immunity in disc herniations, our rationale for utilizing healthy NP tissue stems from its ability to serve as a reliable antigen source while minimizing potential complications associated with diseased tissue. Additionally, previous studies have demonstrated *in vitro* immune reactions to healthy NP cells (344), suggesting their suitability for stimulating an immune response in the context of vaccine development. It is also important to note here that the NP vaccine used in this study was derived from sheep NP material and was therefore immunologically foreign to rabbits in this study, which likely resulted in enhanced immune recognition, compared to immunization against rabbit NP proteins. It would be important to determine in subsequent studies whether immunization with autologous NP proteins derived from rabbit NP material could also induce strong anti-NP antibody responses in rabbits. Our intriguing early findings nonetheless suggest that the exposure of the NP to the immune system by needle puncture, coupled with the administration of an NP vaccine, can generate an enhanced immune reaction, as reflected by higher antibody titers in animals receiving disc puncture and the NP vaccine.

With respect to morphological markers of IDD, we noted a significant decrease in DHI across all three treatment groups, as reflected by sequential imaging. Intriguingly, even though the IVDs in the NP-Vac group were not punctured, baseline MR images revealed that these animals already displayed spontaneous signs of IDD. The observed spontaneous IDD changes at baseline align with previous reports indicating age-dependent alterations in intervertebral discs among rabbits (358,359). This apparent naturally occurring IDD, combined with the immune effects of the NP-Vac, might account for an increase in IDD-related inflammation, leading to a reduction in the DHI for this group. While the NP-Exp (disc puncture) group showed consistent and expected MR changes and Pfirrmann grades to previous studies in rabbits (360–362), NP-Vac+NP-Exp resulted in more severe decreases in signal intensity within the disc. The increase in Pfirrmann grades of the animals from NP-Vac+NP-Exp group at 8 weeks, without significant changes at 12 weeks, suggest that a shortened study of only 8 weeks could be used for the establishment of the proposed accelerated and sustained model of IDD. Developing a more effective model to induce IDD would hasten the currently prolonged periods of time required for IDD progression, thereby reducing model time and costs. Furthermore, identifying and suppressing this immune response could also be used to decrease the development and progression of IDD in patients affected by the condition (352,363,364).

With the progression of IDD, the structure of the IVD becomes disorganized. Histologically, there is loss of distinction between the NP and AF, a reduction in cell density, and NP shape, and a progressive disorganization of AF. Our results show similar histological signs of IDD progression to previously reported IDD in rabbits with different methods to induce IDD (365). However, higher values of degeneration were observed in the NP-Vac+NP-Exp group using the standardized histopathology scoring system for IDD in rabbit models. This supports our

hypothesis that the exposure of NP, in addition to the immune effects of receiving the NP vaccine, induced more severe changes compared to IDD induced through needle puncture alone.

The small sample size is a major limitation of this study, as is the lack of a control group of animals that received no interventions. Nevertheless, despite the limited number of animals in this study, we were able to identify evidence of a treatment effect from NP vaccination combined with surgical disc puncture. Therefore, we propose that there was sufficient evidence of immune activation of the IDD process in this new animal model to warrant further investigation, including studies with larger groups and additional controls, and with an optimized NP vaccine protocol.

Finally, the NP vaccine antibody results combined with significant changes in the Pfirrmann grade and histological evaluation, provide compelling evidence demonstrating the influence of the immune response on the development of IDD in a new *in vivo* model for IDD. In general, these results support our hypothesis that rabbits vaccinated with NP proteins developed a heightened immune response and increased IDD compared to rabbits undergoing IDD via a traditional needle puncture approach. However, further studies are imperative to gain a more comprehensive understanding of the role played by immune responses, particularly the relative importance of humoral responses (measured in the current study) and cellular responses (e.g., T cell responses) in the overall development of accelerated and sustained disc degeneration.

6.6 References

1. Hartvigsen J, Hancock MJ, Kongsted A, Louw Q, Ferreira ML, Genevay S, et al. What low back pain is and why we need to pay attention. The Lancet. 2018 Jun 1;391(10137):2356–67.
2. Oichi T, Taniguchi Y, Oshima Y, Tanaka S, Saito T. Pathomechanism of intervertebral disc

degeneration. JOR Spine. 2020;3(1):1–9.

3. Alini M, Diwan AD, Erwin WM, Little CB, Melrose J. An update on animal models of intervertebral disc degeneration and low back pain: Exploring the potential of artificial intelligence to improve research analysis and development of prospective therapeutics. JOR Spine. 2023 Mar 1;6(August 2022):1–29.
4. Jin L, Balian G, Li XJ. Animal models for disc degeneration-an update. Histol Histopathol. 2018;33(6):543–54.
5. Poletto DL, Crowley JD, Tanglay O, Walsh WR, Pelletier MH. Preclinical in vivo animal models of intervertebral disc degeneration. Part 1: A systematic review. JOR Spine. 2022;(October 2022):1–20.
6. Fusellier M, Clouet J, Gauthier O, Tryfonidou M, Le Visage C, Guicheux J. Degenerative lumbar disc disease: In vivo data support the rationale for the selection of appropriate animal models. Eur Cell Mater. 2020;39:18–47.
7. Feng P, Che Y, Gao C, Zhu L, Gao J, Vo N V. Immune exposure: how macrophages interact with the nucleus pulposus. Front Immunol. 2023;14:1155746.
8. Vadalà G, Russo F, De Strobel F, Bernardini M, De Benedictis GM, Cattani C, et al. Novel stepwise model of intervertebral disc degeneration with intact annulus fibrosus to test regeneration strategies. Journal of Orthopaedic Research. 2018;36(9):2460–8.
9. Sun Z, Zhang M, Zhao XH, Liu ZH, Gao Y, Samartzis D, et al. Immune cascades in human intervertebral disc: The pros and cons. Int J Clin Exp Pathol. 2013;6(6):1009–14.
10. Xu H, Li J, Fei Q, Jiang L. Contribution of immune cells to intervertebral disc degeneration and the potential of immunotherapy. Connective Tissue Research. Connect Tissue Res; 2023.

11. Wang L, He T, Liu J, Tai J, Wang B, Zhang L, et al. Revealing the Immune Infiltration Landscape and Identifying Diagnostic Biomarkers for Lumbar Disc Herniation. Front Immunol. 2021;12(May):1–13.

12. Sun Z, Liu B, Luo ZJ. The immune privilege of the intervertebral disc: Implications for intervertebral disc degeneration treatment. Int J Med Sci. 2020;17(5):685–92.

13. Liu ZH, Sun Z, Wang HQ, Ge J, Jiang TS, Chen YF, et al. FasL expression on human nucleus pulposus cells contributes to the immune privilege of intervertebral disc by interacting with immunocytes. Int J Med Sci. 2013;10(8):1053–60.

14. Ye F, Lyu FJ, Wang H, Zheng Z. The involvement of immune system in intervertebral disc herniation and degeneration. JOR Spine. 2022;5(1):1–12.

15. Geiss A, Larsson K, Rydevik B, Takahashi I, Olmarker K. Autoimmune properties of nucleus pulposus: An experimental study in pigs. Spine (Phila Pa 1976). 2007;32(2):168–73.

16. Bobechko WP, Hirsch C. Auto-Immune response to Nucleus Pulposus in the rabbit. J Bone Joint Surg Br. 1965;47:574–80.

17. Murai K, Sakai D, Nakamura Y, Nakai T, Igarashi T, Seo N, et al. Primary immune system responders to nucleus pulposus cells: Evidence for immune response in disc herniation. Eur Cell Mater. 2010;19:13–21.

18. Wan J, Zhang XS. Pre-operative blood test for antibody to nucleus pulposus may distinguish types of lumbar disc herniation. Med Hypotheses. 2010 Nov;75(5):464–5.

19. Jiang H, Liu J tao, Hui R hua, Wang Y jun. [An experimental study on the influence of radix astragali on the ressorption of ruptured disc herniation]. Zhongguo Gu Shang. 2009 Mar;22(3):205–7.

20. Geiss A, Larsson K, Junevik K, Rydevik B, Olmarker K. Autologous nucleus pulposus primes T cells to develop into lnterleukin-4-producing effector cells: An experimental study on the autoimmune properties of nucleus pulposus. Journal of Orthopaedic Research. 2009;27(1):97–103.

21. Satoh K, Konno S, Nishiyama K, Olmarker K, Kikuchi S. Presence and distribution of antigen-antibody complexes in the herniated nucleus pulposus. Spine (Phila Pa 1976). 1999;24(19):1980–4.

22. Capossela S, Schläfli P, Bertolo A, Janner T, Stadler BM, Pötzel T, et al. Degenerated human intervertebral discs contain autoantibodies against extracellular matrix proteins. Eur Cell Mater. 2014;27:251–63.

23. Zaks K, Jordan M, Guth A, Sellins K, Kedl R, Izzo A, et al. Efficient Immunization and Cross-Priming by Vaccine Adjuvants Containing TLR3 or TLR9 Agonists Complexed to Cationic Liposomes. 2006;(8).

24. Ko KH, Cha S Bin, Lee SH, Bae HS, Ham CS, Lee MG, et al. A novel defined TLR3 agonist as an effective vaccine adjuvant. Front Immunol. 2023 Jan 24;14.

25. Jeon D, Hill E, McNeel DG. Toll-like receptor agonists as cancer vaccine adjuvants. Hum Vaccin Immunother. 2024 Dec 31;20(1).

26. Luo TD, Marquez-Lara A, Zabarsky ZK, Vines JB, Mowry KC, Jinnah AH, et al. A percutaneous, minimally invasive annulus fibrosus needle puncture model of intervertebral disc degeneration in rabbits. Journal of Orthopaedic Surgery. 2018;26(3):1–8.

27. Lee NN, Salzer E, Bach FC, Bonilla AF, Cook JL, Gazit Z, et al. A comprehensive tool box for large animal studies of intervertebral disc degeneration. JOR Spine. 2021;(July 2020):1–36.

28. Masuda K, Aota Y, Muehleman C, Imai Y, Okuma M, Thonar EJ, et al. A novel rabbit model of mild, reproducible disc degeneration by an anulus needle puncture: Correlation between the degree of disc injury and radiological and histological appearances of disc degeneration. Spine (Phila Pa 1976). 2005;30(1):5–14.

29. Pfirrmann CWA, Metzdorf A, Zanetti M, Hodler J, Boos N. Magnetic resonance classification of lumbar intervertebral disc degeneration. Spine (Phila Pa 1976). 2001;26(17):1873–8.

30. Gullbrand SE, Ashinsky BG, Lai A, Gansau J, Crowley J, Cunha C, et al. Development of a standardized histopathology scoring system for intervertebral disc degeneration and regeneration in rabbit models-An initiative of the ORS spine section. JOR Spine. 2021;(December 2020):1–12.

31. Kang H, Dong Y, Peng R, Liu H, Guo Q, Song K, et al. Inhibition of IRE1 suppresses the catabolic effect of IL-1β on nucleus pulposus cell and prevents intervertebral disc degeneration in vivo. Biochem Pharmacol. 2022;197:1–16.

32. Kim NH, Kang ES, Han CD, Kim JD, Kim CH. Auto-immune response in degenerated lumbar disk. Yonsei Med J. 1981;22(1):26–32.

33. Erwin WM, DeSouza L, Funabashi M, Kawchuk G, Karim MZ, Kim S, et al. The biological basis of degenerative disc disease: proteomic and biomechanical analysis of the canine intervertebral disc. Arthritis Res Ther. 2015 Dec 5;17(1):240.

34. Urano T, Narusawa K, Shiraki M, Sasaki N, Hosoi T, Ouchi Y, et al. Single-nucleotide polymorphism in the hyaluronan and proteoglycan link protein 1 (HAPLN1) gene is associated with spinal osteophyte formation and disc degeneration in Japanese women. European Spine Journal. 2011 Apr 15;20(4):572–7.

35. Rodriguez E, Roughley P. Link protein can retard the degradation of hyaluronan in proteoglycan aggregates. Osteoarthritis Cartilage. 2006 Aug;14(8):823–9.

36. Tiaden AN, Klawitter M, Lux V, Mirsaidi A, Bahrenberg G, Glanz S, et al. Detrimental Role for Human High Temperature Requirement Serine Protease A1 (HTRA1) in the Pathogenesis of Intervertebral Disc (IVD) Degeneration. Journal of Biological Chemistry. 2012 Jun;287(25):21335–45.

37. Clouet J, Pot-Vaucel M, Grimandi G, Masson M, Lesoeur J, Fellah BH, et al. Characterization of the age-dependent intervertebral disc changes in rabbit by correlation between MRI, histology and gene expression. BMC Musculoskelet Disord. 2011 Dec 4;12(1):147.

38. Leung VYL, Hung SC, Li LC, Wu EX, Luk KDK, Chan D, et al. Age-related degeneration of lumbar intervertebral discs in rabbits revealed by deuterium oxide-assisted MRI. Osteoarthritis Cartilage. 2008 Nov;16(11):1312–8.

39. Jin Y, Mao G, Yang C, Xia C, Chen C, Shi F, et al. Establishment of a New Model of Lumbar Intervertebral Disc Degeneration With Pathological Characteristics. Global Spine J. 2021;(158).

40. Tayebi B, Molazem M, Babaahmadi M, Ebrahimi E, Hajinasrollah M, Mostafaei F, et al. Comparison of Ultrasound-Guided Percutaneous and Open Surgery Approaches in The Animal Model of Tumor Necrosis Factor-Alpha-Induced Disc Degeneration. Cell J. 2023;25(5):338–46.

41. Ishikawa T, Watanabe A, Kamoda H, Miyagi M, Inoue G, Takahashi K, et al. Evaluation of lumbar intervertebral disc degeneration using T1ρ and T2 magnetic resonance imaging in a rabbit disc injury model. Asian Spine J. 2018;12(2):317–24.

42. Gao Y, Chen X, Zheng G, Lin M, Zhou H, Zhang X. Current status and development direction of immunomodulatory therapy for intervertebral disk degeneration. Front Med (Lausanne). 2023 Dec 21;10.

43. Xiang H, Zhao W, Jiang K, He J, Chen L, Cui W, et al. Progress in regulating inflammatory biomaterials for intervertebral disc regeneration. Bioact Mater. 2024 Mar;33:506–31.

44. Capogna EA, Brown E, Walrath E, Furst W, Dong Q, Zhou CM, et al. ISSLS Prize in Bioengineering Science 2022: low rate cyclic loading as a therapeutic strategy for intervertebral disc regeneration. European Spine Journal. 2022;31(5):1088–98.

CHAPTER 7. CONCLUSIONS AND FUTURE DIRECTIONS

7.1 Conclusions

The research presented in this document provides significant insights into the pathophysiology of IVDD and the development of novel animal models for studying this condition. Through an integrative approach that includes surgery, proteomics, imaging, histology, biomechanics, and immunology, this work underscores the critical importance of employing animal models, to understand the mechanisms underlying IVDD and evaluate potential therapeutic interventions.

The current data indicate that the prevalence of LBP is expected to increase in the coming years, especially in middle- and low-income countries, which will place an even heavier burden on their economic and healthcare systems. Therefore, it is imperative for the scientific community to seek solutions to this issue. Although not directly, our efforts to enhance the understanding of the pathophysiology of these conditions, along with our advancements in refining animal models for preclinical research, will contribute to the goal of alleviating and mitigating this global health problem.

The ovine model, despite its natural limitations, offers an incredible opportunity to learn more about the progression of disc degeneration. The spontaneous aging process of disc degeneration in sheep closely resembles what occurs in humans, providing a unique window to investigate this pathology in this species rather than in humans or other animal species due to ethical and economic constraints. Utilizing ovine models for IVDD research presents a highly translatable approach, given the cellular, anatomical, and physiological similarities between sheep and humans. Our results provide groundbreaking evidence of the proteomic profile associated with the IVDD

process in this common large animal model. The ovine model is often utilized and even mandated by federal and governmental institutions to evaluate the safety and efficacy of new biomedical developments intended for human use. With this new information about the proteomic profile, we provide a powerful tool that can be employed for scientific researchers to assess the efficacy of novel therapeutic strategies for IVDD, including cell-based, genetic, and tissue engineering therapies, in a more precise and scientifically rigorous manner.

In this study, comparative analyses of surgical, imaging, proteomic profiles, and histological characteristics of cervical and lumbar IVDs have uncovered similar degeneration progression patterns in both regions. This finding suggests that treatments developed for lumbar IVDD could be adapted for cervical applications, offering promising implications for clinical practice. Notably, key proteins such as C-reactive protein and Asporin, previously reported in humans and other animal models, have been identified in this study for the ovine model. These proteins hold potential as biomarkers for early diagnosis and the development of targeted treatments.

This thesis also introduces two innovative models for studying IVDD: one utilizing ESWT and the other employing mechanical compression with MRI-compatible materials. While these models effectively induced localized changes, such as new bone formation and alterations in disc biomechanics, they did not produce classical imaging or histological degenerative changes within the study period. These findings emphasize the complexity of inducing progressive degeneration and highlight the necessity for further refinement of these models. However, key insights from this research include the significant bone formation observed in the intervertebral discs following ESWT administration and the ability to visualize the intervertebral disc structure using MRI with the MRI-compatible compression device. These findings are critical for evaluating the safety of ESWT in spinal pathologies and its application in preclinical research, as well as for advancing

the refinement of mechanical compression models in both small and large animal models of IVDD.

Imaging, particularly MRI, plays a recognized and critical role in diagnosing, evaluating the progression of IVDD, and assessing the efficacy of various therapies or surgical interventions for different spinal pathologies. The results from these projects have contributed significantly to our understanding of the progression of IVDD in both cervical and lumbar regions following different types of induction in various models. However, there is a pressing need to standardize imaging methodologies, especially for evaluating cervical intervertebral discs, due to the unique anatomical features of this region. Similarly, efforts should be made to improve the sequence parameters used for different animal models, tailoring imaging evaluations to specific models and adapting them according to the particular research questions being addressed. This standardization will enhance the reliability and reproducibility of imaging assessments across various studies, ultimately advancing the field of IVDD research.

Despite the use of conventional techniques, such as DMMB evaluation, to assess glycosaminoglycans changes in IVDs following various treatments, conversations and experiences shared with other spine researchers have highlighted the need for refinement or replacement of these methods. Traditional techniques often fall short in providing a precise representation of the changes in proteoglycan content characteristic of disc degeneration. This insight was a key factor in our decision to implement a proteomic evaluation approach, aiming to achieve a more detailed visualization of the distinct proteomic alterations that occur in the IVD at various stages of degeneration. By embracing this advanced technique, we hope to enhance the accuracy of our assessments and better elucidate the underlying biochemical changes associated with IVDD, ultimately contributing to more effective therapeutic strategies.

While we acknowledge the importance of histological evaluation in assessing degenerative

changes; overall, our findings did not demonstrate significant degenerative alterations when compared to other outcomes, such as imaging, gross evaluation, or proteomic analyses. Although the limited sample size of our animal studies may have contributed to this lack of significance, it also underscores the necessity for refining the histological scoring systems specifically tailored for ovine intervertebral discs. By developing more precise histological scores, we could better capture the unique changes occurring in the ovine IVD following IVDD induction and even spontaneous aging. This refinement is particularly crucial, as the sheep serves as a valuable model for understanding the progression of IVDD in humans and enhancing our histological evaluation methods could lead to deeper insights into the disease mechanisms shared between species.

Furthermore, these studies were instrumental in tracking changes in various cytokines, which could serve as biomarkers for understanding the progression of the degeneration process. While some of these biomarkers have been utilized in small animal models of IVDD, their application in large animals has been limited due to the scarcity of cytokine profiles available for evaluation and the associated cost limitations. Our results demonstrate that tracking these biomarkers in large animal models is not only feasible but also provides crucial outcomes for the spinal research community. By bridging this gap, we pave the way for more comprehensive investigations into IVDD, enhancing our understanding of this condition and potentially informing the development of targeted therapeutic strategies.

Finally, the introduction of a novel immune-induced model IVDD has shown that immune responses against the NP can accelerate degeneration following disc injury. This study aligns with currently significant interest in understanding the role of the immune system in IVDD and how it can be manipulated to influence disease progression. Various research efforts are underway to elucidate the impact of immune factors at different stages of disc degeneration. This proof-of-

concept *in vivo* experiment successfully demonstrated an immune response that drives the progression of degeneration in a needle puncture animal model. The immune-mediated model presented here opens new avenues for investigating the role of the immune system in IVDD and developing therapeutic strategies that target immune responses to prevent or slow IVDD progression. Additionally, our findings suggest the scientific potential to develop an immune vaccine designed to prime the immune system and sensitize it prior to exposure to NP antigens. Such an approach could be beneficial in preventing the development of pathologies, such as disc herniation, in both animal and human patients.

7.2 Future Directions

Undoubtedly, the results of these studies will serve as a cornerstone for future research aimed at refining these models here presented. Specifically, the information provided about the differences between cervical and lumbar IVDs and the degeneration processes in this species should be utilized to tailor these models accordingly. Insights into strategic and potential proteomic targets can be achieved based on the findings presented here. Similarly, the information regarding the surgical approach offers valuable evidence for effectively addressing these structures when mimicking or inducing IVD models, such as disc degeneration or even disc herniation, in other animal species.

Additionally, the integration of minimally invasive techniques for the induction and treatment of IVDD could be significantly advanced through the animal models presented in this study. The adoption of increasingly precise surgical techniques, such as computer-assisted surgery, represents the next step in enhancing these surgical approaches. This technological advancement promises numerous benefits, including reduced surgery and recovery times, lower risks of

infection, and improved patient outcomes. Moreover, from a preclinical evaluation perspective, these techniques will minimize the influence of surgical factors when assessing novel therapies, allowing for a more accurate evaluation of their efficacy.

Specifically regarding to ESWT, the results presented here will enable researchers to design and refine experiments related to its application in treating IVDD. By adjusting the settings of the therapy and exploring various shock wave devices, researchers can optimize the delivery of energy, allowing for more precise targeting of critical tissues such as the NP, or the endplates. This improved targeting can significantly enhance the efficacy of ESWT, potentially leading to better research outcomes for preclinical and clinical applications. The insights gained from this study will serve as a valuable foundation for long-term research projects aimed at visualizing the effects of ESWT on these anatomical structures over extended periods. By employing advanced imaging techniques and long-term monitoring, researchers can gain a deeper understanding of the biological responses to shock wave therapy, assessing both immediate and delayed effects on tissue health and degeneration. Moreover, the combination of refined experimental settings and innovative shock wave devices could allow for a more tailored approach to therapy, addressing the unique needs of each animal model or patient based on individual anatomical and pathological conditions.

Our findings serve as a proof of concept for the development of an internal mechanical compression device that addresses the challenges we faced, such as infection, and improves the ability to apply dynamic and consistent compression to the intervertebral discs (IVDs). These results contribute to advancing mechanical models in large animals, which are crucial for deepening our understanding of IVD degeneration. Developing such models is especially important given the advantages large animal models offer over small animal models for studying

the mechanical changes that occur in the spine. This will enhance our ability to investigate pathophysiological mechanisms in a more clinically relevant context. In addition, for the mechanical compression models, we foresee that these results will facilitate the use of MRI for diagnosing and monitoring the progression of degeneration across a range of animal models, beyond just sheep. Specifically, the findings from this study highlight the safety and valuable application of MRI-compatible materials within the reported model, reinforcing their significance for preclinical research in spinal health. This is particularly important as mechanical compression models effectively simulate known risk factors for low back pain and disc degeneration, such as obesity and physically demanding occupations. These factors impose substantial mechanical loads on the IVDs, negatively impacting their health and contributing to degeneration. By leveraging MRI technology in this context, researchers can gain crucial insights into the dynamics of IVD health and the influence of various risk factors, thereby enhancing our understanding of spinal pathologies and guiding future therapeutic interventions after using these mechanical compression models.

Building on the proteomic findings, future research is aimed to investigate the roles of specific proteins identified in these studies in the degeneration process. With the identification of proteins that are downregulated and upregulated at various stages of degeneration in the ovine model, this information can be use for the development of targeted therapies aimed at these differentially expressed proteins, allowing researchers to assess their potential in modifying the degeneration process. For instance, the consistent presence of Asporin across all evaluated time points could serve as a valuable biomarker for tracking degeneration in these animal models. Additionally, investigating the signaling pathways associated with these proteins may reveal new approaches for early diagnosis and treatment of IVDD. Furthermore, gene editing technologies

such as CRISPR-Cas9 could be employed to manipulate these targets and evaluate their effects on IVDD progression. In the case of Asporin, researchers could develop genetically modified large animal models by knocking out this protein, thereby creating a unique platform for studying IVDD in a manner that extends beyond small animal models.

The immune-induced model of IVDD presents exciting opportunities for future research. The results from our immune-driven IVDD model are currently being utilized as preliminary data for developing future projects that focus on refining the vaccine used and enrolling larger animal models that are more relevant for translational purposes. Additionally, these findings pave the way for elucidating the identified immune factors in an in vitro environment, which could aid in characterizing the immune response at varying doses or under specific tissue conditions.

Finally, future studies should emphasize the long-term evaluation of potential therapeutic interventions for IVDD in large animal models. Treatments such as cell-based therapies, biomaterials, or pharmacological agents should be tested for their ability to restore disc function and halt degeneration over extended periods. The use of biomarkers identified in this thesis can aid in monitoring treatment efficacy and inform the development of personalized medicine approaches for managing IVDD.

OTHER PROJECTS

Validating a Computer-Assisted Surgical Navigation System in The Equine Cervical Spine

Computer-assisted surgical navigation (CASN) enables real-time identification of surgical validating a computer-assisted surgical navigation system in the equine cervical spine instruments relative to a patient. This technology aids surgeons with pre-operative planning, real-time navigation, and intraoperative assistance, enhancing accuracy and efficiency of surgical procedures. Success in human medicine has demonstrated its benefits, including minimally invasive approaches, reduced risk of infections, decreased surgical time, and reduction in surgical errors. Despite these advancements, CASN has yet to prove its full potential in veterinary medicine. This study aims to validate the Synaptive^{TM} Medical System for use in equine cervical spine procedures. We hypothesized that the system can accurately guide desired anatomical targets. One equine cadaver neck was used to evaluate the accuracy of SMS in approaching four cervical spine targets. Four participants with varying degrees of surgical experience were enrolled. Following a pre-operative (CT) scan, labeled pins were placed by each participant at the desired targets. Anatomical targets were selected for their clinical significance, including the ligamentum flavum at C1-C2, intervertebral foramen at C2-C3, facet joint at C3-C4, and intervertebral disc at C4-C5. Procedure duration was measured to correlate with surgical experience. Postoperative CT was used to evaluate accuracy using the Euclidean distance formula from each target to each pin's point. Statistical analysis in accuracy and duration between participants was performed. This will help determine the feasibility and potential benefits of implementing CASN in veterinary practice, specifically with SMS for surgical procedures in the equine cervical spine.

Comparative Characterization of Dorsal Root Ganglion Across Species: Unraveling Mechanism Of Pain In Animal Models

Chronic pain, a major clinical concern across species, is often mediated through complex neural mechanisms involving the dorsal root ganglion (DRG). The DRG plays a critical role as a hub for sensory input processing, particularly in pain signaling pathways. Understanding its function is essential to elucidate mechanisms underlying pain generation and propagation, providing insight into potential therapeutic targets. This project focuses on characterizing the DRG across different species (equine, ovine, canine, rabbits, guinea pigs, and potentially pigs), to compare its structure and function and examine species-specific mechanisms of pain. The study aims to contribute to veterinary medicine, comparative neuroscience, and translational research that can benefit both human and veterinary applications.

Pain mechanisms, while generally similar, may have species-specific variations, particularly in the structural and functional aspects of the DRG. In veterinary practice, pain management remains a challenge due to the incomplete understanding of these variations. Animals such as horses and sheep serve as models in translational research, offering valuable insights into human conditions like chronic pain syndromes, arthritis, and intervertebral disc degeneration. A detailed understanding of DRG characteristics and their role in pain processing can bridge gaps in both human and veterinary treatment strategies.

Despite its importance, research on the DRG across different species is limited. This comparative approach is justified by the need for species-specific data to improve both veterinary and human healthcare. Equines, for instance, frequently suffer from chronic pain conditions, such as laminitis and osteoarthritis, which could be better managed with a deeper understanding of

equine-specific DRG function. Ovine models are already extensively used in musculoskeletal and pain research, particularly for spine-related conditions. Canines and rabbits, commonly used in experimental pain models, add value to the study due to their established roles in preclinical research. Additionally, guinea pigs offer a small animal model with unique DRG properties, and pigs, with their anatomical and physiological similarities to humans, could provide relevant insights for translational research. By comparing these species, the project expects to highlight key differences and similarities in DRG architecture and function that could influence how pain is perceived and processed.

Identify variations in DRG morphology, molecular expression patterns, and neuronal pathways across the species, which could contribute to species-specific pain responses. Advanced histological, biochemical, and molecular techniques will be used to map DRG neuron types, pain-related biomarkers, and receptor distributions. The findings could reveal new therapeutic targets for pain management in both animals and humans. Furthermore, the study anticipates that certain species, like equine and ovine, may present unique DRG features that make them more suitable for modeling human pain conditions. The long-term goal is to improve pain management strategies by leveraging this interspecies understanding of DRG function, potentially leading to the development of species-specific analgesic treatments and better translational models for human pain research.

Characterization of Equine Intervertebral Disc Across Cervical, Thoracic, Lumbar, and Coccygeal Regions

The equine spine, spanning cervical, thoracic, lumbar, and coccygeal regions, is a complex structure supporting a range of movements essential for equine biomechanics and performance. In recent years, there has been increasing attention to intervertebral disc (IVD) health in horses, as degeneration or injury to these structures can contribute to chronic pain, mobility issues, and reduced athletic performance. This project seeks to characterize the intervertebral discs across various spinal regions in equine species, specifically focusing on the cervical, thoracic, lumbar, and coccygeal regions. A detailed understanding of the IVD morphology and biomechanical properties in horses is critical, as it will aid in identifying region-specific susceptibilities to degeneration and other pathological changes.

Intervertebral disc degeneration (IVDD) in equines, though less studied compared to humans and other species, can have profound effects on the animal functionality and well-being. Horses, especially those involved in athletic activities, are exposed to repetitive stress on the spine, potentially leading to structural changes in their IVDs. IVDD in horses is often underdiagnosed, but it is a significant contributor to pain and limited performance, particularly in high-performance or aged animals. Understanding the anatomical and histological differences in the IVDs across the cervical, thoracic, lumbar, and coccygeal regions is important because these regions are subject to different mechanical loads and functional demands. Each region's IVDs may display unique adaptations or vulnerabilities to degeneration, making a comprehensive study of all spinal regions essential.

The project also seeks to address gaps in veterinary diagnostics and therapeutics for spinal conditions. Current diagnostic tools and treatments for equine spine health often rely on human or

small animal models, which may not be fully applicable to horses due to differences in biomechanics and spinal structure. Characterizing equine IVDs on a regional level will not only improve diagnosis but also aid in developing targeted therapeutic interventions and preventative strategies for IVDD in horses.

Furthermore, the project has broader implications beyond equine veterinary medicine, as it could serve as a comparative model for understanding spinal health in large animals, including humans. The unique insights gained from this research could open new avenues for the development of region-specific therapies to manage IVDD and improve the welfare and performance of equine species and other species, including humans.

LIST OF ABBREVIATIONS

Advanced Glycation End-Products (AGE)

Annulus Fibrosus (AF)

Cartilage Endplates (CEPS)

Differentially Expressed Proteins (DEP)

Dorsal Root Ganglion (DRG)

Extracellular Matrix (ECM)

Extracorporeal Shock Wave Therapy (ESWT)

False Discovery Rate (FDR)

Glycosaminoglycan (GAG)

Green Fluorescent Protein (GFP)

Intervertebral Disc (IVD)

Intervertebral Disc Degeneration (IVDD)

Low Back Pain (LBP)

Magnetic Resonance Imaging (MRI)

Mesenchymal Stem Cells (MSCS)

Non-Steroidal Anti-Inflammatory Drugs (NSAID),

Nucleus Pulposus (NP)

Range of Motion (ROM)

U.S Food and Drug Administration (FDA)

Years Lived with Disability (YLD)